

Strategic Environmental Research and Development Program

**Development of an Adaptive Framework for Management of
Military Operations in Arid/Semi-Arid Regions to Minimize
Watershed and Instream Impacts from Non-Point Pollution**

Project SI-1340

Final Report

**Mark Wigmosta
Leonard Lane¹
Andre Coleman
Jerry Tagestad
Damon Roberts²**

¹ L.J. Lane Consulting, Inc.

² Yakima Training Center, Washington.

December 2007

**Pacific Northwest National Laboratory
P.O. Box 999
Richland, WA 99352**

Approved for Public Release; distribution is unlimited

This report was prepared under contract to the Department of Defense Strategic Environmental Research and Development Program (SERDP). The publication of this report does not indicate endorsement by the Department of Defense, nor should the contents be construed as reflecting the official policy or position of the Department of Defense. Reference herein to any specific commercial product, process, or service by trade name, trademark, manufacturer, or otherwise, does not necessarily constitute or imply its endorsement, recommendation, or favoring by the Department of Defense.

Table of Contents

EXECUTIVE SUMMARY	1
BACKGROUND.....	1
APPROACH.....	1
RESULTS	1
DISCUSSION	3
1.0 OBJECTIVES	5
2.0 BACKGROUND	7
2.1 PROBLEM DEFINITION.....	7
2.2 SELECTED R&D ACTIVITIES PRECEDING THIS PROJECT	8
2.3 APPLICATION OF MODELING FEATURES IN THIS STRATEGIC ENVIRONMENTAL RESEARCH AND DEVELOPMENT PROGRAM (SERDP) PROJECT	10
2.4 THE YAKIMA TEST SITE.....	11
3.0 MATERIALS AND METHODS	13
3.1 ADAPTIVE MANAGEMENT FRAMEWORK.....	13
3.1.1 <i>Management Alternatives at the Yakima Training Center</i>	13
3.1.2 <i>Training Activities</i>	13
3.1.3 <i>Environmental Management</i>	16
3.2 THE ADAPTIVE MANAGEMENT FRAMEWORK (SERDP PROJECT, SI-1340).....	19
3.2.1 <i>Framework Design</i>	19
3.2.2 <i>Scope and Limitations</i>	20
3.2.3 <i>Overview of the Framework</i>	21
3.2.4 <i>Adaptive Management System for a Military Training Site</i>	22
4.0 RESULTS AND ACCOMPLISHMENTS.....	23
4.1 HYDROLOGIC ANALYSIS OF THE YAKIMA TRAINING CENTER	23
4.1.1 <i>Environmental Setting</i>	24
4.1.2 <i>Runoff Production</i>	25
4.1.3 <i>Sedimentation Ponds</i>	26
4.2 ENHANCEMENTS TO THE DISTRIBUTED HYDROLOGY SOIL VEGETATION MODEL	27
4.2.1 <i>Snow Accumulation and Melt</i>	28
4.2.2 <i>Surface Soil Temperature</i>	29
4.2.3 <i>Green-Ampt Infiltration</i>	30
4.2.4 <i>Selah Creek Peak Flow Analysis</i>	32
4.3 ENHANCEMENTS TO THE HILLSLOPE EROSION MODEL	33
4.3.1 <i>Winter Processes</i>	36
4.4 TESTING THE COUPLED DHSVM-HEM MODEL AT THE YTC SEDIMENTATION PONDS	39
4.4.1 <i>Field Data Collection</i>	39
4.4.2 <i>Model Application</i>	40
4.4.3 <i>Discussion</i>	42
4.5 APPLICATION OF REMOTELY SENSED DATA IN MODELING SOIL EROSION AT THE YTC	44
4.5.1 <i>Data Collection</i>	45

4.5.2	<i>Comparison of Remotely Sensed and Field Measured Data</i>	46
4.5.3	<i>HEM Sediment Yield Estimates for Remotely Sensed and Field-Measured Input</i>	50
4.5.4	<i>Revised Method to Estimate Ground Cover</i>	53
4.6	ESTIMATING SOIL EROSION CONDITION CLASSES FOR THE YTC	57
4.6.1	<i>Analyses of Measured and Simulated Soil Erosion Rates</i>	58
4.6.2	<i>Determining Generalized Soil Erosion Condition Classes</i>	59
4.6.3	<i>Using the Decision Tools</i>	60
4.6.4	<i>Mapping Site-Wide Erosion Condition Classes</i>	63
4.6.5	<i>Discussion</i>	64
4.7	DEVELOPMENT OF A DYNAMIC SEDIMENT BUDGET FOR THE YTC	65
4.7.1	<i>Geospatial Watershed Development</i>	65
4.7.2	<i>Virtual Transect Model</i>	65
4.7.3	<i>Spatial Data Viewer</i>	73
4.8	SPATIAL AND TEMPORAL ANALYSIS OF SEDIMENT YIELD	75
4.8.1	<i>Basin-Scale Sediment Yield</i>	75
4.8.2	<i>Interpretation and Utilization of Distributed Sediment Yield Data</i>	78
4.8.3	<i>Temporal Variations in Sediment Yield – Role of Large Storms</i>	79
4.8.4	<i>Role of Large Storms in Determining Sediment Yield at the YTC</i>	82
4.8.5	<i>Discussion</i>	83
4.9	DECISION SUPPORT SYSTEMS	84
4.9.1	<i>The Spreadsheet Implemented Multi-objective Decision Support System (SIMDSS)</i> 84	
4.9.2	<i>Example Application – Analysis of Firebreak Road Alternatives</i>	85
4.9.3	<i>Example of User Input to the DSS – Firebreak roads at the YTC</i>	89
4.9.4	<i>Discussion</i>	90
5.0	CONCLUSIONS	93
6.0	REFERENCES	97

List of Figures

Figure 1. A map of the YTC showing its location in south-central Washington.	12
Figure 2. Land-use zones at the YTC (YTC 2002).	15
Figure 3. YTC Management Plan decision flow diagram (YTC 2002).	17
Figure 4. Schematic overview of the AMF for SERDP Project SI-1340.	21
Figure 5. Locations of five historic crest-stage gages and four meteorological stations relative to the YTC boundary.	25
Figure 6. Seasonal distribution of observed and simulated annual peak flows in the YTC vicinity. The simulation results are discussed in a later section of the paper.	26
Figure 7. A map of the YTC showing training areas and pond locations. Hillslope measurements were taken on pond watersheds during April–May 2003, and these are marked with an asterisk. Measurements on the remaining ponds were taken in May 2004.	27
Figure 8. DHSVM-simulated hourly snow water equivalent (red) vs. HMS daily-observed snow cover for the winters of Water Years 1992–1997.	29
Figure 9. Percent of time the model predicted the correct hourly soil thermal state vs. percent of the winter (Nov–Mar) with observed frozen soil. Each dot represents a single winter.	30
Figure 10. Field data were collected on three broad land-use types: (1) rangeland, (2) unimproved roads, and (3) firebreak roads.	39
Figure 11. Average annual sediment yield predicted by the DHSVM-HEM (blue), RUSLE (green), and WEPP (gray) models at each pond compared with measured yield in 1985–1990 (red square) and 1990–1994 (red circle). Note that WEPP values are off the scale in Ponds 1 and 12.	42
Figure 12. Mean annual sediment yield predicted by DHSVM-HEM for each pond by cover type for rangeland (green), unimproved roads (blue), and firebreaks (red).	43
Figure 13. Analysis of field-measured vs. SPOT-modeled vegetative canopy cover data for transect segments >20 m in length (two pixel sizes). The data are for 136 transect segments.	47
Figure 14. Analysis of field measured vs. SPOT-modeled bare soil data for transect segments >20 m in length (two pixel sizes) and with >60% vegetative canopy cover. The data are for 111 transect segments.	48
Figure 15. Analysis of field-measured vs. SPOT-modeled slope steepness data for transect segments >20 m in length (two pixel sizes). The data are for 138 transect segments.	49

Figure 16. Analysis of field-measured vs. SPOT-modeled flow length data for transect segments >20 m in length (two pixel sizes). The data are for 52 transect segments.	50
Figure 17. Variation of HEM estimated sediment yield for “mean” input data and “mean” plus or minus the standard deviation for each of four input variables.	51
Figure 18. Comparison of “means” \pm SD simulated sediment yield values from field data estimates and remotely sensed data estimates of “means” and standard deviations.	53
Figure 19. Regression analyses for mean GC% as a function of mean CC% for the rocky soils at YTC.	56
Figure 20. Regression analyses for mean GC% as a function of mean CC% for the non-rocky soils at YTC.	56
Figure 21. Comparison of cropland conservation tillage-soil loss results with normalized soil erosion vs. ground surface cover, GC%, for rocky and non-rocky rangeland soils at the YTC.	58
Figure 22. Generalized Canopy cover vs. normalized soil erosion for rocky soils at the YTC. Notice the paired (CC%, GC%) values indicating the soil erosion condition classes.	59
Figure 23. Generalized Canopy cover vs. normalized soil erosion for non-rocky soils at the YTC. Notice the paired (CC%,GC%) values indicating the soil erosion condition classes.	60
Figure 24. Percent vegetation canopy cover derived from SPOT 10-m resolution multi-spectral imagery. Notice the low canopy linear features in the zoom window representing unimproved road (running east-west) and a firebreak (running northwest-southeast).	63
Figure 25. A site-wide soil erosion condition class map derived using three land-use classes (rangeland, unimproved roads, and firebreak roads), two soil classes (rocky and non-rocky), and four soil erosion condition classes (poor, fair, good, and excellent).	64
Figure 26. A total of 3,469 first-order subbasins were developed as a base for multi-scale sediment yield analysis.	67
Figure 27. The Virtual Transect Model derives a flow path from a given starting point in a subbasin until it reaches a point of concentrated flow. A transect is broken into segments based on changes in slope.	68
Figure 28. A spatial comparison of field measured flow paths and flow paths derived from the virtual transect model.	69
Figure 29. Total sediment yield (t/ha/yr) for subbasins fully contained within the YTC.	70
Figure 30. Sediment yield (t/ha/yr) generated from rangeland areas on subbasins fully contained within the YTC.	71

Figure 31. Sediment yield (t/ha/yr) generated from firebreaks. Only subbasins which contain firebreaks are shown.	72
Figure 32. Sediment yield (t/ha/yr) generated from unimproved roads. Only subbasins which contain unimproved roads are shown.	73
Figure 33. An easy-to-use spatial data viewer was developed for the YTC to allow easy access to spatially based model input and modeled sediment yield results.	74
Figure 34. The spatial data viewer allows interactive queries to the underlying database of information, which includes information on sediment yield, soil types, land use, canopy, and ground cover. Also shown is the presence of unimproved roads (brown) and firebreaks (red) overlain on the classified subbasin boundaries.	75
Figure 35. Illustration of the relationship between the percent of the YTC area and the percent of the total sediment delivery to streams. Simulations are for 42 years using the DHSVM-HEM model.	78
Figure 36. Illustration of the role of large storms in determining sediment yield from a small rangeland watershed in Arizona, United States.	80
Figure 37. Illustration of the role of large storms in determining sediment yield for bare plots on cropland soils in New Zealand.	81
Figure 38. Illustration of the role of large storms in determining mean annual sediment yield from four small rangeland watersheds in Arizona, United States.	82
Figure 39. Illustration of the role of large storms in determining mean annual sediment yield from all transects on the YTC.	83
Figure 40. Illustration of the data entry page for the SIMDSS. Alternatives are shown in the left-most column, and decision variables (evaluation criteria) are shown in the columns under the row labeled "Evaluation Criteria and Objectives."	86
Figure 41. Illustration of minimum, maximum, and average scores for the reference management system for firebreak roads and three alternative management systems.	88
Figure 42. Illustration of a scoring function used to score sediment yield from alternative management practices for firebreak roads. In this example less sediment yield is desirable and thus alternatives which control erosion and result in less sediment delivery to streams scores higher than those with greater amounts of sediment yield.	90

List of Tables

- Table 1. Representative or default values of the Green-Ampt infiltration parameters and HEM soil erodibility grouped by soil texture class. Default values are for bare soil. 31
- Table 2. Summary of HEM sediment yield estimates (t/ha) for a “mean” or representative hillslope profile transect at YTC. Simulations are for a silt loam soil and 10 mm of runoff. Inputs are mean and mean \pm SD for the four variables shown in the column headings. Values are the overall means for the field data and remotely sensed data are shown in each column. The resulting HEM output data are **bold** and in parentheses. 51
- Table 3. Statistical summary of transects’ segment vegetative canopy cover and ground surface cover by land use and soil texture. Note, CC% = percent vegetative canopy cover and GC% = percent ground surface cover. 54
- Table 4. Summary of mean vegetative canopy cover, CC%, and mean ground surface cover, GC%, for rocky soils and for non-rocky soils at the YTC. 55
- Table 5. Generalized Canopy Cover – Soil Erosion Condition Classes for Rocky Soils at the YTC. 62
- Table 6. Generalized Canopy Cover – Soil Erosion Condition Classes for Non-Rocky Soils at the YTC. 62
- Table 7. Sediment yield class intervals by subbasins for the YTC. Computed values of sediment yield are from the DHSVM-HEM model in units of t/ha/y. 77
- Table 8. User estimates and sources for scores in the firebreak road example. Under the conventional alternative 1.33 tons of sediment reach the adjacent stream and the cost index is 100. 89

Acronyms

AM	adaptive management
AMF	adaptive Management framework
BMP	Best Management Practice
DEM	digital elevation model
DHSVM	Distributed Hydrology Soil Vegetation Model
DoD	U.S. Department of Defense
DoE	U.S. Department of Energy
DSS	decision support system
HMS	Hanford Meteorological Station
GIS	Geographic Information System
HEM	Hillslope Erosion Model
MPRC	Multi-Purpose Range Complex
MPTR	Multi-Purpose Training Range
NRC	National Research Council
RUSLE	Revised Universal Soil Loss Equation
SD	standard deviation
SERDP	Strategic Environmental Research and Development Program
SWE	snow water equivalent
TMDL	Total Maximum Daily Load
USLE	Universal Soil Loss Equation
VTM	Virtual Transect Model
WEPP	Water Erosion Prediction Project
WMS	Web Mapping Services
YTC	Yakima Training Center

Acknowledgements

We wish acknowledge

We would like to thank the Strategic Environmental Research and Development Program (SERDP) for the financial assistance which enabled us to undertake this project. Appreciation for technical assistance is extended to Mr. Bradley Smith, Executive Director and Dr. John Hall, Sustainable Infrastructure Program Manager, and to the HydroGeoLogic, Inc., staff for their administrative assistance.

Executive Summary

Background

To ensure sustainability and adaptability in managing training operations while minimizing impacts on watersheds, the U.S. Department of Defense (DoD) needs to identify activities that contribute to non-point source pollution, and strategically locate and schedule operations. During land-based training exercises, the potential exists for extreme spatial and temporal variability in hydrologic conditions. This can directly influence the level of associated environmental impacts from non-point-source pollutants such as eroded sediment, petroleum products, and heavy metals. We are developing decision tools to provide information to articulate tradeoffs between alternative management actions and resultant impacts and/or benefits to training range or adjacent downstream water bodies. These decision tools, and the data, science, technology, and knowledge upon which they are based, are necessary to bring the best science to bear on practical decision making.

Approach

The overall approach to this project is to develop, assemble, link, and integrate the tool set for an adaptive management framework (AMF); demonstrate its use and value; and operationalize the framework for general application in arid and semi-arid regions. The site-specific demonstration is focused on managing training operations and minimizing impacts on training areas and downstream receiving waters at the Yakima Training Center (YTC) in south-central Washington State.

Results

This report presents a Geographic Information System (GIS)-based decision support framework. This framework provides the YTC stakeholders and DoD user community with the ability to plan training activities, map the erosion potential response in a system designed to be easy to use, and provide meaningful results to help formulate the decision-making process. The presented methods, tools, and designs provide a new and unique ability to incorporate a multi-modal system incorporating field data, remote sensing, geospatial modeling, hydrologic and erosion modeling, and a decision support system (DSS) linked by a GIS-based user interface. The system works to articulate the multi-objective tradeoffs of management alternatives based on stakeholder decision criteria that allow for a scientifically defensible method of evaluating alternatives for the YTC site management needs.

This report documents work completed under this project during 2003–2007. Field data have been collected on more than 100 hillslope profile transects across the YTC. These data were used to parameterize, test, and evaluate hydrologic/erosion models and to provide ground-truth data for remote sensing and smart change technology development. The Distributed Hydrology Soil Vegetation Model (DHSVM), Green-Ampt infiltration model, and the Hillslope Erosion Model (HEM) were enhanced and linked to simulate winter (along with summer) processes, water balance, runoff, and sediment yield from rangeland, roads, firebreaks, and vehicle tracks associated with training activities at the site. The models were validated successfully against

measured sediment yield from 12 sedimentation ponds within the YTC. The coupled DHSVM-HEM hydrologic and erosion models simulate the seasonal distribution of runoff and the resulting soil erosion at YTC as well as, or better than, the Revised Universal Soil Loss Equation (RUSLE) and Water Erosion Prediction Project (WEPP). The coupled DHSVM-HEM modeling system represents a new generation of runoff and erosion prediction technology heretofore unavailable to land managers at the YTC and to managers of lands hydrologically similar to the YTC.

The validated models were used with YTC hillslope profile data to develop “soil erosion condition classes” of poor, fair, good, and excellent in relation to the worst soil erosion conditions on the YTC. The classes were based upon the following criteria:

- Poor = 0 to 25% reduction in erosion
- Fair = 25 to 50% reduction in erosion
- Good = 50 to 75% reduction in erosion
- Excellent = > 75% reduction in erosion.

The soil erosion condition classes can now be used for analyses, on scales from individual subbasins to the entire YTC, evaluating existing conditions with respect to soil erosion. Because the erosion potential is analyzed on a pixel-by-pixel basis, in which each pixel is independent of another, it cannot be used to estimate total sediment yield in a subbasin under varying conditions. However, for uses where assessments of the influence of soil, vegetation, and land use on potential soil erosion are adequate, this methodology represents a new and unique decision tool for soil management on the YTC.

A complete, dynamic site-wide sediment budget was calculated, in a GIS environment, for thousands of virtual transects describing approximately 3500 subbasins, representing a new and unique technology. The resulting sediment budget represents the extensive field data transects used for model calibration and evaluation, the thousands of virtual transects derived from remote sensing databases, the thousands of subbasin sediment yield calculations using state-of-the-art simulation models, and the GIS spatial analysis and display capabilities. This modeling effort thus represents a heretofore unavailable methodology for using remote sensing and geospatial technology to parameterize distributed hydrology and soil erosion models.

A Spatial Data Viewer was developed to allow the non-GIS specialist to easily navigate and query spatial data from the site-wide sediment budget and associated vegetation and soils data. With the goal of providing a functional and easy-to-use decision environment, a simple user-interface based on Environmental Systems Research Institute’s Java-based ArcExplorer software allows for easy identification of classified sediment yield areas. In addition, the software provides an interactive query capability so the user can view the underlying database information. This database provides information such as subbasin area, total subbasin sediment yield, sediment yield by land use type, mean elevation, mean slope, soil types, mean percent

canopy, and mean percent ground cover. In addition to the basic maneuvering and query capabilities of the viewer, the user has the ability to do the following:

- Reclassify data to define more detailed sediment yield patterns
- Develop customized data queries (e.g., define subbasins with silt loam soils and a combined sediment yield > 3.2 t/ha/yr)
- Add a user's own data for overlays or access web-ready data via Web Mapping Services (WMS) (e.g., National Wetlands Inventory)
- Develop customized map layouts, and perform linear measurements.

Finally, a Spreadsheet Implemented Multi-objective Decision Support System (SIMDSS), adapted from an early standalone USDA-ARS prototype called WQDSS, was developed. The SIMDSS uses a spreadsheet environment to evaluate multiple-criteria alternative weighting into an easy-to-understand format for the end-user by providing summary statistics, graphs, and a familiar spreadsheet environment to facilitate various management scenarios. Data supporting SIMDSS can come from various sources including simulation models, measured data, and/or expert opinion to quantify decision criteria; SIMDSS provides this flexibility by utilizing a scoring function that converts numerical values into a dimensionless quantity. This built-in capability enables system users to mesh data from differing sources to arrive at the best possible decisions.

Discussion

Under a wide variety of land-use and climatic conditions and at locations around the world, studies show that large storms dominate sediment yield from experimental plots and small watersheds (e.g., Lane 2007). This project found that only 13% of the drainage area at YTC contributes nearly one third of the total sediment yield. A management philosophy that targeted, or ranked in priority, those high-sediment-yield subbasins for remediation measures, in general, would maximize return on investment on erosion control measures. Of course, some streams may be more important for a variety of reasons, and this is easily included in the prioritization for remediation.

The single largest sediment yield year (percentage of years simulated = $1/42 = 2.4\%$) produced more than 10% of total simulated sediment yield in the entire 42-year period. In addition, the four largest years produced more than 30% of the total sediment yield. Finally, the combined sediment yield from the largest half of the 42 years produced more than 90% of the total sediment yield. These simulated results are quite similar to measured data from a variety of locations throughout the globe, suggesting that the DHSVH-HEM model is preserving the property of large storm dominance of long-term or mean annual sediment yield from small watersheds.

For decades, the question of scale effects in hydrology has been a principal scientific problem. Synergistic effects of combining databases from long-term watershed monitoring programs, geospatial data acquisition and analysis technology, distributed hydrologic modeling, and targeted field data acquisition programs have resulted in a new and unique ability to simulate spatial and temporal sediment yield across a range of space-time scales. However, this has not been purely a theoretical result of synergy; it has broad practical applications. Hydrologic problems positively impacted by these new developments include the development of targeting monitoring and remediation efforts to maximize return on investment of remediation resources to that fraction of the landscape producing soil erosion and sediment yield at a much higher rate than the spatial average. Implicit in these developments is the ability to display and analyze geospatial data based on combining sound scientific modeling procedures with improved databases.

Temporal analyses and results such as shown herein also have profound implications for monitoring programs, hydrologic and hydraulic design criteria, and simulation model evaluation using extreme event simulation, within a long time series, to replicate the large storm dominance on sediment yield as observed in nature. Simulation models, which lack the ability to account for the significance of large storms in a time series, are of limited value in determining required monitoring periods, estimation of frequency distributions for event or annual sediment yields, and thus for design of hydraulic structures based on exceedance probabilities, or for evaluating management actions against typical environmental regulatory requirements,. In summary, simulation models, which do not reproduce the large storm dominance of sediment yield (e.g., Universal Soil Loss Equation [USLE]/RUSLE) significantly underestimate uncertainty of the processes producing soil erosion and sediment yield. The same is true for models that do not capture the spatial distribution of sediment yield.

Fortunately, the synergistic effects of combining databases, geospatial technology, distributed simulation modeling, and simulation models that capture the large storm dominance features on sediment yield were developed over expanded space-time scales. These synergistic effects were developed to meet the needs of managing natural resources on large military training areas such as the YTC.

1.0 Objectives

This project's two principal objectives focus on improved understanding of processes that contribute to non-point source pollution from military training activities in arid and semi-arid regions and developing and demonstrating impact assessment and decision tools for improved management. These objectives are as follows:

1. Develop an integrated set of decision tools, process models, and Geographic Information System (GIS) databases. These tools and data will be assembled as an adaptive management framework (AMF) for managing field-training activities in arid and semi-arid regions. This will minimize constraints on scheduling and implementing training exercises while ensuring protection and total maximum daily load (TMDL) compliance of watersheds and receiving water bodies.
2. Demonstrate the practical utility of the AMF and its components for managing training operation environmental impacts in arid and semi-arid regions. The adaptive implementation framework is being demonstrated at the Yakima Training Center (YTC) where Pacific Northwest National Laboratory (located within approximately 40 mi) has considerable experience, knowledge of hydrologic and biological processes, and extensive data.

2.0 Background

2.1 Problem Definition

To ensure adaptability in managing training operations while minimizing impacts on watersheds, the U.S. Department of Defense (DoD) needs to identify activities that contribute to non-point source pollution and strategically locate and schedule operations. In arid and semi-arid regions, the potential for extreme spatial and temporal variability in hydrologic conditions during land-based training exercises can directly influence the level of associated environmental impacts. These environmental impacts are a result of non-point source pollutants such as eroded sediment, petroleum products, and heavy metals. Decision tools are needed that provide information to articulate tradeoffs between alternative management actions and resultant impacts and/or benefits to training range or adjacent downstream water bodies. These decision tools, and the data, science, technology, and knowledge upon which they are based, are necessary to bring the best science to bear on practical decision making.

The DoD requires data and technologies that advance the state of knowledge and the ability to model the contributions of DoD non-point source to TMDLs. The objective of the TMDL program is attainment of ambient water quality standards through the control of both point and non-point source pollution. The National Research Council (NRC 2001) notes that related to the paucity of data available in most locations to comply with program requirements, scientific uncertainty is a reality that must be considered directly in the process.

For the TMDL program to proceed in spite of data and information limitations, the NRC recommends that TMDL employ an adaptive implementation approach. This approach calls for newly implemented plans to be reviewed periodically to determine if they are meeting intended objectives. If not, the approach should then be revised based on scientific data and information.

Adaptive implementation, as described by the NRC (2001), is the process of "...taking actions of limited scope commensurate with available data and information to continuously improve our understanding of a problem and its solutions, while at the same time making progress toward attaining a water quality standard." The notion of adaptive implementation is founded on the concepts of adaptive management (AM). Walters and Holling (1990) defines this as a systematic and rigorous, scientifically defensible program of learning from the outcomes of management actions, accommodating change, and improving management. Although generally advocated, AM has proven difficult to implement. This difficulty is in part due to the lack of readily available, widely implemented tools for resolving critical natural resource management issues (scientific methods for analyzing, understanding, and managing problems within complex and anthropogenically altered environmental systems). The NRC (1999) also discusses the need to provide resource managers the means to apply such tools (e.g., simulation models) more routinely. There remains the need for system tools to "operationalize" the AM process for comprehensive ecosystem management.

2.2 Selected R&D Activities Preceding this Project

Three soil erosion/sediment yield prediction technologies either are in use or recommended for use on military facilities. The first technology is the USLE/RUSLE soil erosion prediction technology. The USLE (Wischmeier and Smith 1978) is the simplest and historically most widely used erosion prediction technology for soil conservation. It is also the basis of the RUSLE (Renard et al. 1997). The RUSLE has been recommended for use on military facilities such as the YTC (DoE et al. 1999). The WEPP is an advanced, processes-based model designed to provide USDA agencies and their cooperators with a state-of-the-art erosion and sediment yield prediction capability. The HEM (Lane et al. 2001) is a simplified, process-based upland erosion and sediment yield model that captures the influence of spatial variability in topography, vegetative canopy cover, and ground surface cover on erosion and sediment yield from hillslopes. The HEM was documented and published online in 1998 and in print in 2001. Therefore, the HEM was not available for the DoE et al. analyses and review published in 1999.

Lane et al. (1992) summarized the development and application of erosion prediction technology in the USDA, which included models available at that time and of interest herein (i.e., USLE, RUSLE, and WEPP). This paper provided a synopsis of the USDA's experience in developing and applying soil erosion prediction technology in its research and development activities and its soil conservation programs. Over a nearly 50-year period, equations to predict soil erosion by water have been useful in developing plans for controlling soil erosion and sedimentation. As stated earlier, the USLE is the most widely known and used of the erosion prediction equations. The USLE presents a simply understood and easily applied technology that has been of immense benefit to soil conservation and land management around the world. In 1985, the USDA in cooperation with the U.S. Bureau of Land Management and several universities initiated a national project called the WEPP to develop a next generation water erosion prediction technology. The RUSLE is an update of the USLE intended to improve erosion prediction in the interim before WEPP was adopted and to provide an adjunct technology thereafter. The HEM was not generally available in 1992 and thus was not included in Lane et al. (1992).

The RUSLE procedure is a modification of the USLE to improve determination of its factor values, broaden its geographical and cropping-land-use-management bases, and to improve and update estimates of the rainfall-runoff factor and seasonal variations of the soil erodibility factor (K) due to winter processes (e.g., snow and snowmelt, freezing-thawing soil). However, Figure 3.5 on p. 96 of the RUSLE User Guide is a map of the western United States defining a line generally from the Big Bend area of Texas; through eastern New Mexico, central Colorado, Wyoming, and Montana; and, generally east of the continental divide, west of which the time-varying K values should not be used. Areas where the time-varying K values in RUSLE should not be used include all of Arizona, Utah, Idaho, California, Nevada, Oregon, Washington, and western portions of Texas, New Mexico, Colorado, Wyoming, and Montana. On p. 86 of the RUSLE User Guide it is recommended that in these areas where the time-varying K procedures should not be used, the user should estimate K as was done in the past, i.e., the USLE nomograph, soil properties, or the USLE K factor equation (Equation 3-1 in Renard et al. 1997). The limitations of the USLE, with respect to seasonal variations in soil erodibility including winter processes, in much of the West is thus carried over into the RUSLE erosion prediction technology.

The WEPP model is composed of sub-models or components to include climate, hydrology, hydraulics, plant growth, soil and management practices, as well as erosion and sediment transport processes for plot to watershed scales of applications. It is complex, process-based, and state of the art (Laflen et al. 1991b). WEPP is also based on extensive field experiments (including rainfall simulator studies) and databases (Laflen et al. 1991a). Given it is processes-based, complex, and operates in a continuous simulation mode, the WEPP model requires a great deal of input data and user expertise.

To solve the problems identified above, our (and others') research findings indicate that simulation models should possess the following general characteristics.

Process-Based

A major goal of managing military training lands is to assess the natural resource impacts of past management land-use and management practices (hind casting or assessment) and to predict consequences of future management and land-use practices on natural resources (forecasting and evaluating alternative management scenarios). To encode the ability to predict future consequences, and thus to choose among alternative natural resource management practices, the models must be process-based. Data-based or empirical models (e.g., the Universal Soil Loss Equation [USLE; Wischmeier and Smith 1978] and the Revised Universal Soil Loss Equation [RUSLE; Renard et al. 1997]) are often useful for analyzing historical data. However, because they are not based on mimicking hydrologic and sedimentation processes, the models lack predictability.

Distributed

Spatial variability in geology, topography, soils, vegetation, land use, and climate dominate hydrologic response across a range of scales. Moreover, on large complex areas there may be thousands of subbasins contributing runoff and sediment to complex stream networks. Simulation models, which incorporate distributed (rather than lumped) input of these watershed characteristics, are required to capture watershed response. Because not all of the thousands of subbasins can be monitored, distributed models are required to generalize monitoring results over a range of spatial scales.

Designed to Accept Geospatial Inputs from Remotely Sensed Data

Given the need for distributed models applicable across a range of scales, and given the inability to characterize watershed properties across thousands of sub-basins using field data, models that are designed to use remotely sensed data in conjunction with target monitoring data are required.

Continuous Simulation

Event-based models have proved very useful in flood frequency analyses and in design of hydraulic structures for a given design flood. However, to capture the dynamics of winter processes (e.g., snow accumulation and melt, rain on snow, rain on frozen ground) continuous simulation is required. Because soil moisture is critical in predicting initial conditions for warm season rainfall-runoff simulation and in predicting such properties as trafficability and low-flow water quality, continuous simulation is required in all seasons.

Compatibility of Integrated Process Models

This Project has integrated models of climate, hydrologic processes, soil erosion, and sedimentation into a coupled or linked modeling system. To enable use of common databases, help ensure system stability and robustness, and improve predictability, these components should be approximately comparable in their degree of process representation and complexity.

2.3 Application of Modeling Features in this Strategic Environmental Research and Development Program (SERDP) Project

The hydrologic modeling conducted in this project addresses directly the YTC's need to quantify erosion rates and sediment loading under alternative land uses. The complex topography, meteorology, vegetation, soils, and land-use patterns at YTC dictate the use of spatially distributed models to capture critical variability in runoff/erosion processes. The episodic nature of surface runoff and erosion in semi-arid locations such as the YTC limits the opportunity for calibration, favoring physically based models with a limited number of input parameters. We have linked two distributed, physically based models of intermediate complexity; the Distributed Hydrology Soil Vegetation Model (DHSVM) (Wigmosta et al. 1994; Stork et al. 1998; Wigmosta et al. 2002) is used to simulate runoff production and the Hillslope Erosion Model (HEM) (Lane et al. 1995b; Lane et al. 2001) is used to estimate erosion and sediment yield.

The DHSVM (<http://hydrology.pnl.gov/watershed.asp>) is a physically based distributed parameter model that provides an integrated representation of watershed processes at the spatial scale described by digital elevation model (DEM) data. The modeled landscape is divided into computational grid cells centered on DEM nodes. This characterization of topography is used to model topographic controls on absorbed shortwave radiation, precipitation, air temperature, and downslope moisture redistribution. Vegetation characteristics and soil properties assigned to each model grid cell may vary spatially throughout the watershed. In each grid cell, the modeled land surface can be composed of a combination of vegetation and soil. At each time step, the model provides simultaneous solutions to energy and water balance equations for every grid cell in the watershed. Individual grid cells are hydrologically linked through surface and subsurface flow routing. The model predicts temporal and spatial changes in hydrologic properties such as snow cover and depth, soil moisture, ground saturation, soil temperature, subsurface water movement, surface runoff, and simplified 1-D channel flow.

The HEM (<http://eisnr.tucson.ars.ag.gov/HillslopeErosionModel/>) was developed by Dr. Leonard Lane and other scientists at the United States Department of Agriculture - Agricultural Research Service (USDA-ARS) Southwest Watershed Research Center in Tucson, Arizona, United States. The HEM simulates rill and interrill erosion down a hillslope profile represented by a cascade of planer hillslope segments using an analytic solution to the coupled kinematic-wave and erosion (sediment continuity) equations for overland flow (Lane et al. 1995b). The solution to the sediment continuity equation for the case of a constant and uniform rainfall excess is integrated through time (Shirley and Lane 1978) to simulate the total sediment yield from the cascade for a given runoff event. The model requires a runoff volume per unit area and a soil-erodibility index for the entire hillslope. Input data for each of the individual segments are slope, length, slope steepness, percent vegetative canopy cover, and percent ground cover. The input data are used in parameter estimation procedures to compute the model's depth-discharge coefficient, interrill erodibility, rill erodibility, and sediment transport coefficient. The HEM calibration and validation studies were based on data from more than 2000 plot events at experimental areas

throughout the western United States (Lane et al. 2001). The parameter estimation procedures in HEM were developed from additional rainfall-simulator data collected in the western United States.

The HEM, as described above, simulates erosion and transport associated with surface runoff generated by rainfall excess (= rainfall – infiltration), but does not simulate snow accumulation and melt. This limitation makes direct application of HEM (and most other erosion models) infeasible at the YTC site, where erosion also results from rapid snowmelt. To overcome this limitation, the hydrologic and soil erosion models were linked so that the hydrologic model in essence “drives” the soil erosion model by computing surface runoff under a variety of precipitation input-soil thermal state conditions. The DHSVM simulates surface runoff generated by (1) both rainfall and snowmelt excess, (2) direct rainfall/snowmelt on saturated soils (saturation overland flow), and (3) subsurface flow returning to the ground surface (return flow). The DHSVM-simulated runoff volume per unit area for a given event is input to HEM along with a soil erodibility index, based on soil type and soil thermal state. The coupling of these two models resulted in a system that simulates continuous runoff, soil erosion, and sediment yield continuously through time including summer storms and winter processes. Thus, the linked DHSVM-HEM system provides a new continuous and spatially distributed simulation capability heretofore unavailable at the YTC.

The DHSVM-HEM linked modeling system was applied to selected watersheds containing sedimentation ponds with measurements of erosion and deposition rates. Key model parameter data such as percent vegetative cover and percent ground surface cover in each test watershed were obtained from field measurements and remote sensing along with segment lengths and slopes derived from GIS-based DEM terrain analysis. The DHSVM-HEM system simulated sediment yields were compared with sedimentation pond measurements.

2.4 The Yakima Test Site

The YTC is a 132,435-ha (327,000-acre) facility located in the arid, high desert region of south-central Washington (Figure 1). The installation lies within the core of the largest remaining contiguous block of shrub-steppe in Washington State and contains several tributaries that flow into 303(d) listed streams, including the Yakima River. Elevated water temperatures and increased sediment loads have contributed to a significant loss of usable habitat for Endangered Species Act-listed species in large portions of these receiving streams. Estimation of current mobile sediment quantities and sources is a major concern for the YTC, and a high-priority concern for DoD lands. Most erosion (and sediment transport/yield) occurs in the YTC during extreme events of short duration, often associated with rapid rain-induced snowmelt. Erosion potential can be further enhanced following natural or man-induced range fires. It is infeasible to make management decisions based entirely on empirical data, given the infrequent nature of these events and the need to consider alternative land management scenarios. For ecosystem management at the YTC, an adaptive combination of data collection and distributed modeling is required to manage military operations properly and minimize environmental impacts.

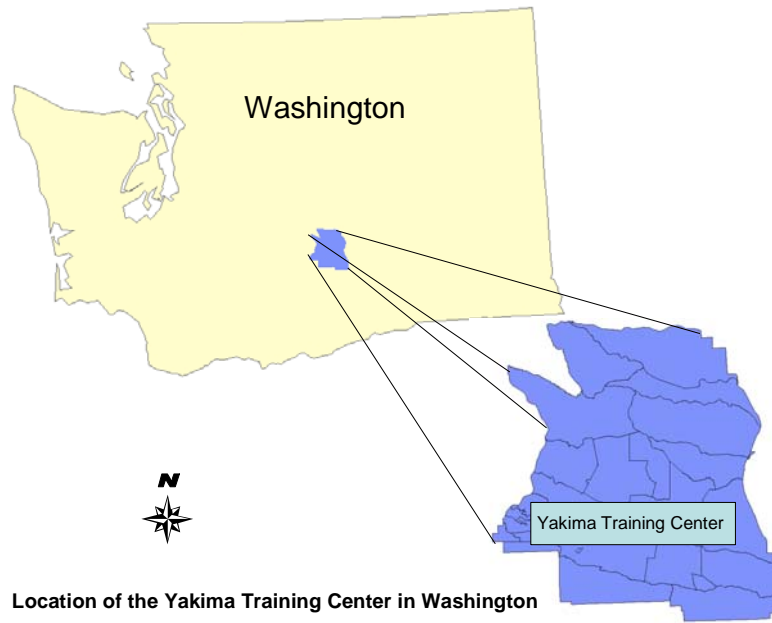


Figure 1. A map of the YTC showing its location in south-central Washington.

3.0 Materials and Methods

The overall approach to this project is to: develop, assemble, link and integrate the tool set for the adaptive management framework; demonstrate its use and value; and operationalize the framework for general application in arid and semiarid regions. The site-specific demonstration (Section 4.0) is focused on management of training operations and ways to minimize impacts to training areas and downstream receiving waters at the Yakima Training Center in south-central Washington.

3.1 Adaptive Management Framework

A conceptual model of management alternatives at the YTC was developed to guide the framework design, user interface and decision support system (DSS), along with the associated data collection and modeling programs. The YTC management alternatives are discussed below, as is the SERDP framework design, user interface, and DSS, respectively.

3.1.1 Management Alternatives at the Yakima Training Center

The mission of the YTC is to provide a variety of field training opportunities that develop and maintain the combat readiness of military units. Environmental management at YTC helps ensure that training activities are not constrained due to (1) environmental degradation that may reduce the ability to support training activities or (2) restrictions on use imposed by state and/or Federal agencies (for instance, TMDLs). Environmental degradation may reduce access to training areas and reduce the types, quantity, and quality of training activities that the YTC can support. Independent of any regulatory actions or penalties, environmental degradation directly undermines the ability of YTC to support its mission. A vision toward long-term stewardship of the YTC is critical to ensure the YTC will continue to support its mission.

3.1.2 Training Activities

As a training facility, the YTC provides the opportunity, facilities, and support for military units, including both active and reserve component forces, to enhance troop readiness and train for mobilization and post mobilization exercises. All branches of the armed forces and allied military units train at YTC to sustain and improve unit readiness for both wartime and contingency operations.

Training includes individual and crew gunnery, small arms qualification, engineer and communications training, and collective (unit) maneuver and live fire training. Military units use the YTC to train Brigade, Battalion, Company, Platoon, and Crew gunnery and maneuver. The YTC is also used for air assaults, air drops (personnel and equipment), and special operations gunnery and maneuver. Availability of the Multi-Purpose Range Complex (MPRC), artillery-firing points adjacent to ground maneuver corridors, the Multi-Purpose Training Range (MPTR), and other ranges provide opportunities for multiple live fire training iterations.

Twenty-six developed ranges at the YTC are used for a variety of live fire training activities. Sixteen training areas, ranges, and impact areas are contained within ten watershed complexes.

Use of training land is scheduled based upon historical use, current military requirements, and environmental practices and policies. As the mission continues to evolve, land-use patterns at the YTC may change.

To aid in resource management, the YTC is divided into five land-use zones (Figure 2). These planning designations identify allowable military training activities and acceptable levels of impact to resources thereby maximizing military training opportunities, while simultaneously safeguarding resources. Management and land-use activities are undertaken within the context of the zone designation.

The following are descriptions of these land-use zone designations (YTC 2002):

- **Zone 1 Land Bank.** This zone covers 10,000 ac (3%) of the YTC. It is managed for significant and sensitive natural and/or cultural resources (e.g., wetlands, riparian areas, archeological, or sacred sites). Most forms of training, including all tracked and wheeled vehicle use, digging and bivouacking are prohibited. Protection and restoration of these sites is a primary objective.
- **Zone 2 Conservation.** This zone is the Sage Grouse Protection Area and covers 44,320 ac (13.5%) of the YTC. Most forms of training are permitted within these areas, but are highly controlled. Digging and bivouacking activities are not permitted within this zone. Army rest/rotation training regimes and restoration or rehabilitation activities are designed to maintain or enhance these areas.
- **Zone 3 General Use.** This zone covers 245,914 ac (75%) of the YTC and includes the MPRC, MPTR, Cantonment Area and all the primary training and vehicle maneuver areas. With the exception of the Cantonment Area and portions of the MPRC and MPTR, all forms of training are permitted, including bivouac and digging activity, as long as surface water quality, soil stabilization, and potential long-term habitat reservoirs are maintained.
- **Zone 4 High Use.** This zone covers 7742 ac (2.4%) of the YTC. It accommodates heavy use and high-impact activities, such as Brigade Support Areas and gravel pits. Reclamation or remediation activities are used to ensure protection of soil and water resources.
- **Zone 5 Impact Areas.** This zone covers 19,126 ac (5.8%) of the YTC. Included are impact and dud areas and the Selah Airstrip. Due to unexploded ordnance in impact and dud areas, these sites are off limits. Due to the hazardous nature of these areas, on-the-ground management of these sites is not feasible other than the protection of soil and water resources. These sites are however included in remotely sensed data collection efforts including satellite imagery and aerial photographs.

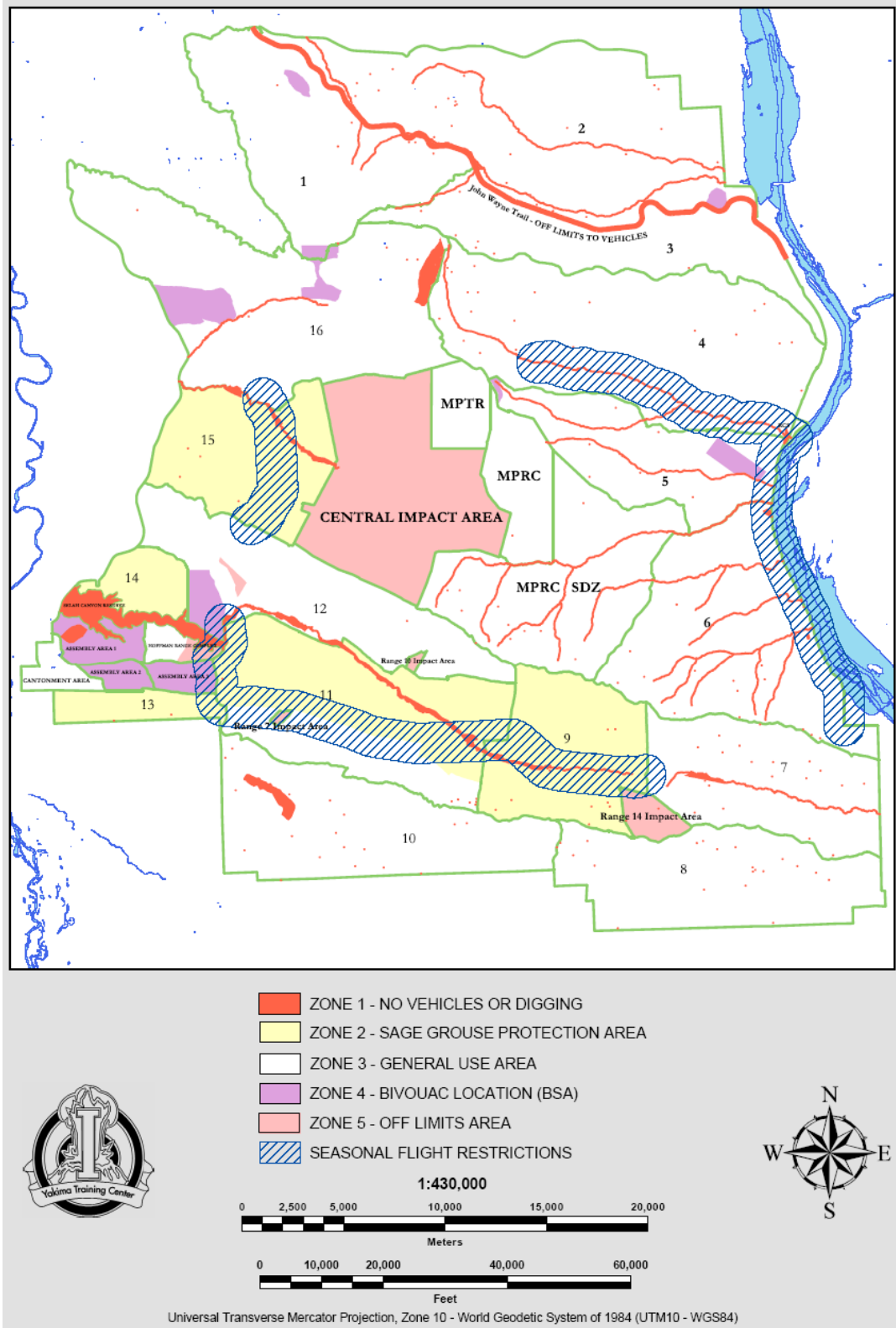


Figure 2. Land-use zones at the YTC (YTC 2002).

In addition to use policies, other factors effect the evaluation of military training alternatives such as recent or forecast weather events, range fire or other conditions that exacerbate the potential for short- or long-term environmental disturbance. Other management and land-use actions that must also be considered in conjunction with military actions are road construction and closure, recreation, cultural resource management, and fire management.

3.1.3 Environmental Management

Environmental management at the YTC helps ensure that training activities are not constrained due to environmental degradation that may reduce the ability to support training activities. By maintaining a proactive and positive relationship with regulators, such as Washington State Department of Ecology, YTC environmental managers have reduced the risk that training operation constraints will be imposed by outside agencies. The willingness of YTC staff to exceed requirements established by regulators reflects the considerable indirect costs associated with restrictions being imposed on training activities. This positive relationship allows the YTC more flexibility and quicker responses from those agencies with environmental oversight.

The YTC employs an ecosystem approach to environmental management that consists of a combined coarse, mid- and fine scale approach. The coarse scale applies to the installation as a whole, the mid-scale to watersheds, and the fine-scale to specific projects, species, or resource management activities. The Ecosystem Management process at YTC is diagrammed in Figure 3 (YTC 2002). This includes identifying installation-wide and watershed specific resource goals and objectives, developing thresholds for individual resources to measure their condition, and applying management actions (through Management Action Descriptions) to improve the resource. If thresholds are not met, the reason is identified and management actions are revised or objectives evaluated to determine their validity (YTC 2002). Throughout this process, YTC will continue to implement Best Management Practices (BMPs). As appropriate thresholds are determined and implemented, BMPs may be modified, added, or eliminated.

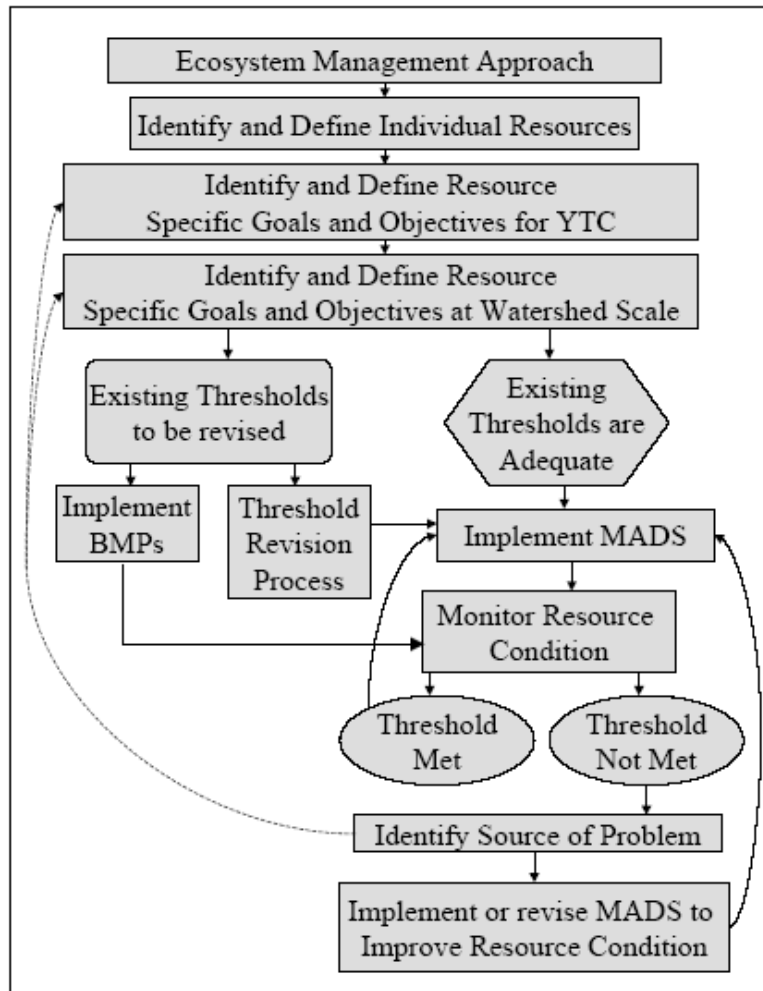


Figure 3. YTC Management Plan decision flow diagram (YTC 2002).

Site-specific experience and expertise have been developed to maintain natural and cultural resources. The YTC has an established array of BMPs to limit erosion and other impacts that have specific attributes including costs, schedule requirements, and impact on land availability. Examples include:

- Training management:
 - Locate and map areas of sufficient soil moisture to limit specific activities.
 - Pre-planning with Using Units to balance mission requirements with minimizing disturbance.
 - Rotate training areas to provide for recovery of vegetation and soils resources.
 - Prioritize areas for types and intensity of training.
 - Locate and map critical habitat areas.

- Rangeland vegetation management:
 - Re-vegetate areas with appropriate native or desirable non-native grass and forb species where military training has affected vegetation.

- Prioritize types of plants for revegetation in specific areas.
- Prioritize timing of revegetation efforts.
- Control exotic plants species.
- Road Management:
 - Improve existing roads to reduce erosion.
 - Redesign existing roads, culvert, and stream crossings to reduce erosion.
 - Continue closures of steep roads, roads adjacent to streams, or those not maintained to reduce associated soil loss.
 - Improve existing roads to reduce time to reach remote training sites.
 - Construct new roads to improve traffic capacity (including access for fire suppression).
- Rangeland fire management:
 - Alter the density and location of firebreaks to reduce erosion.
 - Prioritize areas for specific types of training activities to minimize fire risk.
 - Selective use of fire management to control rangeland fuel levels.
 - During the fire season, schedule live-fire to avoid high temperature and low humidity times of the day.
- Support for ongoing AM:
 - Continue to implement and revise the Land Condition Trend Analysis monitoring protocols that provide soil resource data.
 - Continue to implement and revise water quality monitoring protocols to evaluate BMP effectiveness and needs.
 - Implement Watershed Assessment to identify issues related to soil erosion and function.

Managers need to know what species, communities, and ecosystems occur in an area to focus management objectives on the most critical components of the system to facilitate management planning, analysis, and decision making (YTC 2002). By focusing on the most critical components, managers streamline planning and clarify objectives. Managers identify landscape and ecosystem elements (compositional, structural, or functional) that are essential for conservation and management of cultural and natural resources. Individual resources within the landscape including soils and geology, water, upland vegetation, riparian and wetland areas, fish and wildlife, cultural resources, and outdoor recreation act, or are acted upon, by landscape-level processes and functions. The YTC uses several elements to accomplish individual resource management including (YTC 2002):

Developing goals that represent the desired condition of a resource:

- Determining objectives (incremental steps) used to meet resource goals.
- Implementing management strategies.
- Monitoring effectiveness of management actions.

- Determining and applying thresholds to monitor whether management strategies are successfully reaching resource goals.
- Applying AM.

The relatively small number of staff in the YTC environmental management unit allows decisions about the allocation and scheduling of environmental management resources to be made with the active participation of the staff that will be carrying out the associated activities. The YTC management encourages innovative activities to maintain and restore proper environmental conditions. Before funding is provided to support a demonstration project of an innovative environmental management approach, staff must estimate the probable benefits that could be achieved if the approach proves to be successful at the demonstration plot scale and was then applied to some or all of the YTC. Benefits can be estimated in a variety of metrics, of which one may be annualized cost reduction. Benefits can also be expressed in other non-monetary units, such as: the expected number of lost training days due to rangeland fires; the reduction of the likelihood of runoff exceeding water quality standards; increase of allowable traffic speeds on certain undeveloped roads. Communicating the tradeoffs between such incommensurable benefits to staff and management is a key service provided by the AMF for decision support being developed under this project.

3.2 The Adaptive Management Framework (SERDP Project, SI-1340)

The framework was designed to encompass, complement, interface, and improve the environmental management activities described in Figure 3. The adaptive combination of methods employed by this project will improve the “Monitor Resource Condition” activities conducted by YTC staff, and add an improved scientific basis to the decision process “Threshold Met/Threshold Not Met.” The framework integrates field work, remote sensing, geospatial modeling, hydrologic modeling, and scientific interpretations and expert judgment together in a decision support component that will provide a repeatable scientific basis for decision making required to implement the management activities illustrated in Figure 3.

Restrictions on training activities for environmental management must be balanced against the YTC’s training mission. Ultimately, the YTC Commander is responsible for deciding on the optimal balance of environmental management and training activities. By clearly communicating the environmental and training tradeoffs to the commander, YTC’s environmental managers can provide a clear and defensible basis for their requests for resources.

3.2.1 Framework Design

An AM system, in the context of natural resources management, is adopting a management plan that typically integrates monitoring, databases, simulation modeling, decision theory, and expert judgment to evaluate management alternatives and adapt them as necessary to continually improve the management of natural resources. The defining characteristic of AM is learning, and subsequently adapting, to improve as you manage. Thus, AM is a methodology between “trial and error,” wherein different management plans are tried until a “good one” is found and inflexible management plans, i.e., the infamous 5-year plans of the old centrally planned economies.

Problems suitable for AM have several key elements or characteristics as listed below:

- The problems are large and complex. Because many stakeholders are involved, a multi-objective approach is required.
- There is a mandate for action. The stakeholders (clients, regulators, public, etc.) recognize the problem and want action and progress toward solutions.
- There are high levels of uncertainty (e.g., highly variable weather, spatial variations in land use, sparse or missing data).
- Decisions, actions, evaluations, and adaptations are all documented.
- Management actions are measurable and testable so they can be evaluated.
- Decisions are open to re-evaluation.
- Communication: good science and common sense.

AM is flexible and as new things are learned, alternative land-management practices are adopted. Contrasted with the inflexible plan (one way) and the trial and error plan (wandering around and improving by the luck of the draw), AM seeks to improve by learning as each alternative management action is evaluated.

This framework was designed for the SERDP Project SI-1340 to develop an AMF for improved management of military training lands (emphasizing soil and water problems for sustainability of training lands). This framework is being implemented. Our example application is the YTC with emphasis on training area rehabilitation alternatives (e.g., current practices, rotation of training areas, and revegetation), road management alternatives (e.g., current, improve existing roads, redesign roads and crossings, and remove some existing roads), and fire break roads (e.g., current, improved turnouts or water bars, improved crossings, and herbicides for weed control).

3.2.2 Scope and Limitations

The concepts and component integration described herein have broader applications to arid and semi-arid areas. For specific illustrative purposes and to provide a specific example application, this document is limited to the YTC. Most runoff and erosion occurs in the YTC during extreme events of short duration, often associated with rapid rain-induced snowmelt over frozen or partially frozen soils. The surface runoff and erosion phenomena typically occur during a discrete period. They can be modeled with acceptable accuracy using efficient, physically based storm event models (i.e., Green-Ampt Infiltration model for runoff and HEM for erosion). However, accurate representation of snow accumulation/melt and soil temperature requires the use of more complex, computationally and data intensive continuous simulation models such as DHSVM that track water and energy balances in time and space.

3.2.3 Overview of the Framework

A schematic overview of the AM process for this project is shown in Figure 4. Beginning in the upper left-hand corner of Figure 4, the training site is subject to natural inputs (e.g., weather and biological activity) and anthropogenic inputs (e.g., land-management and training activities). During operation and management of the training site, monitoring data and observations are collected. The box in the lower left-hand corner shows that the site data and observations go into databases. These databases allow parameterization of simulation models that are used to help interpret the data and provide a predictive capability. In the lower right-hand corner, the observations, data, simulation model results, and expert judgment are used for interpretations and analyses with respect to site operations and management plans. The decision box in the right-hand portion of Figure 4 represents the processes of comparison, analyses, and decision making related to judging whether current management plans and operations are meeting site objectives. If the decision is yes, the current management practices and the overall evaluation process continue. However, if the decision is no, then a new alternative management strategy is adopted and implemented, and the site management plan is adjusted to reflect the new practices. Databases, simulation models, and the DSS aid in developing a new management plan by evaluating alternative changes to the current plan, and thereby helping to move the best plan forward. Then, the new management practices and the overall evaluation process continue. Ideally, continued operations, monitoring, analyses, and decisions on meeting the management plan objectives result in selection of a series of alternative management practices that continually improve natural resources management.

Conceptual Model of Adaptive Management & Role of Decision Support Systems (DSS)

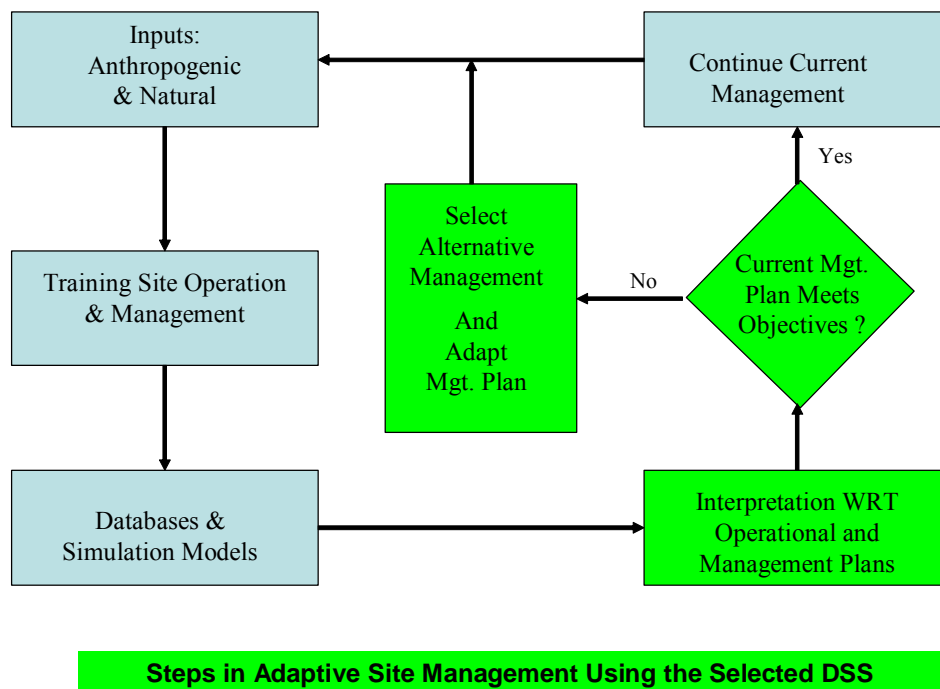


Figure 4. Schematic overview of the AMF for SERDP Project SI-1340.

Role of Monitoring in AM: Monitoring as defined herein is composed of observations, field data collection, and collection of remote sensing data and organizing them into databases for interpretation; these are key elements in AM.

Role of Databases in AM: Statistical evaluations, trend analyses, and professional judgment of the monitoring databases provide a picture of site operations by showing how the site is responding to them and the natural inputs. The databases resulting from monitoring also are used to initialize and parameterize simulation models used to interpret the data further and to make predictions of future site performance (i.e., water balance, soil erosion, etc.).

Role of Simulation Modeling in AM: Simulation models are used to interpret the data further and to make predictions of future site performance (i.e., water balance, soil erosion, etc.). Simulation models also provide predicted time series of key variables upon which management decisions are made (decision variables).

Role of DSS in AM: DSSs are used to evaluate the existing (conventional) management practices and proposed alternatives using decision variables, databases, and expert opinion and to compare them with respect to their performance in reaching site management objectives. A DSS is an integrator of information from observations, data, and our best science as represented by the simulation and decision models, expert judgment and opinions, and our ability to bring them together to assist the decision maker. As such, the DSS is one of the most complex and important components of an AM system as it is the principal way to bring our best science to bear on decision making.

Role of Management Plans and Objectives in AM: Site management plans and their objectives in evaluating, improving, and sustaining natural resources drive AM planning and operations. In this role, they provide the basis for all steps (shown schematically in Figure 4).

3.2.4 Adaptive Management System for a Military Training Site

As stated earlier, our example application is the YTC with emphasis on training area rehabilitation alternatives (e.g., current practices, rotation of training areas, and revegetation), road management alternatives (e.g., improve existing roads, redesign roads and crossings, remove some existing roads), and firebreak roads (e.g., improved turnouts or water bars, improved crossings, and herbicides for weed control).

Primary simulation modeling emphasis herein is on the hydrology and soil erosion/sediment yield aspects of site performance with other decision variables (metrics related to wildlife habitat, operational costs, description of management practices, and suitability of practices/decisions with respect to Army and site policies and constraints) to come from observations, databases, expert judgment, and plans.

4.0 Results and Accomplishments

The results and accomplishments described here are directly related to the Objectives listed in Section 3. However, for continuity and a clearer presentation, objectives are tracked through development and then to applications at the YTC. This section begins with an analysis of hydrologic conditions at the YTC, followed by the development and testing of the coupled DHSVM-HEM runoff-erosion model (Sections 4.2 and 4.3). The development and testing of remote sensing technologies used for process model input and to derive soil erosion condition classes is presented in Sections 4.5 and 4.6. Development and evaluation of a dynamic site wide sediment budget is presented in Sections 4.7 and 4.8, including discussion of GIS databases and their integration with process models and the AMF (described in Section 3.2). The Section concludes with a discussion of the spreadsheet DSS.

4.1 Hydrologic Analysis of the Yakima Training Center

Environmental degradation through soil erosion and transport is a major concern of resource managers, including the DoD, which oversees millions of hectares at sites distributed throughout the United States. Geology, topography, soil characteristics, vegetation, and climate interact in a complex manner to determine the types, intensities, and locations of runoff production and the associated soil erosion and transport of sediments. The locations and magnitude of active erosion and transport will change in space and time depending on hydrologic conditions. Natural or operationally induced changes to the landscape will alter the hydrologic response across a range of scales from a point to a drainage basin. Prediction of the resulting changes in runoff production, erosion, and sediment transport requires an accurate, explicit representation of the spatial and temporal variations in hydrologic processes, as well as the relationships between local site hydrology, topography, soils, vegetation, climate, and land use. The need for predictability under future conditions requires process representation within the models and incorporation of site-specific conditions in estimation of model parameter values (see, for example, Clark et al. 2006 and Lane and Wigmosta 2006).

This project developed and employed a coupled hydrologic-erosion model and targeted field data collection program to quantify erosion rates and sediment loading in arid regions under alternative land uses. The methodology is illustrated at the YTC in south-central Washington, United States. The primary water quality concern at the YTC is the introduction of fine sediment into streams and discharge to the Yakima and Columbia Rivers (YTC CNRMP 2002). Estimation of current mobile sediment quantities and sources is a major concern for the YTC, and a high-priority concern for DoD lands. Most erosion (and sediment transport/yield) occurs in the YTC during extreme events of short duration, often associated with rapid rain-induced snowmelt on frozen soil. Erosion potential can be further enhanced following natural or man-induced range fires. Infrequent runoff events have been monitored resulting in sporadic data that are difficult to interpret, particularly whether changes in water quality are due to management practices or natural processes associated with arid land hydrology (YTC CNRMP 2002). It is infeasible to make management decisions based entirely on empirical data, given the infrequent nature of these events and the need to consider alternative land-management scenarios.

The complex topography, meteorology, vegetation, soils, and land-use patterns at the YTC are typical of many arid regions and dictate the use of spatially distributed models to capture critical variability in runoff/erosion processes. The episodic nature of surface runoff and erosion in these locations limits the opportunity for calibration, favoring physically based models with a limited number of input parameters. We have linked and enhanced two distributed, physically based models of intermediate complexity; the DHSVM (Wigmosta et al. 1994; Storck et al. 1998; Wigmosta et al. 2002) is used to simulate runoff production and the HEM (Lane et al. 1995b; Lane et al. 2001) is used to estimate erosion and sediment yield. The coupled model was evaluated for its ability to predict long-term sediment yield using measurements from 12 sedimentation ponds at the YTC that receive runoff from areas subject to a ranges of operations and activities. Model results were also compared to results from the RUSLE (Renard et al. 1997) and the Water Erosion Prediction Project (WEPP) (Laflen et al. 1991b) models.

The mission of the YTC is to provide a variety of field training opportunities that develop and maintain the combat readiness of military units. Environmental management at the YTC helps ensure that training activities are not constrained due to environmental degradation that may reduce the ability to support training activities or restrictions on use imposed by state and/or Federal agencies (e.g., TMDLs). Independent of any regulatory actions or penalties, environmental degradation directly undermines the ability of YTC to support its mission.

4.1.1 Environmental Setting

More than 97,605 ha (241,000 ac) of the YTC's 132,435-ha (327,000-acre) land area are dominated by big sagebrush (*Artemisia tridentata*), three tip sagebrush (*Artemisia tripartita*), and stiff sagebrush (*Artemisia rigida*) plant communities (YTC CNRMP 2002). Soils at the YTC are mostly shallow light silt loams that are fragile and erode easily (YTC CNRMP 2002). Elevations vary from about 150 m (500 ft) at the banks of the Columbia River to an elevation of 1,277 m (4,191 ft) along Yakima Ridge in the southeast portion of the YTC. Ridges generally range from 900–1,220 m (3,000–4,000 ft) in elevation with slopes varying from 8–60%.

Data collected at weather stations on the YTC between 1984 and 2000 indicate variability across the installation with annual average precipitation ranging from a high of 241 mm (9.5 in.) to a low of 160 mm (6.3 in.) The average across YTC was 190 mm (7.5 in.) of precipitation, with most accumulating in the months of October through May (YTC CNRMP 2002). The YTC receives a large portion of its annual precipitation in the form of snow. While no data have been collected at the YTC to monitor annual snow depth accumulations, data from monitoring stations at Yakima, Ellensburg, Priest Rapids, and Hanford reflect conditions at the YTC (see Figure 5). Annual average accumulations at neighboring sites are 594 mm (23.4 in.) at Yakima, 729 mm (28.7 in.) at Ellensburg, 147 mm (5.8 in.) at Priest Rapids, and 373 mm (14.7 in.) at the Hanford Meteorological Station (HMS). Monthly average minimum daily temperatures remain below freezing November through February at these four locations, while average maximum daily temperatures are above freezing throughout the year. This results in the episodic occurrence of frozen soils during cold snaps.

4.1.2 Runoff Production

Four active stream gauging stations at the YTC record discharge, turbidity, temperature, and total suspended solids. However, they have received little runoff during their short period of record, making it difficult to quantify runoff processes at the YTC or calibrate the hydrological models. Therefore, a review of active and historic USGS stream gauging stations was made to identify stations with relatively long records, in locations subject to climatic and hydrologic conditions similar to the YTC. No active stations met all these criteria; however, five historic stations were identified, including one (Selah Creek Tributary) that was located within the YTC boundary (Figure 5).

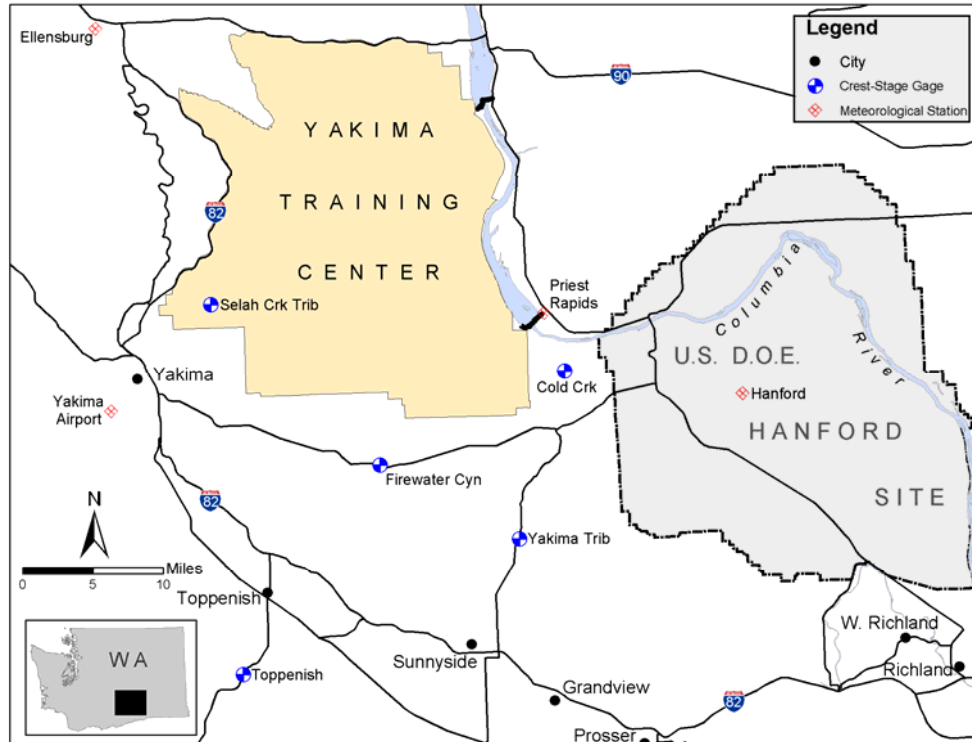


Figure 5. Locations of five historic crest-stage gages and four meteorological stations relative to the YTC boundary.

A total of 84 years of annual instantaneous peak flows were recorded at the five crest-stage stations. As expected, runoff is episodic in this arid region with streamflow occurring in about half the years. Most of the annual peak flows, as well as the highest flow rates, occurred during the winter. An analysis of local meteorological records indicates they are likely the result of rain-on-snow over frozen soils. However, some peak flows also result from summer thunderstorms, so it was necessary to address runoff production throughout the year, which requires the use of a continuous simulation model. An example of the seasonal distribution of peak flows is presented in Figure 6.

84 Years of Peak Annual Flow by Month for 5 Stations On or Near the YTC

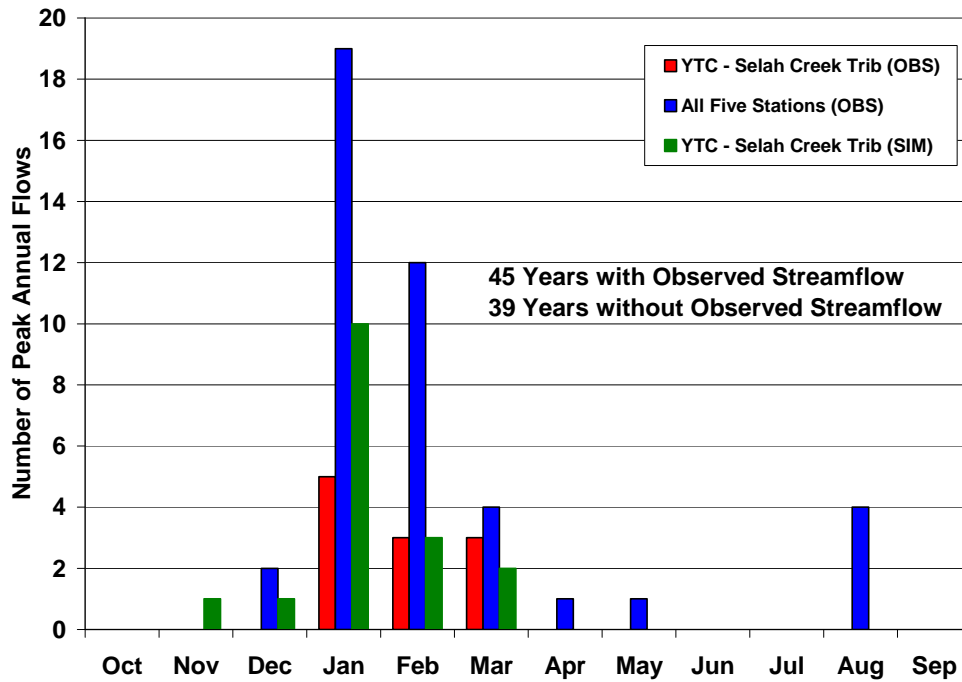


Figure 6. Seasonal distribution of observed and simulated annual peak flows in the YTC vicinity. The simulation results are discussed in a later section of the paper.

4.1.3 Sedimentation Ponds

Twelve sedimentation ponds are located within the YTC (Figure 7) that receive runoff from areas subject to a range of operations and activities. Although some of these ponds collect sediment from lightly used areas at or near the background rate, other ponds are in areas subject to heavy use with unimproved roads and firebreaks. The ponds were installed in 1984 and surveyed in 1985, 1986, 1990, and 1994. These ponds provide critical information on soil erosion as a function of both environmental conditions such as natural topography, soils, vegetation, and climate, as well as the type and intensity of site training and operations. These ponds consist of small earthen dams, which trap water and sediment as they flow down from the hillsides above the basins. The basins slow the runoff to a speed that allows the suspended sediment to deposit in the basin. The basins are full only after runoff has occurred, and they dry up quickly. This makes it easy to measure the volume of sediment that has been deposited in the basin, referred to here as sediment yield.

**Yakima Training Center
Training Area Boundaries and Sediment Ponds**

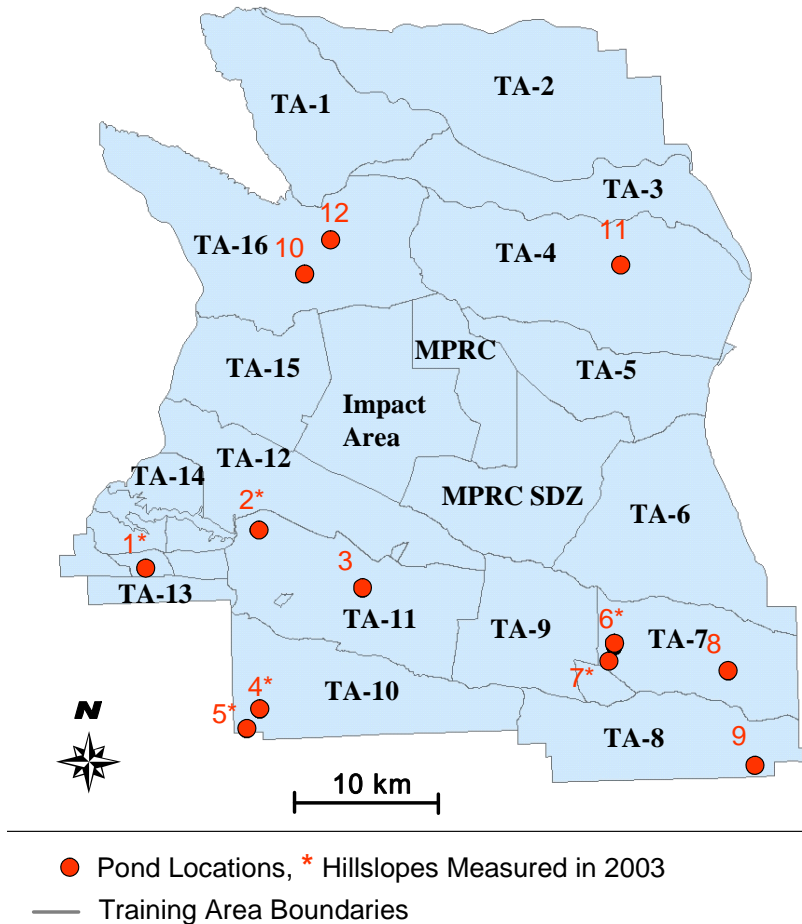


Figure 7. A map of the YTC showing training areas and pond locations. Hillslope measurements were taken on pond watersheds during April–May 2003, and these are marked with an asterisk. Measurements on the remaining ponds were taken in May 2004.

4.2 Enhancements to the Distributed Hydrology Soil Vegetation Model

The DHSVM (Wigmosta et al. 1994, 2002; Storck et al. 1998) is a physically based distributed parameter model that provides an integrated representation of watershed processes at the spatial scale described by DEM data. The modeled landscape is divided into computational grid cells centered on DEM nodes. This characterization of topography is used to model topographic controls on absorbed shortwave radiation, precipitation, air temperature, and downslope moisture redistribution. Vegetation characteristics and soil properties are assigned to each model grid cell and may vary spatially throughout the basin. In each grid cell, the modeled land surface can be composed of a combination of vegetation and soil. At each time step, the model provides simultaneous solutions to energy and water balance equations for every grid cell in the watershed. Individual grid cells are hydrologically linked through surface and subsurface flow routing. The model predicts temporal and spatial changes in hydrologic properties such as snow

cover and depth, soil moisture, ground saturation, soil temperature, subsurface water movement, surface runoff, and simplified 1-D channel flow. The DHSVM was used to provide a time series of surface runoff volumes to the HEM. Key components of the model used to provide this information are described below.

4.2.1 Snow Accumulation and Melt

The snowpack is modeled as two layers: a thin surface layer and a (generally) deeper pack layer. Energy exchange between the atmosphere, overstory canopy, and snowpack occurs only with the surface layer. The energy balance of the surface layer expressed in forward finite difference form over the model time step (Δt) is

$$W^{t+\Delta t}T_s^{t+\Delta t} - W^tT_s^t = \frac{\Delta t}{\rho_w c_s} (Q_r + Q_s + Q_e + Q_p + Q_m) \quad (1)$$

Where:

c_s is the specific heat of ice

ρ_w is the density of water

W is the water equivalent of the snowpack surface layer

T_s is the temperature of the surface layer

Q_r is the net radiation flux

Q_s is the sensible heat flux

Q_e is the latent heat flux

Q_p is the energy flux given to the snowpack via rain or snow

Q_m is the energy flux given to the pack due to liquid water refreezing or taken from the pack during melt. Energy fluxes into the surface layer are defined as positive.

The snow accumulation and melt component of DHSVM were tested for use in arid regions using 42 years of hourly data collected at the HMS (Figure 5), which has climatic conditions similar to the YTC. The DHSVM simulated hourly snow water equivalent (SWE) correlates well with daily HMS snow depth measurements (SWE is not measured at the HMS). Typical results are presented in Figure 8 for a six-year period that includes the greatest measured annual snowfall on record (Water Year 1993) and the highest month on record (December 1996 in Water Year 1997), as well as years with little and moderate snowfall. An exact agreement is not expected because SWE is compared to snow depth (the snow depth to water equivalent ratio is typically between 2:1 and 10:1).

The presence or absence of snow cover influences the occurrence of interrill erosion. DHSVM correctly simulated the presence or absence of snow cover 92% of the time during the winter months of November–March. Results for individual years were generally greater than 80%, typically above 90%, indicating an excellent ability to model the presence or absence of snow cover.

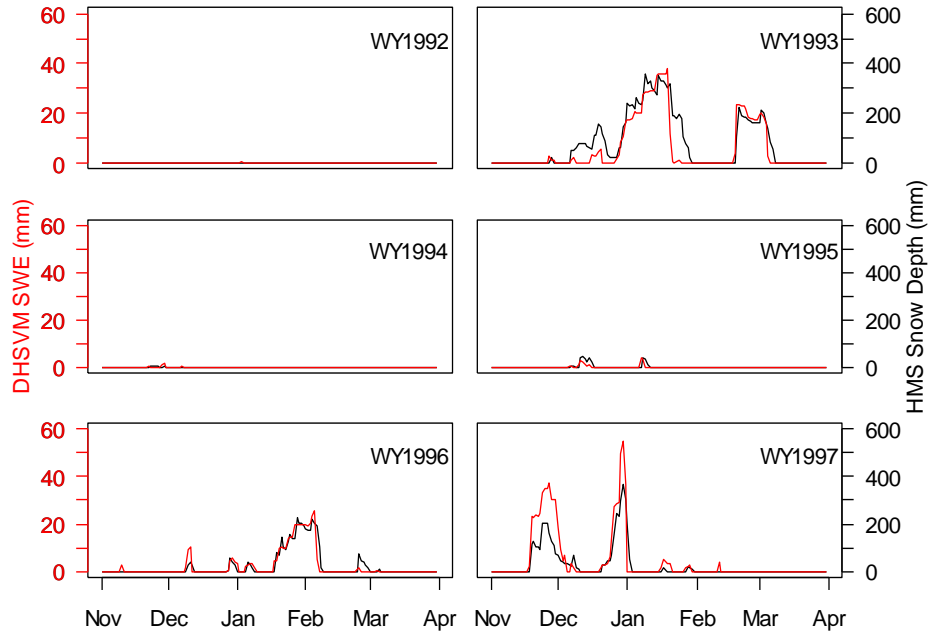


Figure 8. DHSVM-simulated hourly snow water equivalent (red) vs. HMS daily-observed snow cover for the winters of Water Years 1992–1997.

4.2.2 Surface Soil Temperature

A relatively simple frozen soil algorithm for DHSVM was tested using 42 years of hourly soil temperature data from the HMS

$$T_s^t = T_s^{t-\Delta t} + w(T_a^t - T_s^{t-\Delta t}) \quad (2)$$

Where:

T_s (°C) is the near-surface soil temperature

T_a (°C) is the air temperature, w is a weighting coefficient, and t and $t - \Delta t$ represent the current and previous time step, respectively.

To account for the insulating effects of snow cover, if T_a is greater than zero, it is taken equal to zero in (2) when snow is on the ground. The near-surface soil is assumed frozen when $T_s \leq 0$.

With a weighting coefficient of 0.4, the model predicting the correct soil state (either frozen or thawed) 87% of the time (Figure 9). This accuracy is probably well within the current ability to prescribe meteorological conditions across most locations.

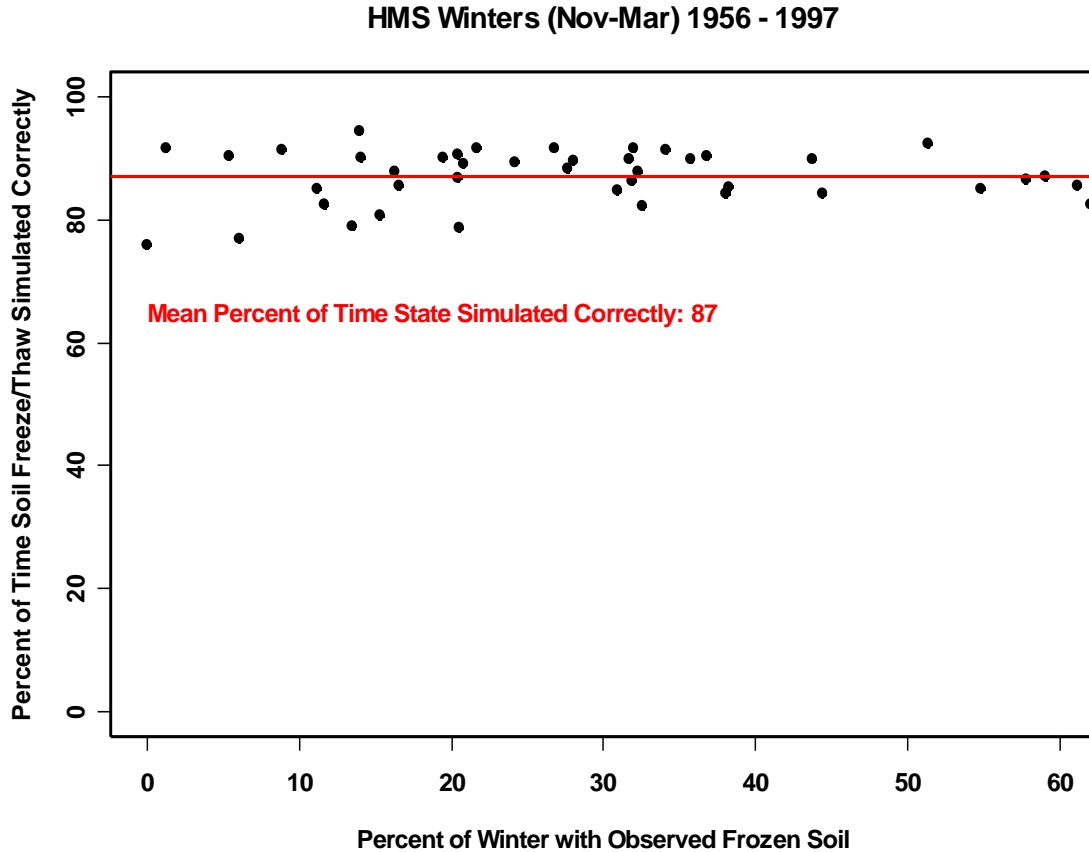


Figure 9. Percent of time the model predicted the correct hourly soil thermal state vs. percent of the winter (Nov-Mar) with observed frozen soil. Each dot represents a single winter.

4.2.3 Green-Ampt Infiltration

Soil infiltration is modeled using the Green-Ampt approach. The Green-Ampt parameters used are based on generalized soil texture–hydraulic properties derived by Rawls et al. (1982) and specific values for use in this approach were presented by Stone et al. (1992). The Green-Ampt infiltration equation can be written as:

$$f = K_s + K_s \frac{N_s}{F} \quad (3)$$

Where:

f = infiltration rate (mm/hr)

K_s = effective saturated hydraulic conductivity (mm/hr)

N_s = effective matric potential (mm)

F = cumulative infiltration (mm). Also, the effective matric potential is defined in terms of the soil porosity, ϕ (dimensionless), average potential across the wetting front, ψ (mm), and the relative effective soil saturation, S_e (dimensionless, $0 \leq S_e \leq 1$).

In equation form:

$$N_s = \psi(1 - S_e)\phi \quad (4)$$

The effective saturation is defined as the ratio of the absolute water content of the soil to the effective porosity. Therefore, oven dry soil has a S_e value of 0.0 and when the soil is saturated to the effective porosity, $S_e = 1.0$. Default values of the Green-Ampt infiltration parameters used in this study are summarized in Table 1.

Table 1. Representative or default values of the Green-Ampt infiltration parameters and HEM soil erodibility grouped by soil texture class. Default values are for bare soil.

Soil Texture	K_s (mm/h)	ϕ	ψ	S_e		Erodibility ¹
				(-1/3 bar)	(-15 bar)	
Sand	118.	0.40	49.	0.22	0.08	--
Loamy Sand	30.	0.40	63.	0.30	0.15	2.03 (1.31-2.75)
Sandy Loam	11.	0.41	90.	0.49	0.22	2.31 (0.33-4.29)
Loam	6.5	0.43	110.	0.60	0.28	1.84 (0.03-3.65)
Silt Loam	3.4	0.49	173.	0.63	0.26	1.74 (1.18-2.30)
Silt	2.5	0.42	190.	0.67	0.21	2.26
Sandy Clay Loam	1.5	0.35	214.	0.77	0.48	0.56 (0.23-0.89)
Clay Loam	1.0	0.31	210.	0.89	0.52	1.38
Silty Clay Loam	0.9	0.43	253.	0.84	0.49	1.86
Sandy Clay	0.6	0.32	260.	0.78	0.52	--
Silty Clay	0.5	0.42	288.	0.87	0.59	3.34 (0.92-5.76)
Clay	0.4	0.39	310.	0.86	0.59	1.41 (0.23-2.59)

¹ First line is base value. Second line is range for those soil classes with more than four experimental sites representing a soil texture class.

Values of K_s are modified for the effects of vegetative canopy cover and ground surface cover. The modification is based on relationships derived from rainfall simulator data from Arizona and Nevada (Lane et al. 1987) and in equation form is:

$$K_{se} = K_s [\exp(c_c CC\%)] [\exp(c_g GC\%)] \quad (5)$$

where K_{se} = effective saturated hydraulic conductivity (mm/hr) modified for the influence of canopy cover and ground cover, K_s = original effective saturated hydraulic conductivity (mm/hr), c_c = coefficient in the exponential relationship between percent vegetative canopy cover ($CC\%$)

and saturated hydraulic conductivity, and c_g = coefficient in the exponential relationship between percent ground surface cover ($GC\%$) and saturated hydraulic conductivity. Values of the coefficients in (5) were estimated as $c_c = 0.0105$ and $c_g = 0.009$ using rainfall simulator data from experimental plots in Arizona and Nevada (Lane et al. 1987).

Values of K_{se} are modified for the effects of frozen soil conditions based on a simplification of the approach used by the WEPP Model (Laflen 1991a, b), which assumes:

$$K_{sef} = c_f K_{se} \quad (6)$$

Where:

K_{se} is determined through (5)
coefficient $c_f = 1.0$ for thawed soils and is less than one for frozen soil.

The coupled Green-Ampt and kinematic wave runoff routing model, called IRS9, is described by Stone et al. 1992, and was the basis for modifications to the DHSVM model described herein.

4.2.4 Selah Creek Peak Flow Analysis

The enhanced DHSVM was evaluated using historical peak flow data from the Selah Creek basin located within the YTC (Figure 5). Many of the historical peak flows summarized in Figure 6 are obviously the result of localized metrological conditions, which is reflected by the inconsistency of peak flow dates between stations for a given year. The rather sparse meteorological network available will likely miss this type of small-scale spatial variability, making these events of limited value in model evaluation. However, peak flow in 1963, 1970, 1971, and 1974 occurred on the same day (or within one day for 1970) at each site. This indicates the runoff resulted from more widespread meteorological conditions, which is more likely to be captured by the meteorological network. These winter events resulted from rapid snowmelt and were among the largest recorded at each site. At the Selah Creek Tributary station, the 1971, 1963, 1974, and 1970 peak flows ranked first, third, fourth, and sixth, respectively.

DHSVM was run at an hourly time step over the Selah Creek Tributary for the period of record (Water Years 1956–1974). The output, including water available at the soil surface through snowmelt, throughfall, and direct precipitation (potential runoff), were used as input to the Green-Ampt infiltration equation. Application of the Green-Ampt equation requires the cumulative infiltration (F) to be set to zero at the start of individual storm events, while all other parameters in equations (3) and (4) remain constant during the storm. Individual storms were separated by a minimum of 12 consecutive hours without input to the soil surface when the ground was snow covered and one hour in the absence of snow cover.

Soil parameters for the Green-Ampt equation were taken from Table 1 for Silt Loam, the dominate soil type in the Selah Creek Tributary. K_{se} was determined through equation (5) with a

canopy cover of 74% and a ground cover of 67%, based on field measurements taken in close proximity to the basin. Soil temperature was calculated through equation (2). The coefficient c_f in equation (6) is based on the soil state (frozen or thawed) at the start of the storm (i.e., the soil is assumed to remain either frozen or thawed throughout the storm). This coefficient was adjusted until flow was simulated in 11 of the 19 years during the Selah Creek period of record ($c_f=0.038$), in agreement with observations.

Streamflow was simulated in 9 of the 11 years with recorded flows, with the simulated date of peak annual flow within one day of observed during the key years of 1963, 1970, 1971, and 1974. Results are also favorable for the simulated ranking of these peak flows. The seasonal distribution of peak annual flows for Water Years 1956–1997 generally agrees with observations (Figure 6). The model simulated flow in 17 of 42 years (40%) versus 11 of 17 years based on observations.

4.3 Hillslope Erosion Model (HEM)

4.3.1 HEM Enhancements

The HEM (Lane et al. 2001) is a simple and robust model, and it was developed to estimate erosion and sediment yield at the hillslope scale. This model is a time-averaged solution of the coupled kinematic wave equations for overland flow and the sediment continuity equation. Thus, the solution emphasizes spatially distributed soil erosion and sediment yield processes averaged over a specified period. The model is made continuous for simulating long-term mean annual averages by coupling it with the DHSVM (described above). The HEM was developed specifically for hillslopes and tested, evaluated, and parameterized primarily for applications in semi-arid regions of the United States but it has also been used around the world (e.g., Cogle et al. 2003).

The model is used to simulate erosion and sediment yield as a function of position on the hillslope and to simulate the influence of spatial variability in topography, vegetative canopy cover, and ground surface cover on erosion and sediment yield from hillslopes. The single-event model has an analytic solution, simplified input, relatively few parameters, and internal relationships to relate slope steepness, soil erodibility, vegetative canopy cover, and ground surface cover to the model parameters.

Lane et al. (1995) described the model and its application in rangeland areas in detail, and the following material is an abbreviated version of that description. Notice that the hydraulics of overland flow on a plane are approximated in the development of HEM by the kinematic wave equations:

$$\frac{\partial(h)}{\partial t} + \frac{\partial(q)}{\partial x} = r \quad (7)$$

and

$$q = Kh^m, \quad (8)$$

Where:

h = the average local flow depth in meters (m)

t = time in seconds (s)

q = discharge per unit width in m^2/s

x = distance in the direction of flow in m

r = rainfall excess rate in m/s

the depth-discharge coefficient is $K = CS^{1/2}$ where

C = the Chezy hydraulic resistance coefficient for turbulent flow in $m^{1/2}/s$

S = the dimensionless slope (slope steepness) of the land surface.

Notice that the exponent m in equation (8) is 1.5 when the Chezy hydraulic resistance formula is used.

A simplifying assumption required for an analytic solution is that rainfall excess rate is constant and uniform:

$$r(t) = \begin{cases} r & 0 \leq t \leq D \\ 0 & \text{otherwise} \end{cases} \quad (9)$$

where $r(t)$ is rainfall excess rate and D is the duration of rainfall excess in sec. The analytic solution eliminates all the problems of numerical solutions at the expense of simplifying the complex rainfall excess pattern to a simple step function.

The sediment continuity equation for overland flow is:

$$\frac{\partial(ch)}{\partial t} + \frac{\partial(cq)}{\partial x} = E_i + E_r, \quad (10)$$

Where:

c = total sediment concentration in kg/m^3

E_i = the interrill erosion rate per unit area in $kg/s/m^2$

E_r = net rill erosion or deposition rate per unit area in $kg/s/m^2$.

Since rills can be significant sources of erosion or the locations of significant deposition, E_r in equation (10) accounts for both processes.

A simplifying assumption for the interrill erosion rate is:

$$E_i = K_i r \quad (11)$$

where K_i is the interrill erosion coefficient in kg/m^3 . Simplifying assumptions for the rill erosion/deposition equation component are:

$$E_r = K_r(T_c - cq) = K_r[(B/K)q - cq] \quad (12)$$

where K_r is the rill erosion coefficient in $1/\text{m}$, T_c is the sediment transport capacity in kg/s/m and is assumed equal to $(B/K)q$, and B is a transport-capacity coefficient in $\text{kg/s/m}^{2.5}$. Equations (7) – (10) are called the coupled kinematic-wave and erosion equations for overland flow.

Equations (11) and (12) were suggested by Foster and Meyer (1972) and represent significant simplifications of the erosion and sediment transport processes. Nonetheless, these assumptions did allow derivation of analytic solutions to the coupled equations.

The solution to the sediment continuity equation for the case of constant rainfall excess was integrated through time (Shirley and Lane 1978; Lane et al. 1988) and produced a sediment-yield equation for individual runoff events as:

$$Q_s(x) = QC_b = Q\{B/K + (K_i - B/K)[1 - \exp(-K_r x)]/K_r\} \quad (13)$$

Where:

Q_s = total sediment yield per unit width of the plane in kg/m

Q = the total storm runoff volume per unit width in m^3/m

C_b = mean sediment concentration over the entire hydrograph in kg/m^3

x = distance in the direction of flow in m , and the other variables are as described above.

A major limitation of the analytic model represented by equation (13) was that it was described for a single plane, not complex topography required to represent hillslopes.

The above sediment-yield equation for a single plane (13) was extended to irregular slopes (Lane et al. 1995a). This extension was accomplished mathematically by transforming the coupled partial differential equations to a single ordinary differential equation (integration through time). As an ordinary differential equation, the solution on a segment of the plane could easily be solved for sequential segments of the entire plane. Finally, the extension was accomplished practically by approximating irregular hillslope profiles by a cascade of plane segments. With the extension of the model equation (13) to irregular slopes, inputs for the entire hillslope model are runoff volume per unit area and a dimensionless, relative soil-erodibility parameter. Input data for each of the individual segments are slope length and steepness, percent vegetative canopy cover, and percent ground surface cover. Additional efforts were made to parameterize the model using physically measurable characteristics. This was successful (as shown below) for all parameter values except the dimensionless soil erodibility.

From the input data, parameter estimation procedures were derived by calibrating the model using rainfall simulator data, to compute the depth-discharge coefficient, K , the interrill erosion coefficient, E_i , the rill erosion coefficient, E_r , and the sediment-transport coefficient, B . The calibration was done using rainfall-simulator data from 10.7-m by 3.0-m rangeland plots across

the western United States and USLE fallow plot data from throughout the eastern United States. These calibration results, corresponding relationships from the literature, and expert judgment were used to relate soil properties, slope length and steepness, vegetative canopy cover, and ground surface cover with the model parameters (coefficients) described above. These relationships were incorporated as a subroutine within the computer program to simulate sediment yield. The entire program is called the simulation model for sediment yield on hillslopes, or hereafter, the HEM.

4.3.2 Winter Processes

The HEM was derived and calibrated for soil erosion from rainfall-runoff events on thawed soil, i.e., under warm season or summer conditions. Thus, to be used at the YTC and other sites where winter processes (e.g., snow, soil freeze-thaw cycles, and snowmelt) are significant, the HEM needed modification, particularly with regard to its representation of soil erodibility under winter conditions. An extensive literature search was conducted on two winter processes: (1) the erodibility/erosion of frozen soils and (2) the erodibility/erosion of thawing soils. Information gleaned from this review was used to improve estimates of the relative (or dimensionless) erodibility term of the HEM under frozen and thawing soil conditions as it is used to estimate sediment yield, interrill detachment, rill detachment or deposition, and mean sediment concentration for each segment that has been specified for a hillslope profile. The relative erodibility input (for thawed soils) is based generally on optimized values derived from erodibility-soil textural class relationships (Table 1, last column, adapted from Lane et al. 2001). Section 4.2 in Lane et al. (2001) gives a detailed description of the methods used to optimize the relative erodibility parameter and a table of representative values and ranges for relative soil erodibility by soil textural class. See Lane et al. (2002) for a discussion of the extensive model calibration, based on more than 2000 rainfall simulator runs, and the derivation of Table 1 values.

Based on results from the literature and our synthesis of the resulting data and relationships, we derived erodibility estimation equations for the mean values of erodibility (*erod*) shown in Table 1. These erodibility estimation equations have the following form:

$$erod_f = a(erod) \quad (14)$$

for the erodibility of frozen soil, $erod_f$, as a dimensionless coefficient, a , times the erodibility of soil in its normally thawed condition ($erod$), i.e., under summer conditions. The corresponding equation for the dimensionless erodibility of thawing soil, $erod_t$ is:

$$erod_t = (1 + b)erod \quad (15)$$

where b is a dimensionless coefficient to be determined. Notice that $0 < a < 1$ and $b \geq 0$.

Currently, we do not plan on making the coefficients, a and b , vary with textural class, initial soil moisture at the time of freezing/thawing, soil organic matter content, soil structure, or other soil properties. This is because of the high uncertainty in the nominal values of $erod$ and the paucity

of field data on erodibility of frozen and thawing soils. These topics are the subject of future research (e.g., see Seyfried and Flerchinger 1994 for a discussion or our current inability to predict infiltration and erosion on frozen and thawing soil). We recognize that the use of single values for a and b in equations (14) and (15) represent a significant simplification. However, we do feel that given the problems of defining a and b and their temporal and spatial variability at the hillslope scale on ungauged watersheds, the significant simplification is warranted at this time. Clearly, additional research and field experiments are needed to improve on equations (14) and (15). Nonetheless, inclusion of equations (14) and (15) in the HEM erodibility estimation give us the ability to estimate seasonality via simulation of summer and winter processes.

In general, soils are least erodible when frozen solid. Haupt (1967) reported that, except at very low ice contents, soil is not very erodible when still frozen. An impermeable concrete frost layer can form when sudden and severe freezing occurs if high soil water content is present at the time of the initial freezing, resulting in extremely low soil erodibility. Studies of seasonal variability of erodibility on cropland soils have shown that in areas with hard winter frosts, frozen soil erodibility remains at a minimum value until spring thawing begins (Young et al. 1990; Renard et al. 1997).

When completely frozen soil conditions exist, particularly where hard winter frosts occur, we recommend using erodibility coefficient values (a values in equation (14)) that are very low or approach zero. Measured data from a Barnes loam soil near Morris, Minnesota, indicate that erodibility was zero from the beginning of November through about the middle of March. However, the influence of an undisturbed A horizon, surface organic material, and undisturbed soil structure on rangeland soils may make them more erodible than cultivated agricultural soils; indicating an " a value" somewhat greater than zero. Likewise, based on the research reviewed, we recommend that if snow cover is present, interrill erosion due to raindrop impact is zero because of the snow cover's insulating-protective effects.

Many of the papers reviewed indicated that both cropland and rangeland soils are at their most erodible as they begin to thaw. Soil frost strongly influences water infiltration and soil erosion on both croplands and rangelands in parts of the Northwest and Intermountain West of the United States. These areas are characterized by cold winters, transient snow cover, and multiple freeze-thaw cycles (Blackburn et al. 1990; Haupt 1967; Zuzel and Pikul 1987). Wischmeier and Smith (1978, pp 7-8) in the USLE Handbook discussed "R Values for Thaw and Snowmelt" and concluded that runoff played a more important role than rainfall. In fact, Wischmeier and Smith (1978, p. 7) stated

"In the Pacific Northwest, as much as 90 percent of the erosion on the steeply rolling wheatland has been estimated to derive from runoff associated with surface thaws and snowmelt."

They concluded that additional research on erosion processes in the Northwest are needed and then stated (Wischmeier and Smith 1978, pp 7-8):

“In the meantime, the early spring erosion by runoff from snowmelt, thaw, or light rain on frozen soil may be included in the soil loss computations by adding a subfactor, R_s , to the location’s erosion index to obtain R .”

They followed this statement with an example calculation for a location in the Palouse area, which showed an increase in R value from 20 to 38 as a result of adding the subfactor. This indicates a ratio of corrected to nominal mean annual soil loss of $38/20 = 1.9$ or about a factor of two.

Experimental data, modeling results, and our syntheses of them, suggest that the erodibility of frozen rangeland soils compared to their nominal erodibility (erodibility of the soils in a thawed condition as in the summer) should be significantly less (i.e., $a \ll 1$ in (14)). The erodibility of thawing rangeland soils compared to their nominal erodibility should be significantly greater, with a factor of two suggested by empirical plot data from the Palouse region of the Northwest (i.e., $b \sim 1$ in (15)).

We have taken $a = 0.4$ in equation (14) based on the requirement that $0 < a < 1$ and the assumption that erodibility of frozen rangeland soils is greater than comparable cropland soils where the coefficient a approaches zero for frozen soils in the ‘concrete’ condition and is greater than zero for frozen soils with less hardness. We have taken $b = 1.0$ in equation (15), supported by limited empirical data from the Northwest as described earlier. We feel that these first-order values are consistent with available data and our limited understanding of winter processes affecting soil erosion on rangelands.

Given the assumption that the soil condition remains constant during an event, there are five Soil State options depending on precipitation phase (rain or snow), snow cover (bare or snow covered soil), and soil thermal state (thawed, thawing, or frozen):

1. Rainfall on bare-thawed soil; no change to parameters, normal rainfall model, use nominal value of erodibility.
2. Rainfall on bare-frozen soil; decrease erodibility for frozen soil.
3. Rainfall or snowfall on snow-covered thawing soil; eliminate interrill erosion, and increase erodibility for thawing soil.
4. Rainfall or snowfall on snow-covered frozen soil; eliminate interrill erosion and decrease erodibility for frozen soil.
5. Snowfall on bare-thawed soil; eliminate interrill erosion and use nominal value of erodibility

Therefore, the HEM was modified to implement the above options based on providing it one additional input, Code = 1, 2, 3, 4, or 5, from the hydrologic model. We further assumed that the soil for the entire hillslope profile is in one of the five soil condition classes (bare-thawed, bare-frozen, snow covered-thawing, snow covered-frozen, and snowfall-thawed). These assumptions

allowed us to use the spatially uniform runoff and erodibility version of HEM to modify as a new version of HEM for applications where winter processes are significant in the erosion process.

In the new version of HEM, spatial variability in sediment delivery to stream channels on small watersheds is represented by topographic, soil, and cover variations between the n profiles used to represent a sub watershed, spatial variations in snow pack, and the profiles' status in one of the soil condition classes. Temporal variation over a season or over several years is represented by changes in the time series of rainfall and/or snowfall input, changes in snow pack, and the changing status of the soil condition class for the n hillslope profiles used to represent the sub watersheds or sub basins.

4.4 Testing the Coupled DHSVM-HEM Model at the YTC Sedimentation Ponds

The DHSVM-HEM model was evaluated for its ability to predict long-term sediment yield using measurements from the 12 sedimentation ponds. In addition, the DHSVM-HEM results were compared to results from the RUSLE and WEPP models, which were generated in an independent study by Gatto (personal communication 2004). Aerial photos were used to determine the location and fractional area of improved roads, unimproved roads, and firebreaks that existed in the ponds watershed during the pond measurement period.

4.4.1 Field Data Collection

Field data on representative hillslopes distributed across the YTC were collected in 2003 and 2004. Data were collected to represent three broad classes of land use: (1) rangeland, (2) firebreak roads, and (3) unimproved roads (see Figure 10). Within each of these three broad classes, data were collected to represent a range of land-use intensity and soil types.



Figure 10. Field data were collected on three broad land-use types: (1) rangeland, (2) unimproved roads, and (3) firebreak roads.

Hillslope profile data were measured using transect sampling methodology designed to enable a field crew of three or more people to collect hillslope transect data sufficient (when used with

data from existing soils, topography, etc. databases) to parameterize the DHSVM-HEM model. Hillslope profiles are transects that follow the apparent flow path down the hillslope from the crest of the ridge to the toe of the slope where it intersects a defined drainage. In developed or disturbed areas, the hillslope profile can terminate at any feature that ends the overland flow path on the land surface (e.g., constructed drainage, pond, or road). It should be noted that roads of various types can be significant features of the watersheds above these ponds and thus can be represented by the hillslope profile data.

Each transect is composed of three or more segments defined by a significant change in vegetation density, vegetation community, soil type, or slope steepness. The initial data recorded for each segment are length, percent slope steepness, and compass bearing. Each segment is divided into a minimum of 20 increments for data collection—to record the vegetative canopy cover and ground surface cover. Vegetative canopy cover is classified as grass, shrub, forb, tree, cactus, half-shrub, etc., and ground surface cover may be litter, gravel, rock, bedrock, cryptogam, or plant basal area. The number of vegetative canopy cover hits divided by the number of increments in the segment multiplied by 100 equals the percent vegetative canopy cover (simplified to % canopy cover herein) for the segment. Similarly, the number of hits on ground surface cover divided by the number of increments in the segment multiplied by 100 equals the percent ground surface cover (simplified to % ground cover herein) for the segment.

4.4.2 Model Application

The DHSVM was run at an hourly time step from October 1, 1955, through September 30, 1997, using data from the Yakima Airport (Figure 5). Air temperature and precipitation were lapsed from the Yakima Airport to each pond location using differences in mean monthly values of these variables at the two locations obtained from the PRISM data sets available without cost from the Spatial Climate Analysis Service (<http://www.ocs.orst.edu/prism/products/>). The DHSVM simulated hourly time series of water available at the ground surface (precipitation and/or snowmelt) was broken into a sequence of storms. Rainfall-dominated storms (i.e., defined by lack of snowpack) were further disaggregated using the double exponential method (Nicks and Lane 1989), while snowmelt dominated storms remained at the one-hour time step. Soil state (frozen or thawed) and the HEM soil condition code at the start of the storm were determined through equation (2) and assumed constant throughout the storm.

The time series of storms was input to Green-Ampt Infiltration Model to estimate surface runoff volume from each storm for each transect (hillslope profile), based on soil type, soil thermal state, and transect-average percent canopy and ground cover. Sediment yield was then calculated by HEM using the runoff volumes and soil condition code, along with soil type and transect segment properties. At each pond, the median value of sediment yield for each cover type (rangeland, unimproved roads, and firebreaks) was multiplied by the fractional area of the cover type and the products summed to determine the total basin sediment yield.

Mean annual sediment yield for DHSVM-HEM was obtained by summing yield from all individual storms and dividing the total by the simulation length of 40 years. These results are compared with the commonly used RUSLE model and to the pond measurements in Figure 11. The DHSVM-HEM was also compared with WEPP results from Gatto (unpublished manuscript, 2004) in the same figure. The measurement data were divided into two periods (1985-1990 and

1990-1994) to indicate the potential range and variability of runoff and measured erosion across the YTC. The results are quite encouraging and indicate that DHSVM-HEM may be a viable alternative to the RUSLE model in the arid western United States. The WEPP model produced the poorest results, although Gatto (personal communication, 2004) felt this may have resulted, in part, from his lack of familiarity with the model and its larger number of parameters (personal communication, 2004).

From the results illustrated in Figure 11, notice that the RUSLE predictions matched the observed data (red bars) best on Ponds 3 and 4 and were comparable to the accuracy of the DHSVM-HEM predictions on Ponds 5 and 6. As expected from a continuous simulation model, the DHSVM-HEM predictions matched the observed data best on Ponds 1, 2, 7, 8, 9, 10, 11, and 12. On rangeland areas, the annual coefficient of variation ($CV = SD$ divided by the mean) usually varies from about 1 to more than 2 (Lawrence et al. 1997). Based on an annual CV of 2 for the observed data, the DHSVM-HEM predictions were within about a factor of 2 of the measured data for 9 of the 12 watersheds while the RUSLE predictions met this criterion on 4 of the 12 ponds with a suggestion of significant over-prediction on the majority of the ponds. Finally, for both the RUSLE and DHSVM-HEM procedures comparisons of model predictions of erosion on the uplands with measured pond sediment yields did not include any channel erosion or deposition predictions or adjustments.

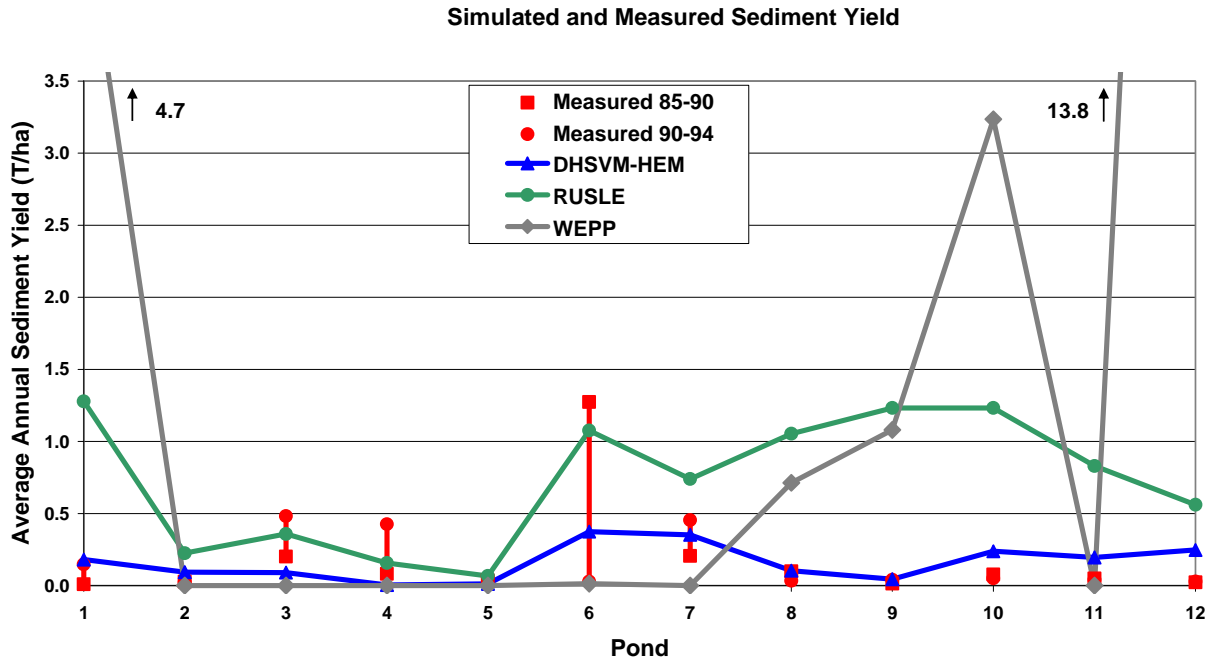


Figure 11. Average annual sediment yield predicted by the DHSVM-HEM (blue), RUSLE (green), and WEPP (gray) models at each pond compared with measured yield in 1985–1990 (red square) and 1990–1994 (red circle). Note that WEPP values are off the scale in Ponds 1 and 12.

4.4.3 Discussion

Results from the DHSVM-HEM application to the 12 sedimentation pond watersheds indicate that while unimproved roads and firebreaks yield more sediment per unit area, rangeland yields the most sediment in total because of its much larger total area. Rangeland yields 86% of the total, with firebreaks and unimproved roads contributing 9 and 5%, respectively. However, when roads are present, even as a small fraction of the total area, they can contribute a disproportionate amount of sediment as indicated in Figure 12. Roads and firebreaks in Ponds 6 and 7 represent 3 and 2% percent of the total area, but contribute 66 and 48% of the sediment, respectively.

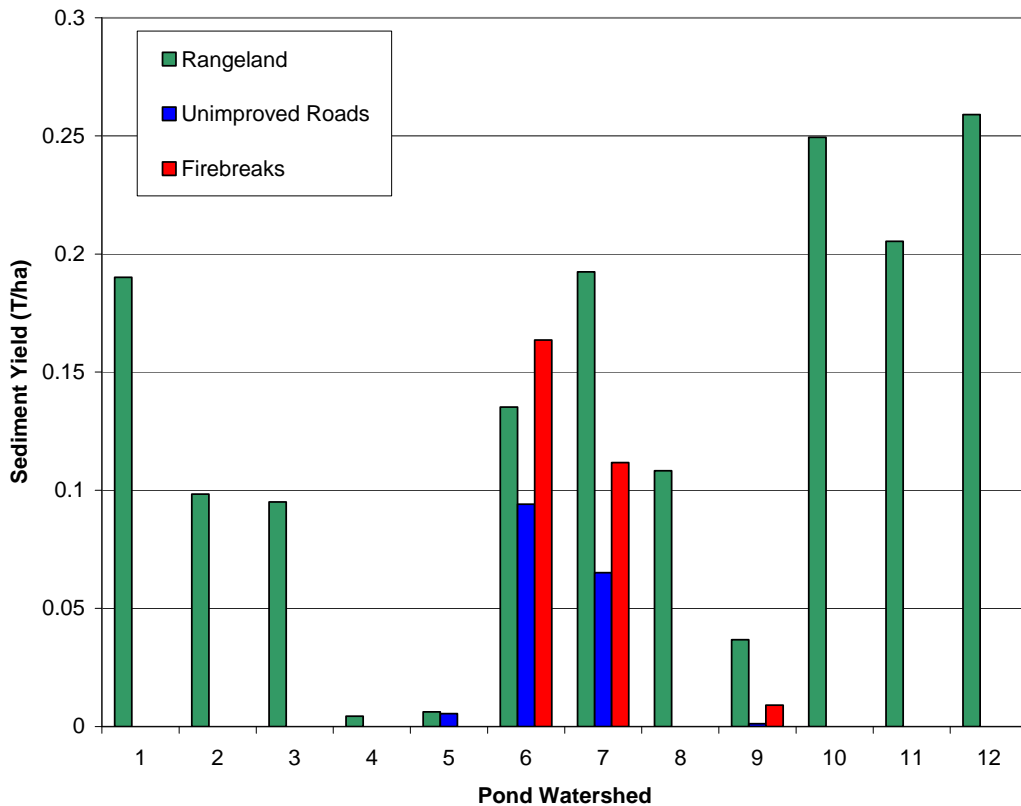


Figure 12. Mean annual sediment yield predicted by DHSVM-HEM for each pond by cover type for rangeland (green), unimproved roads (blue), and firebreaks (red).

In summary, the DHSVM-HEM procedure appeared to perform best when compared with the RUSLE and WEPP models. However, these results are not definitive because of the short records of observed data (1985–1994), because RUSLE and DHSVM-HEM were estimating upland erosion delivered to the stream channel system, and because there were additional uncertainties in applying WEPP at the YTC. However, the DHSVM-HEM procedure appears to be a viable alternative to RUSLE and WEPP and conceptually DHSVM-HEM is superior to RUSLE because it is more physically based and because of its continuous simulation capability including winter processes. The DHSVM-HEM procedure is simpler and less “data-hungry” than WEPP and this may be an advantage under conditions of human and monetary resource limitations.

From these experiments and analyses, we make the following conclusions:

- Winter processes dominate runoff and soil erosion at the YTC; however, summer thunderstorms do occur.
- Simulation models applicable to areas such as the YTC where winter processes dominate the hydrology and erosion should be based on continuous simulation throughout the year,

including the winter season, when such models are used to compute average and average annual values of runoff and erosion.

- The coupled DHSVM-HEM hydrologic and erosion models simulate the seasonal distribution of runoff and the resulting soil erosion at YTC as well as, or better than, RUSLE and WEPP.
- The coupled DHSVM-HEM modeling system represents a new generation of runoff and erosion prediction technology heretofore unavailable to land managers at the YTC, and to managers of lands hydrologically similar to the YTC.

However, additional research is needed to test and evaluate the coupled DHSVM-HEM modeling system's winter routines and their parameter values beyond those from south-central and southeastern Washington used herein. This is especially true for the parameter values associated with the soil erosion component.

4.5 Application of Remotely Sensed Data in Modeling Soil Erosion at the YTC

Physically based soil erosion and sediment yield models (erosion models hereafter) require input of (1) directly measured physical characteristics (e.g., topography and hydrography), (2) geospatially estimated values of directly measured inputs (e.g., spatially distributed precipitation), and (3) input derived from direct measurements (e.g., spatially distributed soils, vegetative canopy cover, and ground surface cover). All these inputs can be based upon field measurements or remotely sensed data with various schemes to distribute them spatially and temporally as required by the erosion models.

A key area of research in hydrology (erosion) and geospatial analyses is how model inputs and processes vary as functions of spatial scale, intensity scale, and temporal scale (see, for example NRC 1999; Rodriguez-Iturbe and Rinaldo 1997; Lane et al. 1997; and Goodrich et al. 1997). Examples of spatial scale problems include scaling direct measurements up from point or plot areas to watershed areas, determining the dominance of hydrologic (including erosional) processes on hydrologic response, and measuring spatially distributed hydrologic data to use in model verification and validation (e.g., see Wilson et al. 2001 and Lane and Wigmosta 2006). Different understanding, measurement, and modeling techniques are required as the temporal scale varies from seconds to annual or decadal periods.

Adding to the complexities summarized above, model input data can come from field measurements or from remotely sensed measurements before they enter the geospatial analyses phase to provide the required scale dependence. A central question herein is how model performance varies geospatially depending upon data source—field or remotely sensed. This question is especially important as attempts are made to model erosion over large areas such as the YTC.

We describe field data collection techniques and their products and remote sensing techniques and their corresponding products applied at the YTC (described in Section 2.4). These products are then used to provide input to the hydrologic and erosion model.

These comparable products of field studies and remote sensing are then statistically compared and used in model simulations to allow us to determine the sensitivity and robustness of the HEM to differences in model input from field and remotely sensed data sources. Emphasis is on geospatial analyses and the scope of our analyses and discussions are limited to data from the YTC and to erosion and sediment yield data from simulations using the HEM.

Because it is impractical to field measure data for the YTC's 3469 first-order subbasins (see Figure 26), an alternative method of extracting required HEM model parameters became necessary. Using remote sensing and geospatial processing, HEM model parameters were extracted for three primary topic areas: topography, canopy cover, and soils. These parameters are as follows:

- Hillslope profile length and steepness for each of the profile's n segments
- Hillslope vegetative canopy cover, CC%, and ground surface cover, GC%, for each of the profile's n segments
- Hillslope profile soil texture.

The central idea is to take limited field data on representative hillslope profiles and to calibrate/validate remote sensing-based methods of estimating the above information. Once the remotely sensed information explains as much, and very similar information, of the variation in these variables as is explained by the field data, then coupled remotely sensed information and GIS are used to generate "virtual hillslope transects" at any point on the YTC. Our goal is to have these virtual hillslope transects (Section 0) contain the same or very similar information that would be obtained if they had been determined by field measurements. If this goal is met, then the HEM will give similar results regardless of the source of their parameter inputs (field or remotely sensed data) and, thus, we will be able to compute sediment delivery to all stream channels on the YTC under a variety of management and land-use scenarios.

4.5.1 Data Collection

Training activities that disturb soils can affect the ecosystem through erosion, sediment loading, temperature alterations to aquatic habitats, and physical destruction of key habitats. Remotely sensed imagery is being used to characterize environmental changes across the watershed such as increases in bare soils and changes in vegetative cover. Spectral imaging algorithms for use with sequentially collected imagery were developed to assess quantitative and qualitative changes in key landscape characteristics as a result of military training. Landscape characteristics potentially affected by training that influence watershed processes include relative amounts of upland or riparian vegetative cover and bare soils and the formation of rills, gullies, and channels. Image analysis is used to quantify landscape-level characteristics in the following steps:

1. Identify and analyze vegetative and soil indices that best reflect relative quantities of vegetative cover and bare soils;

2. Use data sets from sequential imagery to detect significant increases or decreases in bare soils as a result of training activities; and
3. Apply sophisticated change-detection methods including textural analyses and linear spectral un-mixing techniques to optimize the detection and characterization of biotic signatures.

Current YTC field sampling (described in Section 4.4) is used to associate field-measured variables with pixel response. The image analysis results are then used in conjunction with topographic data as input data layers for hydrologic modeling to quantify the magnitude and spatial distribution of surface water runoff, soil erosion, and sediment loading to streams. For this study, we used data from the SPOT satellite. This imaging satellite instrument collects data in four spectral bands at a spatial resolution of 10 m. The revisit time of SPOT is 2 to 3 days and we used scenes from July 18, August 13, and September 29, 2003.

4.5.2 Comparison of Remotely Sensed and Field Measured Data

One measure of robustness for the HEM is to compare its response, sediment yield from the hillslope (t/ha), in response to using field measured data and remotely sensed data as model input. The logic is that if by specified statistical comparisons, using the mean values from transects at YTC pond watersheds and \pm the SDs, HEM output to these means and \pm SD from field-measured data and remotely sensed data are comparable, then the HEM is robust with respect to using remotely sensed data.

However, it should be noted that the field measurements and remotely sensed information do not exactly correspond; they are measuring different quantities. For example, field data used to define a hillslope profile are obtained using a line-transect method and segments within the profile can vary from approximately 10^0 to 10^2 m along a line. The corresponding DEM-derived hillslope profile is based on a constrained analyses of 10 m pixels, i.e., if any portion of a pixel was touched by a transect line, that pixel was included in the slope calculation. If 13 pixels are used to define the segment slope, and their properties within a profile, then segments within the profile can vary from approximately 10^1 to 10^2 m along a 10-to-30-m-wide strip. Another problem with this method is that a given transect segment may touch portions of several different pixels. In this case, the median pixel value was used to compare to the field data for that segment.

4.5.3 Canopy Cover

Analysis of field-measured vs. SPOT-modeled vegetative canopy cover data for transect segments >20 m (two pixel sizes) for 136 transect segments are summarized in Figure 13. Notice that the regression equation between data from field measurements (X) and data from remote sensing (Y) is:

$$Y = 0.08 + 0.56 X \quad (16)$$

with $R^2 = 0.51$, mean $X = 68.9\%$ and Mean $Y = 46.2\%$. This means that the remotely sensed data and their analyses techniques (models) result in vegetative canopy cover estimates that explain about 50% of the variation in corresponding field-measured values and that the mean value of the vegetative canopy cover was underestimated by approximately 30% with respect to the field data. (See the above note about comparison of field and remotely sensed hillslope profile data, which are not exactly coincident in space.)

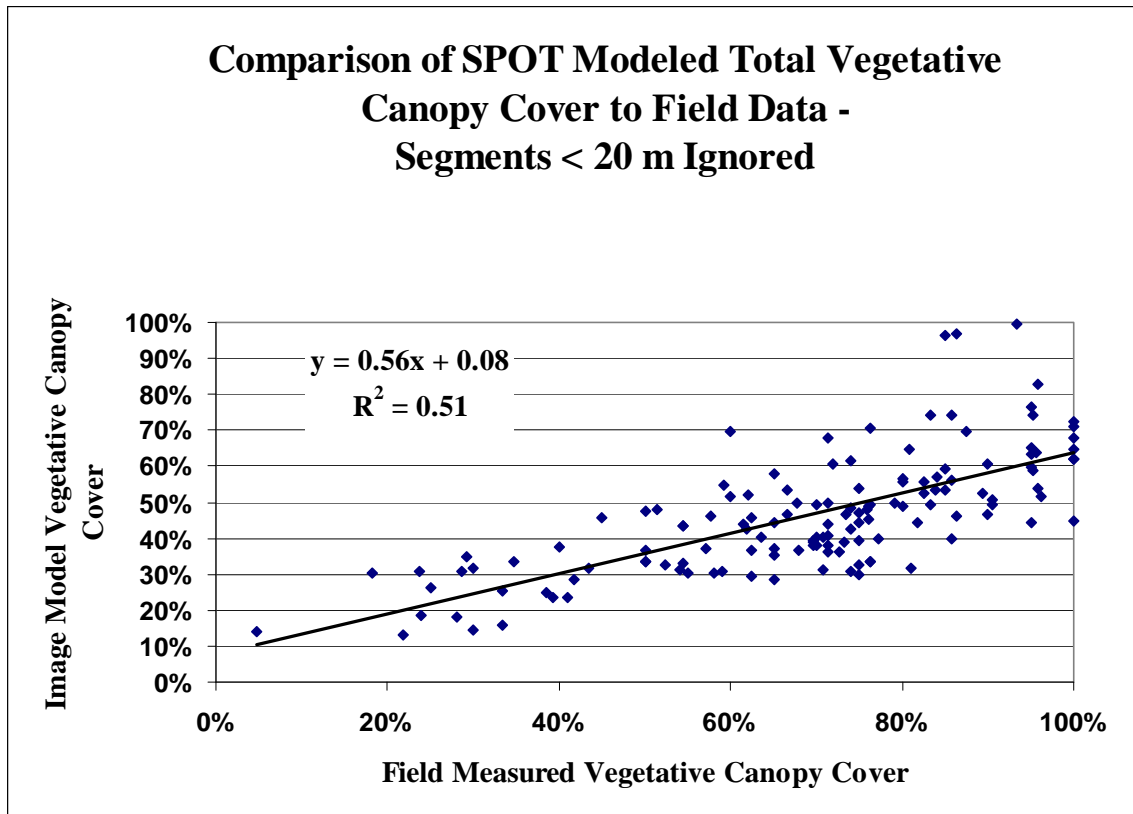


Figure 13. Analysis of field-measured vs. SPOT-modeled vegetative canopy cover data for transect segments >20 m in length (two pixel sizes). The data are for 136 transect segments.

4.5.4 Bare Soil and Ground Cover

Analysis of field-measured vs. SPOT-modeled bare soil data for transects >20 m (two pixel sizes) and <60% vegetative canopy cover for 111 transect segments is summarized in Figure 14. Notice that the regression equation between field data (X) and data from remote sensing (Y) is:

$$Y = 0.06 + 0.68 X \quad (17)$$

with $R^2 = 0.52$, mean $X = 26.7\%$ and mean $Y = 24.5\%$. This means that the remotely sensed data and their models explain about 50% of the variation in corresponding field-measured values and that the mean value of bare soil was underestimated by approximately 8%.

The HEM inputs percent ground surface cover, GC%, which is computed as:

$$GC\% = 100 - \text{Bare Soil}\% \quad (18)$$

for use as model input. It should be noted that equation (18) is used to convert individual and mean values of bare soil to surface ground cover but that the SD of bare soil is equal to the SD of ground surface cover.

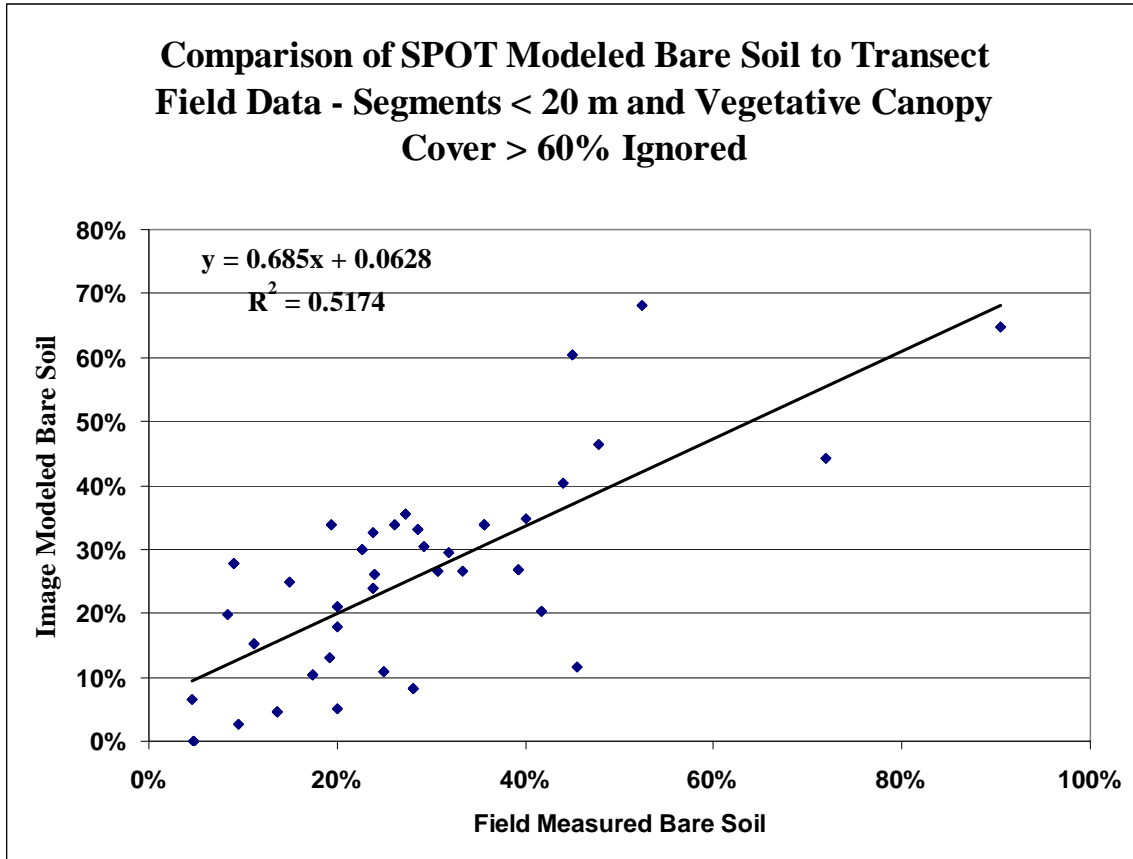


Figure 14. Analysis of field measured vs. SPOT-modeled bare soil data for transect segments >20 m in length (two pixel sizes) and with >60% vegetative canopy cover. The data are for 111 transect segments.

4.5.5 Slope Steepness

Analysis of field-measured vs. SPOT-modeled slope steepness data for transects >20 m (two pixel sizes) for 138 transect segments are summarized in Figure 15. Notice that the regression equation between field data (X) and data from remote sensing (Y) is:

$$Y = 2.79 + 0.84 X \quad (19)$$

with $R^2 = 0.66$, mean $X = 14.7\%$ and mean $Y = 14.3\%$. This means that the remotely sensed data and their models explain about 70% of the variation in corresponding field-measured values and that the mean value of slope steepness was underestimated by approximately 3%.

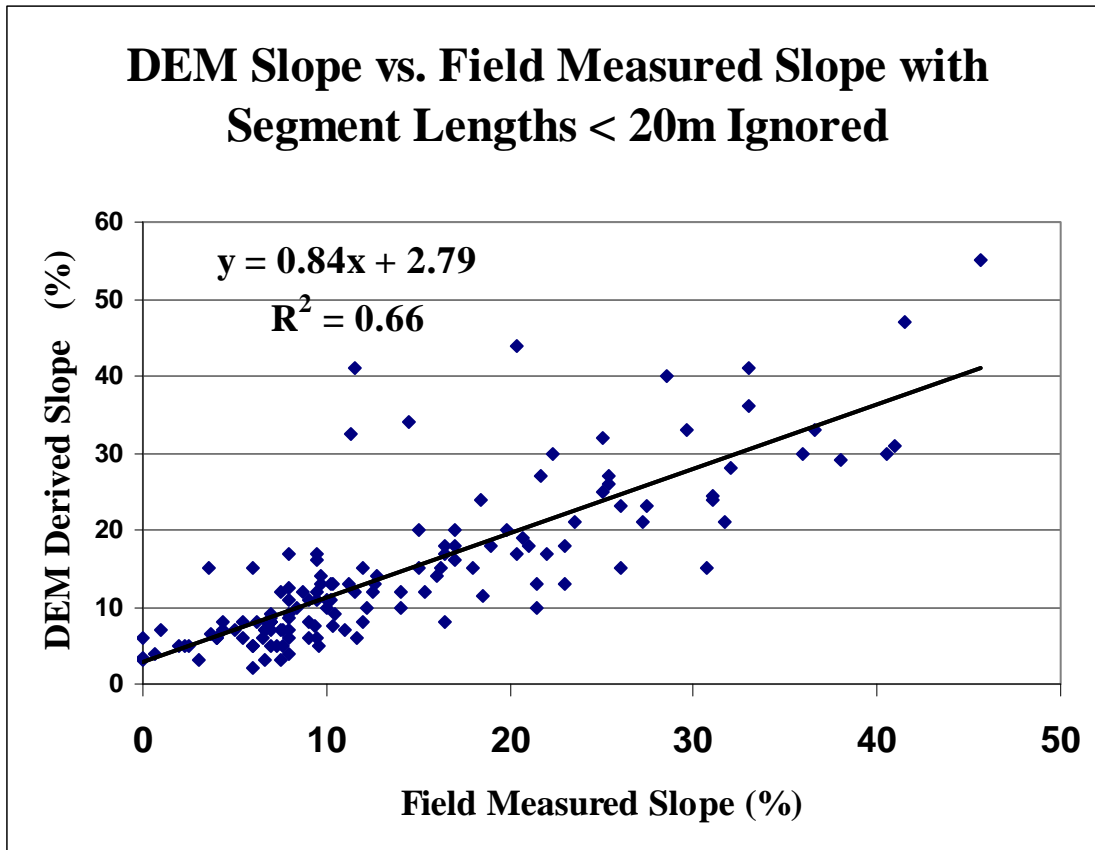


Figure 15. Analysis of field-measured vs. SPOT-modeled slope steepness data for transect segments >20 m in length (two pixel sizes). The data are for 138 transect segments.

4.5.6 Flow Length

Analysis of field-measured vs. SPOT modeled flow length data for transects >20 m (two pixel sizes) for 52 transect segments are summarized in Figure 16. Notice that the regression equation between field data (X) and data from remote sensing (Y) is:

$$Y = 40.8 + 0.89 X \quad (20)$$

with $R^2 = 0.42$, mean $X = 108.7$ m and mean $Y = 137.2$ m. This means that the remotely sensed data and their models explain about 40% of the variation in corresponding field-measured values and that the mean value of slope length was overestimated by approximately 26%.

Comparison of Field Measured and DEM Derived Flow Lengths From Common Starting Point

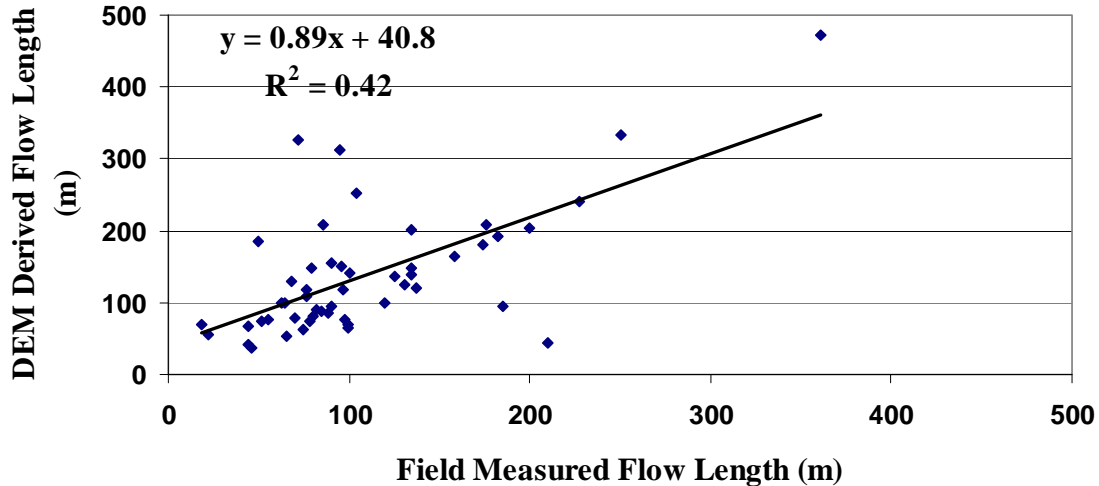


Figure 16. Analysis of field-measured vs. SPOT-modeled flow length data for transect segments >20 m in length (two pixel sizes). The data are for 52 transect segments.

4.5.7 HEM Sediment Yield Estimates for Remotely Sensed and Field-Measured Input

A statistical summary of data from field measurements and remotely sensed data and the resulting sediment yield data for a representative or “mean” hillslope profile transect at the YTC is discussed. To summarize the “mean” or representative response from a “mean” or representative hillslope profile transect, we calculated the mean and SD for hillslope segments over all the measured and corresponding remotely sensed transects for vegetative canopy cover, surface ground cover, slope steepness, and slope length. The overall means were then used as input to the HEM and the resulting “mean” or representative hillslope sediment yield was calculated. These “mean” values are shown in bold in Table 2. Next, we varied “means” for each of the four variables independently by \pm the SD holding “mean” values of the other three variables constant. The “mean” \pm SD values for the four input variables and the resulting sediment yield in t/ha from the HEM are shown in Table 2.

The results from Table 2 are also shown in Figure 17. Notice that the HEM is most sensitive to changes in ground cover and slope steepness, followed by slope length, and least sensitive to changes in canopy cover. In addition, a high correlation exists between the field data input sediment yield and remotely sensed data input sediment yield. Comparison of the 8 “means” \pm SD sediment yield estimates produces eight data points as shown in Figure 17. The field data “mean” is overestimated by about 20% by the remotely sensed data “mean.”

Table 2. Summary of HEM sediment yield estimates (t/ha) for a “mean” or representative hillslope profile transect at YTC. Simulations are for a silt loam soil and 10 mm of runoff. Inputs are mean and mean ± SD for the four variables shown in the column headings. Values are the overall means for the field data and remotely sensed data are shown in each column. The resulting HEM output data are bold and in parentheses.

HEM Calculated Sediment Data (t/ha) for “Mean” Hillslope at YTC								
	Canopy Cover [%]	Sediment Yield (t/ha)	Ground Cover [%]	Sediment Yield (t/ha)	Slope Steepness [%]	Sediment Yield (t/ha)	Slope Length [m]	Sediment Yield (t/ha)
Field Data								
Mean	68.9	(0.79)	73.3	(0.79)	14.7	(0.79)	108.7	(0.79)
-SD	48.1	(0.89)	57.3	(1.40)	4.7	(0.29)	45.5	(0.43)
+SD	89.7	(0.69)	89.3	(0.44)	25.0	(1.29)	172.0	(1.07)
Remotely Sensed Data								
Mean	46.2	(0.94)	75.5	(0.94)	14.3	(0.94)	137.2	(0.94)
-SD	29.9	(1.01)	60.3	(1.55)	4.2	(0.33)	50.6	(0.48)
+SD	62.4	(0.87)	90.7	(0.56)	24.3	(1.55)	223.8	(1.26)

Note: Overall mean sediment yield from field data = 0.79 t/ha and overall mean sediment yield from remotely sensed data = 0.94 t/ha.

Influence of Variations (Mean +/- SD) in Input Data to the HEM From Field and Remotely Sensed Data

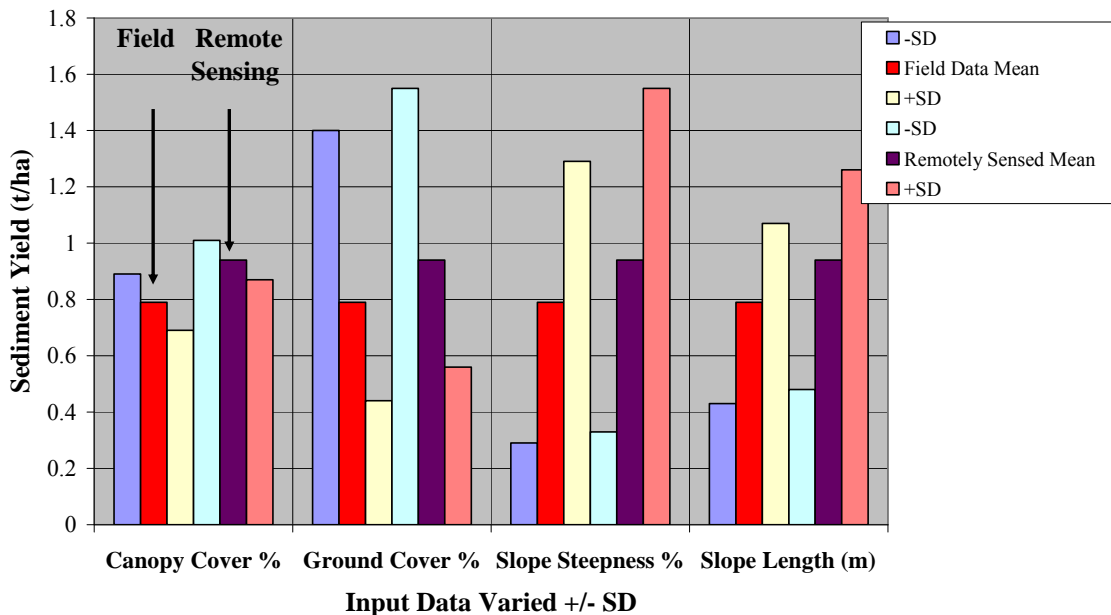


Figure 17. Variation of HEM estimated sediment yield for “mean” input data and “mean” plus or minus the standard deviation for each of four input variables.

The variation or uncertainty in input data values and the resulting HEM estimated sediment yield for a “mean” or representative hillslope profile transect using field data or remotely sensed data are shown in Table 2 and Figure 17. For example, in Table 2, notice that a variation in canopy cover of \pm SD ($68.9\% \pm 20.8\% = 48.1$ to 89.7%) results in about ± 0.10 t/ha (0.79 t/ha ± 0.10 t/ha = 0.69 to 0.89 t/ha) variation in HEM predicted sediment yield for the field data. For the remotely sensed data the corresponding numbers are $46.2\% \pm 16.3\%$ producing a mean sediment yield of 0.94 t/ha ± 0.16 t/ha. = 0.87 to 1.01 t/ha. Similar variations for the other input data and resulting sediment yield are shown in the last three columns of Table 2.

Variation in sediment yield is slightly larger for variations in field data input, largest for variations in surface ground cover and slope steepness, less for variations in slope length, and least for variations in canopy cover. This is a statement of the uncertainty and sensitivity of the HEM for variations in input data for a “mean” or representative hillslope at the YTC. That is, for a “mean” or representative hillslope a variation of input data of \pm SD changes the HEM output as follows: about 7 to 13% for canopy cover, about 40 to 80% for ground cover, about 60 to 65% for slope steepness, and about 30 to 50% for slope length.

From the hundreds of data points shown in Figure 13 through 16 (derived from hundreds of segments on 66 transects), representative or overall “mean” values of canopy cover, ground cover, slope steepness, and slope length were derived and used to compute HEM estimates of sediment yield for the “means” and \pm SD. Variation and sensitivity of estimated sediment yield to these “means” \pm SD are shown in Figure 17 and the degree of correlation between variations of estimated sediment yield using field data input and remotely sensed data input is shown in Figure 18.

In Figure 18, the central point labeled as means represents the overall mean HEM estimated sediment yield from all the field data means (0.79 t/ha) and the corresponding overall mean HEM estimated sediment yield from all the remotely sensed means (0.94 t/ha). This represents a remotely sensed mean “over prediction” of approximately 19%. However, recall that the field and remote sensing methods do not measure precisely the same quantities. The R^2 value of 0.99 in Figure 18 suggests that the HEM predictions from field data mean values \pm SD are highly correlated with corresponding values from remotely sensed data. The mean and mean \pm SD values of field and remote sensing data produce almost exactly the same HEM prediction results with a mean difference, or bias, of some 0.15 t/ha = 20% of the mean from field data.

However, the inability to determine remotely sensed ground surface cover (100% - Bare Soil %) when vegetative canopy cover is above 60%, see Figure 14) suggests the need for an alternative method of estimating ground surface cover. Because ground surface cover is one of the most sensitive inputs to the HEM (and to other soil erosion models), it is necessary to be able to estimate it over the entire range of vegetative canopy cover (0 to 100%).

**Hillslope Erosion Model Response to Input of Means +/- SD for:
Canopy Cover, Ground Cover, Slope Steepness, and Slope Length**

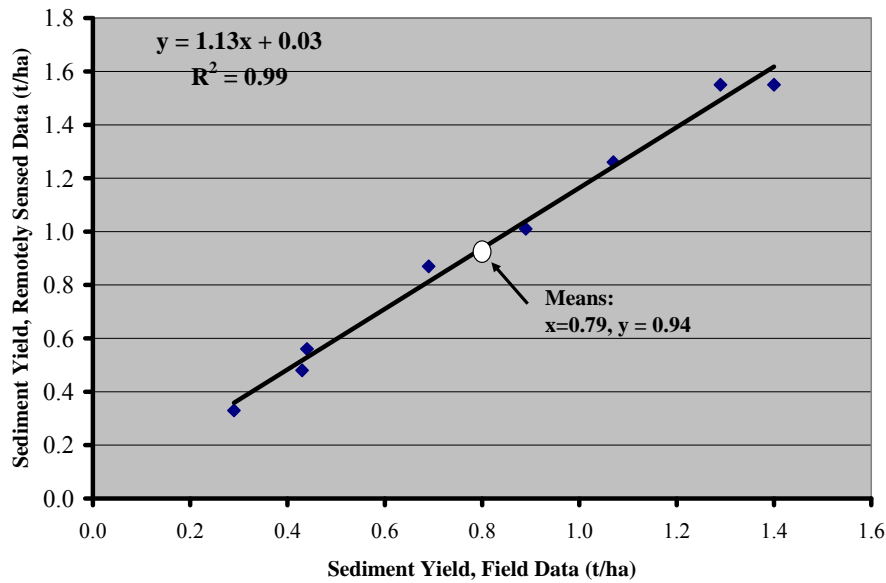


Figure 18. Comparison of “means” ± SD simulated sediment yield values from field data estimates and remotely sensed data estimates of “means” and standard deviations.

Moreover, from Table 2, roughly half of all field-measured segments on YTC hillslopes have vegetative canopy cover in excess of 60% making the relationship shown in Figure 14 inapplicable. Therefore, an alternative method was needed to estimate ground surface cover if process-based erosion models such as HEM are to be used site-wide at the YTC.

4.5.8 Revised Method to Estimate Ground Cover

A new procedure was developed to estimate ground cover from soil type and remotely sensed canopy cover. The soil types included what are generally considered “rocky soils” and “non-rocky soils” depending upon the degree of their rock, cobble, and gravel content. Seven soil textures were sampled on rangelands, and three each on firebreak and unimproved roads. The database of interest here included data from 577 segments from hillslope transects (see Table 3).

The logic in our analyses of these data is as follows. For rocky soils as vegetative canopy cover decreases to near zero, surface fines in the soil would be eroded leaving an “armoring” of the soil surface from the rocks in the soil profile. This would result in a positive value of ground surface cover (GC%) as vegetative canopy cover (CC%) decreased toward zero. Moreover, the degree of armoring would tend to decrease as CC% approached 100% and would be replaced by vegetative components of ground cover – basal plant area, litter, and when present, cryptogams. Conversely, for the non-rocky soils, the soil profile would contain little rocks and as CC% decreased towards zero so would GC%. As for the rocky soils, the vegetative components of GC% would tend to increase as CC% increased towards 100%.

Table 3. Statistical summary of transects' segment vegetative canopy cover and ground surface cover by land use and soil texture. Note, CC% = percent vegetative canopy cover and GC% = percent ground surface cover.

Land Use	Soil	Number of Segments	Statistics of Canopy and Ground Surface Cover			
			Mean CC%	SD CC%	Mean GC%	SD GC%
Rangeland	CBV-L	121	62.2	21.5	71.6	18.3
	CBX-L	6	86.8	8.8	82.9	15.6
	CL	3	55.5	22.0 ¹	47.4	19.3 ¹
	GR-L	21	45.9	24.6	62.6	14.2
	L	68	82.3	10.6	79.9	12.3
	SIL	205	71.9	21.7	69.4	21.1
	STV-L	10	50.8	17.1	61.1	19.5
Total	All Soils	434	69.2	22.0	71.2	19.3
95% CI			(67.1,71.3)		(69.4,73.0)	
Firebreak	CBV-L	18	3.5	6.4	28.8	17.7
Roads	L	22	35.7	33.3	18.2	18.9
	SIL	31	6.0	8.7	13.5	13.6
Total	All Soils	71	14.6	24.1	18.8	17.4
95%CI			(8.9,20.3)		(14.7,22.9)	
Unimproved	CBV-L	8	5.5	5.9	28.0	10.9
Roads	L	15	15.0	9.4	17.5	17.6
	SIL	49	13.2	13.0	23.1	14.4
Total	All Soils	72	12.7	12.0	22.5	14.9
95% CI			(9.9,15.5)		(19.0,26.0)	
Grand Totals	--	577	55.4	32.1	58.7	28.7
95% CI			(52.8,58.0)		(56.4,61.0)	

1. The soil texture abbreviations are as follows:
CBV-L = Very cobbly loam, CL = Clay loam, GR-L = Gravelly loam, L = loam, SIL = Silt loam, and STV-L = Very stony loam.
2. SD refers to the standard deviation.
3. Standard deviation not calculated for n <5, we use standard deviation calculated from all data within the land-use category.

Based upon the above reasoning, we developed regression equations for GC% as a function of CC% for the 6 means from rocky soils and from the 7 means from non-rocky soils. These data are summarized in Table 4. Notice that the mean CC% values are about the same for both rocky and non-rocky soils but that the mean GC% is larger for the rocky soils than for the non-rocky soils, although not statistically different at the 5% level.

Regression analyses were performed, with GC% as a function of CC%, for the data shown in Table 4 and are shown in Figure 19 for rocky soils and Figure 20 for non-rocky soils.

Table 4. Summary of mean vegetative canopy cover, CC%, and mean ground surface cover, GC%, for rocky soils and for non-rocky soils at the YTC.

Rocky Soil	Soil Texture	No of Segments	Mean CC%	Mean GC%	Comments and Notes
	CBV-L	121	62.2	71.6	Largest class in the rocky soils
	CBX-L	6	86.8	82.9	
	GR-L	21	45.9	62.6	
	STV-L	10	50.8	61.1	
	CVB-L	18	3.5	28.8	
	CBV-L	8	5.5	28.0	
	Total	184			Represents 184 of 577 segments or 32%
		Mean	42.45	55.83	
		SD	32.62	22.63	
Non-Rocky Soil	CL	3	55.5	47.4	Largest class in the non-rocky soils
	L	68	82.3	79.9	
	SIL	205	71.9	69.4	
	L	22	35.7	18.2	
	SIL	31	6	13.5	
	L	15	15	17.5	
	SIL	49	13.2	23.1	
	Total	393			Represents 393 of 577 segments or 68%
		Mean	39.94	38.43	
		SD	30.45	27.27	

YTC Segment Data for Rocky Soils
Mean Ground Cover as a Function of Mean Canopy Cover

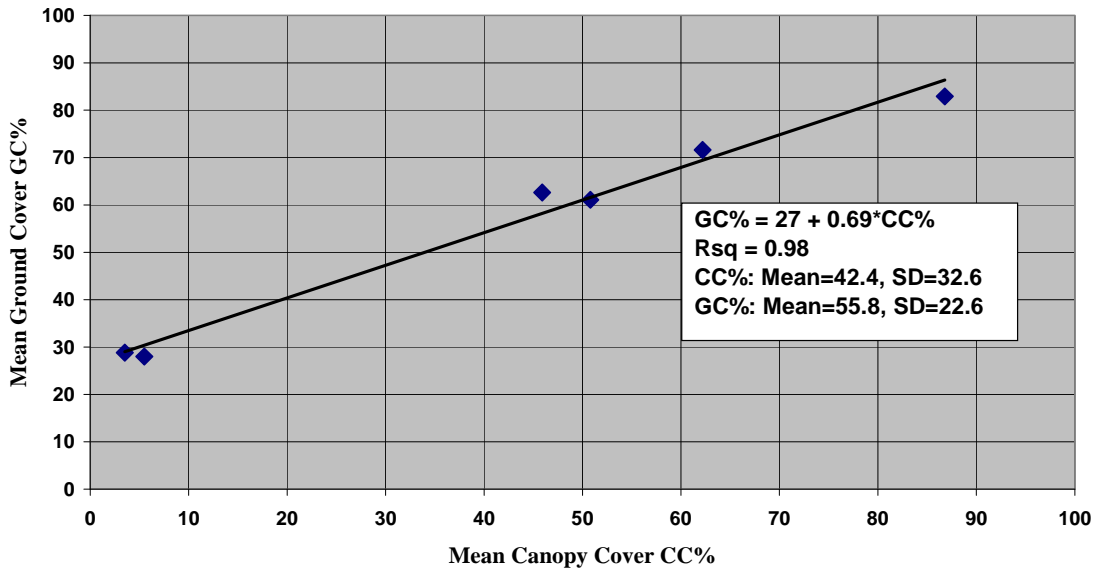


Figure 19. Regression analyses for mean GC% as a function of mean CC% for the rocky soils at YTC.

YTC Segment Data for Non-Rocky Soils
Mean Ground Cover as a Function of Mean Ground Cover

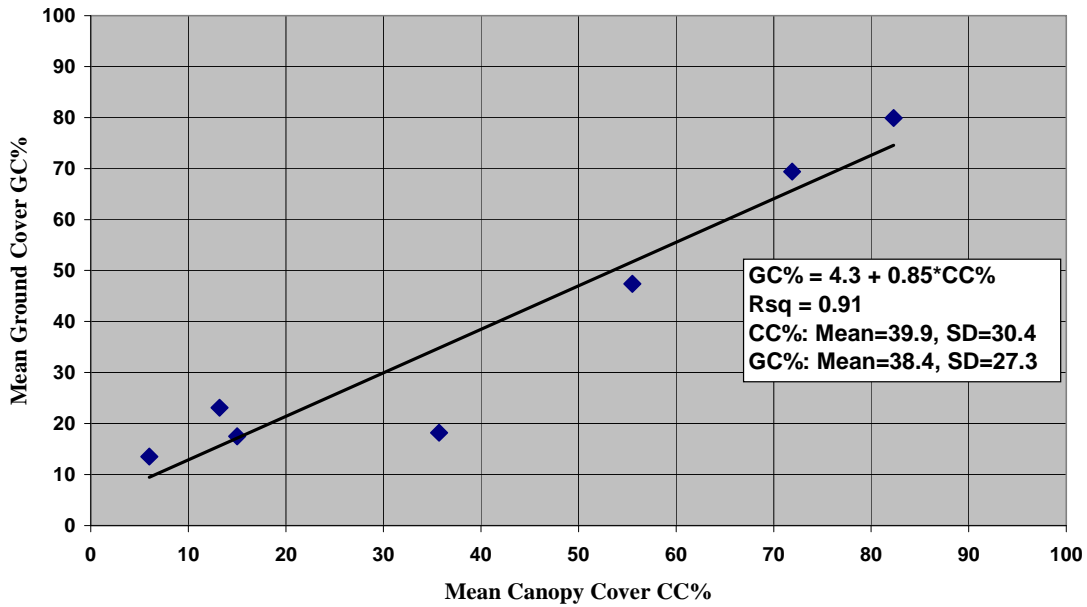


Figure 20. Regression analyses for mean GC% as a function of mean CC% for the non-rocky soils at YTC.

The following equations were derived from the analyses illustrated in Figure 19 and Figure 20. For the rocky soils, the equation is:

$$GC\% = 27 + 0.69 * CC\% \quad (20)$$

with $R^2 = 0.98$.

For the non-rocky soils, the equation is:

$$GC\% = 4.3 + 0.85 * CC\% \quad (21)$$

with $R^2 = 0.91$.

Notice that for the rocky soils (equation 20), as CC% approaches 0.0% that GC approaches 27% and as CC% approaches 100% that GC approaches 96%. For the non-rocky soils (equation 21), notice that as CC% approaches 0.0% that GC approaches 4.3% and as CC% approaches 100% that GC approaches 89.3%. The intercept of 27% in (equation 20) suggests that on rocky bare soil armoring would result in a residual ground surface cover of about 30% while the intercept of 4.3% in (equation 21) suggests that on non-rocky bare soil a residual ground surface cover of only about 4% would develop.

4.5.9 Procedure to Estimate Ground Surface Cover on all Hillslopes at the YTC

At present, we are unable to estimate ground surface cover (GC%) adequately using remote sensing techniques alone. Therefore, we adopted the following steps to provide site-wide estimates of ground surface cover on the virtual transects.

- Use remote sensing techniques to estimate segment and transect topography from DEM data.
- Determine soil texture for each virtual transect and classify it as rocky or non-rocky.
- Use remote sensing techniques to estimate segment vegetative canopy cover, CC%, for each segment in the transect.
- Use equation (20) or (21), as appropriate, to estimate ground surface cover, GC%, for each segment in the transect.
- Build the virtual transect database using the above techniques.

4.6 Estimating Soil Erosion Condition Classes for the YTC

Notice that although only 13 data points are shown in Figure 19 and Figure 20, the 6 points in Figure 19 represent 184 hillslope profile segments and the 7 points in Figure 20 represent 393 hillslope profile segments. Thus, the extensive database of 577 hillslope profile segments

represents most major areas of the YTC including the 12 sedimentation ponds distributed across the training areas.

The left-most data points in Figure 19 and Figure 20 represent the worst conditions (with respect to vegetative canopy cover and ground surface cover disturbance/removal) observed on the range areas of YTC. In fact, these extreme points represent firebreak and unimproved roads.

In the next section, illustrative (relative or normalized) soil erosion rates are compared for cropland soils, rocky rangeland soils at YTC, and relatively non-rocky soils at the YTC. The cropland soils are for conservation tillage practices wherein the crop is harvested and a residue or mulch is left on the soil surface to reduce soil erosion. In contrast, the rangeland soils at the YTC are for soils with a vegetative canopy cover and a ground surface cover. The ground surface cover includes plant basal area, rocks and gravel, cryptogams, as well as the plant litter on the surface. Thus, much more of the ground surface, and subsurface, is bound together with roots, incorporated litter, cryptogams, and plant stems.

4.6.1 Analyses of Measured and Simulated Soil Erosion Rates

As described earlier, conservation tillage data and modeling have been used to derive generalized crop residue–reduction in soil loss curves for cultivated croplands (see for example, McCarthy et al. 2005, as summarized in Figure 21).

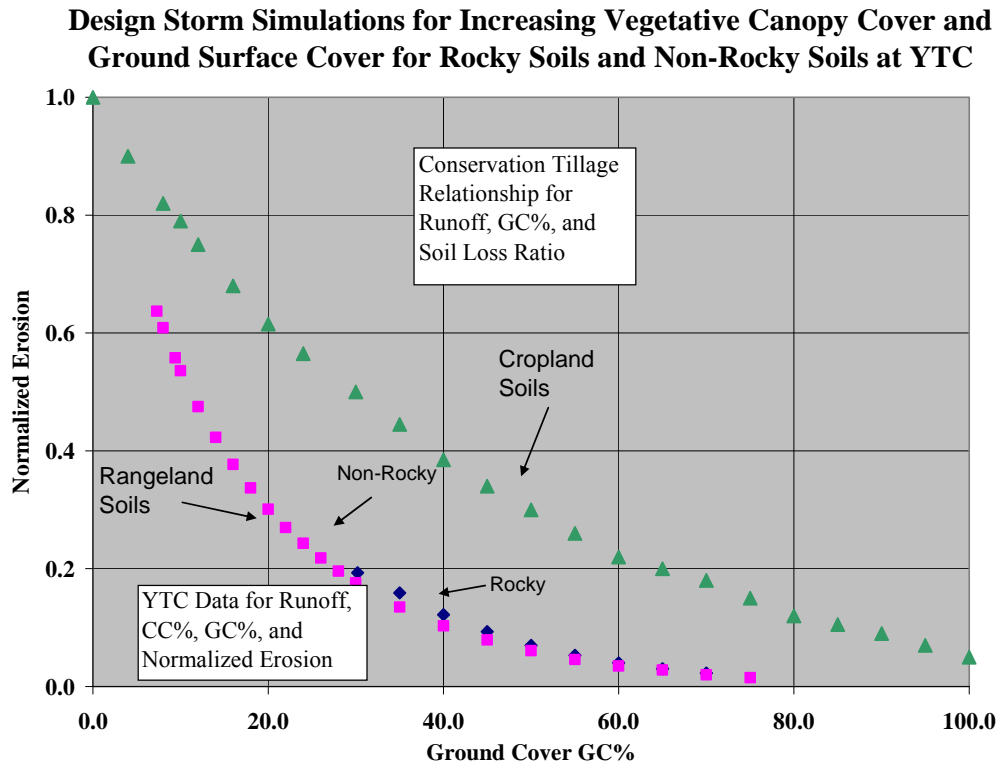


Figure 21. Comparison of cropland conservation tillage-soil loss results with normalized soil erosion vs. ground surface cover, GC%, for rocky and non-rocky rangeland soils at the YTC.

The upper curve (green triangles) in Figure 21 represents residue mulch on cultivated cropland soils. As such, it primarily reflects protection of the soil from raindrop impact and overland flow as well as more long-term reductions in runoff. However it does not reflect permanent vegetation, plant roots, etc. which tend to bind and protect the soil. The next curve labeled “Rocky” represents HEM simulated soil erosion normalized by soil erosion for the left-most point of the data. The final curve labeled “Non-Rocky” represents HEM simulated soil erosion normalized by soil erosion for the left-most point in that data set. Finally, notice that the overall vegetative canopy cover and ground surface cover effects on the relatively undisturbed soils at YTC result in soil erosion rates of about half or less than those observed on cultivated croplands.

4.6.2 Determining Generalized Soil Erosion Condition Classes

To account for the full range of soil erosion response on rangelands, the data for rocky and non-rocky soils were normalized further by the highest relative soil erosion rates in Figure 21 to rescale them to the 0 to 1 range.

The results of this rescaling are shown in Figure 22 and Figure 23 for the rocky and non-rocky soils, respectively. In each case, the minimum value of CC% was taken as the approximate minimum shown in Figure 19 and Figure 20 and then the corresponding GC% values were computed using the regression equations (20 and 21). Combinations of CC% and GC% which resulted in 0 to 25%, 25 to 50%, 50 to 75%, and >75% reductions of the maximum soil erosion rates (from the minimum CC%, GC% pairs) were then calculated from the curves shown in Figure 22 and Figure 23.

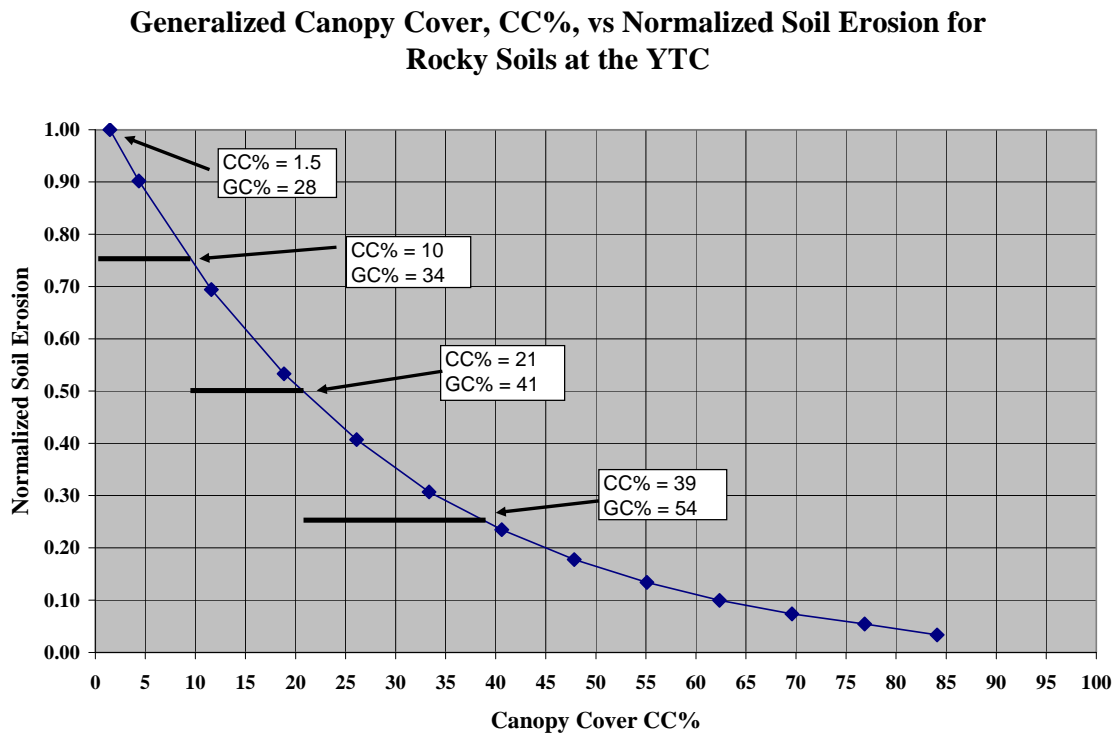


Figure 22. Generalized canopy cover vs. normalized soil erosion for rocky soils at the YTC. Notice the paired (CC%, GC%) values indicating the soil erosion condition classes.

In Figure 22, the rocky soils have a minimum CC% value of 1.5 and a minimum GC% value of 28. As discussed earlier, these rocky soils evolve to a high rock content surface configuration. In contrast, the data summarized in Figure 23 for non-rocky soils have a minimum CC% value of 4.4 and a minimum GC% value of 8.0 and these soils evolve to a much lower rock content surface configuration. As a result, the absolute values of soil erosion observed from the two different soils classifications (rocky vs. non-rocky) will be different with the non-rocky soils generally having higher relative soil erosion rates. However, their relative, or normalized, soil erosion rates are quite similar, as shown in Figure 22 and Figure 23. The greatest degree of difference is in the higher amount of GC% associated with the same level of CC% on the rocky soils.

Generalized Relationship Between Canopy Cover, CC%, and Normalized Soil Erosion for Non-Rocky Soils at the YTC

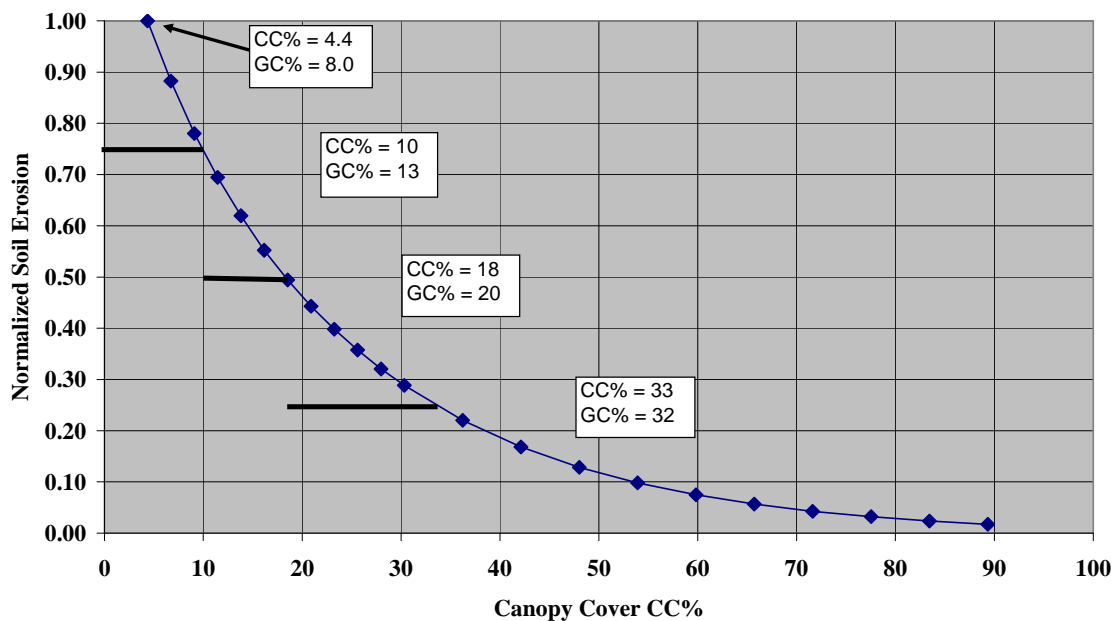


Figure 23. Generalized canopy cover vs. normalized soil erosion for non-rocky soils at the YTC. Notice the paired (CC%,GC%) values indicating the soil erosion condition classes.

4.6.3 Using the Decision Tools

Because the normalized soil erosion rates are similar, they can be used to construct similar soil erosion condition classes as shown in Figure 22 and Figure 23. An example use of the curve shown in Figure 22 might include something like the following. On a rocky soil, a training location in good condition class, that is one with the following cover values, $21 < CC\% < 39$ and $41 < GC\% < 54$, could be moved to a fair condition class if the CC% value fell below 21% or the GC% value fell below 41%, or both, as the result of training activity.

Given the above assessment of an area moving from a good to fair soil erosion condition class, the personnel responsible for making natural resource conservation plans and instituting rehabilitation measures to meet those plans would need to decide if rehabilitation measures were necessary in this example. The way we see this working for applications at YTC are through remotely sensing vegetative canopy cover, CC%, before and after the particular land-use episode, using equation (20) or (21) to estimate ground surface cover, GC%. Next, the before and after CC% and GC% values would be used to classify the soil erosion condition class before and after the particular land use, and the results would be used as a decision tool in remediation decisions. Finally, the coupled models DHSVM-HEM as discussed in Section 4.4 would be used to quantify the actual mean annual soil erosion rates to compare with, for example, regulatory requirements, water quality criteria, and mapping.

In making forward assessments, rather than after action analyses, the existing hillslope conditions (soil, topography, CC%, GC%, and meteorological inputs) would be used as inputs to the coupled DHSVM-HEM models to assess existing and likely future soil erosion rates and their corresponding soil erosion condition classes. In this case, the decision tools would be used, for example, in planning future land-use activities, and evaluating alternatives.

In either mode, assessing past actions (hindcasting) or estimating impacts of future actions (forecasting), the ability to calculate soil erosion and soil erosion condition classes provides the site managers with a valuable, quantitative, and defensible set of decision tools.

Finally, we have summarized the results of the soil erosion condition classes analyses in two tables: Table 5 for the rocky soils on the YTC and Table 6 for the non-rocky soils on the YTC. These two tables summarize the soil erosion condition class concept for the YTC. The header on the tables summarizes the existing and proposed soil erosion condition classes based upon sequential 25% reductions in soil erosion. The first row in the tables summarizes the values of CC% and GC% used to define each of the four soil erosion condition classes. The next three rows of the tables give the results for each of the three major cover types and include the mean values of CC% and GC% for the base conditions. Within each column, the value in parentheses is a representative reduction in soil erosion at the center of each range of cover values and the bold Xs represent where the base, or current, conditions fall with respect to soil erosion condition class.

Table 5. Generalized Canopy Cover – Soil Erosion Condition Classes for Rocky Soils at the YTC.

Cover Type	Base ¹	Poor	Fair	Good	Excellent
		Ranges: CC% < 10% GC% < 34%	Ranges: 10 < CC% < 21% 34 < GC% < 41%	Ranges: 21 < CC% < 39% 41 < GC% < 54%	Ranges CC% > 39% GC% > 54%
Rangeland	Means ² : CC% = 60% GC% = 70% “Excellent”	(0.86) ³ 1.00 – 0.75 ⁴	(0.61) 0.75 – 0.50	(0.35) 0.50 – 0.25	(0.068) < 0.25 X
Firebreak Roads	Means: CC% = 3.5% GC% = 29% “Poor”	(0.86) 1.00 – 0.75 X	(0.61) 0.75 – 0.50	(0.35) 0.50 – 0.25	(0.068) < 0.25
Unimproved Roads	Means: CC% = 5.5% GC% = 28% “Poor”	(0.86) 1.00 – 0.75 X	(0.61) 0.75 – 0.50	(0.35) 0.50 – 0.25	(0.068) < 0.25

1. Base conditions means for the current (2003-2004) conditions for the given Cover Type at YTC.
2. Weighted means for CC% and GC% from the number of segments in each soil textural class.
3. Design storm erosion rate normalized by erosion at center of “poor” range of CC% = 1.5 to 10 and GC% = 28 to 34, i.e., CC% = 6 and GC% = 31 for “Poor” condition, CC% = 15.5 and GC% = 37.5 for “Fair Condition,” etc.
4. Range of normalized soil erosion values which defines the condition class.

Table 6. Generalized Canopy Cover – Soil Erosion Condition Classes for Non-Rocky Soils at the YTC.

Cover Type	Base ¹	Poor	Fair	Good	Excellent
		Ranges: CC% < 10% GC% < 13%	Ranges: 10 < CC% < 18% 13 < GC% < 20%	Ranges: 18 < CC% < 33% 20 < GC% < 32%	Ranges: CC% > 33% GC% > 32%
Rangeland	Means ² : CC% = 74% GC% = 72% “Excellent”	(0.88) ³ 1.00 – 0.75 ⁴	(0.60) 0.75 – 0.50	(0.36) 0.50 – 0.25	(0.043) < 0.25 X
Firebreak Roads	Means: CC% = 18% GC% = 16% “Fair”	(0.88) 1.00 – 0.75	(0.60) 0.75 – 0.50 X	(0.36) 0.50 – 0.25	(0.043) < 0.25
Unimproved Roads	Means: CC% = 14% GC% = 22% “Fair”	(0.88) 1.00 – 0.75	(0.60) 0.75 – 0.50 X	(0.36) 0.50 – 0.25	(0.043) < 0.25

1. Base conditions means for the current (2003-2004) conditions for the given Cover Type at YTC.
2. Weighted means for CC% and GC% from the number of segments in each soil textural class.
3. Design storm erosion rate normalized by erosion at center of “poor” range CC% = 4.4 to 10 and GC% = 8.0 to 13, i.e., CC% = 7 and GC% = 10 for “Poor” condition, CC% = 14 and GC% = 16.5 for “Fair Condition,” etc.
4. Range of normalized soil erosion values which defines the condition class.

4.6.4 Mapping Site-Wide Erosion Condition Classes

A site-wide soil erosion condition dataset was developed by applying geospatial analyses and using (1) the SPOT-based percent canopy cover (CC%) data (Figure 24), (2) the established percent ground cover (GC%) regression equations, (3) land-use classifications, and (4) the parameters for the erosion condition classes. Because the major differences in erosion condition are based upon the characterization of rocky or non-rocky soils, the two soil classes were initially isolated and used as a base for additional analysis and processing. The raster-based CC% data were applied to rocky/non-rocky spatial domains and GC% was derived according to the two previously stated regression equations. Once these parameters were calculated, the data were re-merged and the land-use data were applied. The resulting data were classified into a total of 12 classes representing each of the four soil erosion condition classes by the three broad land-use classes and a site-wide map of soil erosion classes was produced (see Figure 25).

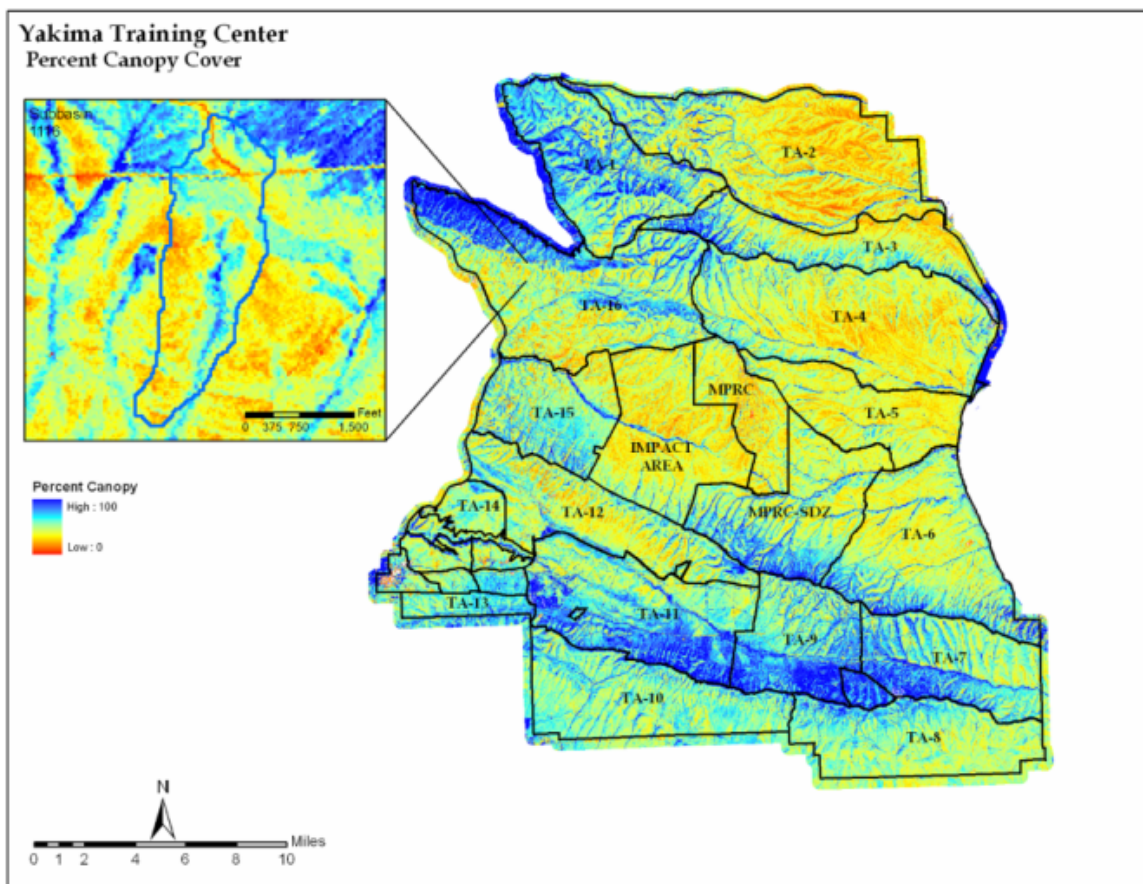


Figure 24. Percent vegetation canopy cover derived from SPOT 10-m resolution multi-spectral imagery. Notice the low canopy linear features in the zoom window representing unimproved road (running east-west) and a firebreak (running northwest-southeast).

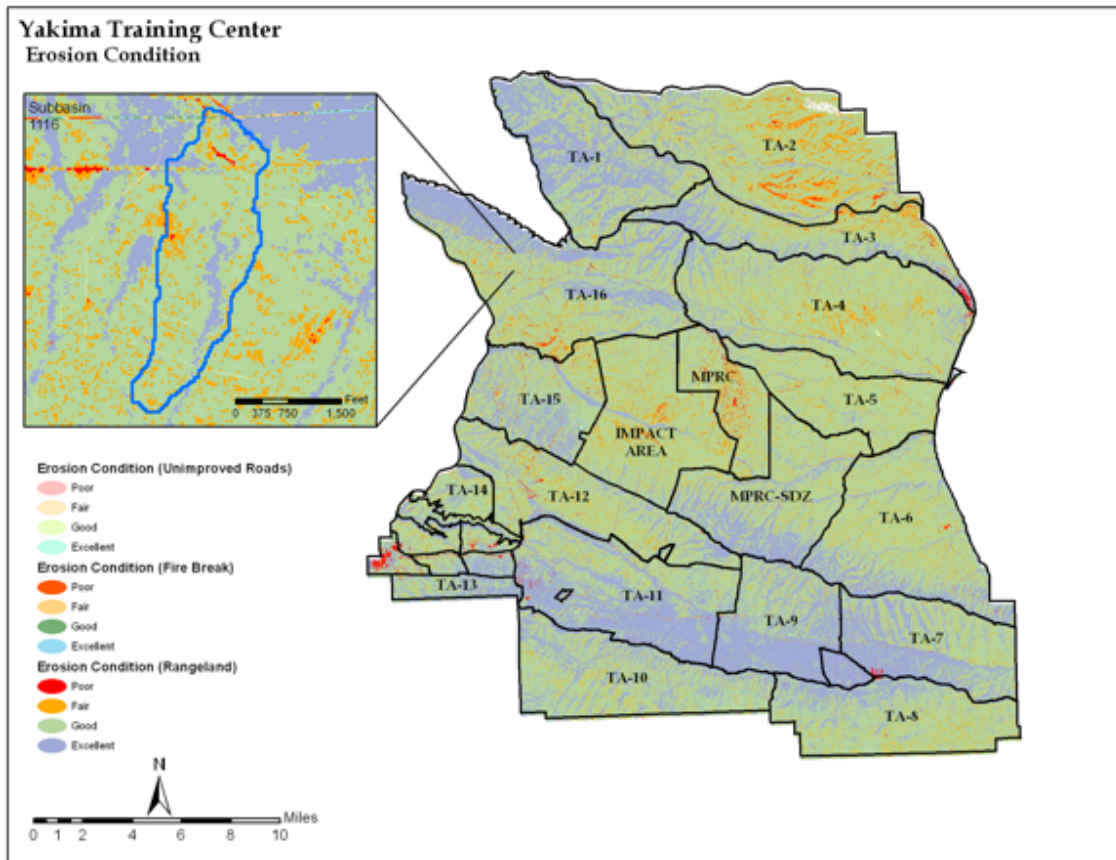


Figure 25. A site-wide soil erosion condition class map derived using three land-use classes (rangeland, unimproved roads, and firebreak roads), two soil classes (rocky and non-rocky), and four soil erosion condition classes (poor, fair, good, and excellent).

4.6.5 Discussion

The hydrologic and sediment transport routing available through application of dynamic models is not directly included in the databases used to construct the map shown in Figure 25. However, the hydrologic and erosion models are used to construct the curves shown in Figure 22 and Figure 23 and are based on runoff and soil erosion simulation and routing, and thus, represent the time-averaged behavior of runoff and sediment transport processes. Thus, the results shown in Figure 25 represent the influence of soil, vegetation, and land use upon soil erosion potential as represented by the soil erosion classes. Because the erosion potential is analyzed on a pixel-by-pixel basis, in which each pixel is independent of another, it cannot be used estimate total sediment yield in a subbasin under varying conditions. However, for uses where assessments of the influence of soil, vegetation, and land use on potential soil erosion are adequate, the YTC site-wide sediment budget for existing conditions, as computed, and mapped in Figure 25, represents as a new and unique decision tool for soil management on the YTC.

To capture the hydrographic impacts on soil erosion under varying conditions, it is necessary to derive topographic-based parameters from a hydrologic boundary (i.e., subbasin). A geospatial-based model, the Virtual Transect Model (VTM) described below (Section 4.7), was developed

to simulate flow paths down random starting points in a given subbasin and collect necessary parameter data to feed the DHSVM-HEM model.

4.7 Development of a Dynamic Sediment Budget for the YTC

4.7.1 Geospatial Watershed Development

To provide a multi-scale capable adaptive management tool, all modeling work was developed in a manner to use the smallest logical unit area which was defined as a first-order watershed. This philosophy provides the end-user the ability to combine and link specific areas to assess resource management needs as deemed necessary. The first-order watersheds were developed using USGS 10-meter Digital Elevation Models (DEM) and the commonly-used Deterministic-8 (D8) method for extracting flow paths and watershed boundaries (O'Callaghan and Mark 1984). Field-survey data and GIS-based upslope drainage area analysis determined that an average drainage area of 2600 m² provided the establishment of concentrated flow at the YTC. The watershed processing resulted in 3469 first-order watersheds with an average basin size of 4200 m² (see Figure 26).

4.7.2 Virtual Transect Model

A GIS-based Virtual Transect Model (VTM) was developed allowing for the estimation of soil erosion conditions on a first-order watershed scale. The intent of the “virtual transect” is to spatially model overland flow paths and collect various data along these paths, just as is observed and performed in the field. A single virtual transect is divided into segments based on changes in slope with a minimum segment length of 1.5-times the resolution of the underlying DEM (see Figure 27). The segments essentially allow a virtual transect to collect detailed data along its natural flow path including percent vegetative canopy cover, percent ground surface cover, soil type, soil texture, slope steepness, segment length, accumulated length, majority land use for the segment, azimuth, long-term mean precipitation, and long-term mean temperature. A spatial validation of data results from the VTM and field-determined flow paths show a high degree of agreement (see Figure 28), which makes it possible and realistic to collect virtual transect data for the entire YTC.

The virtual transect path is based on the idea of a raindrop model, where a point in the subbasin is selected and the overland flow path of the raindrop is traced downslope to the channel network (locations of concentrated flow obtained from GIS Terrain Analysis). This method assumes a non-permeable and frictionless surface where the flow path is based strictly on DEM elevation values, and DEM-derived flow direction and flow accumulation data. Early efforts in the VTM produced transect start points in which a centroid was determined in a given subbasin, and then an eight-directional ray separated at 45° angles was delivered to the subbasin boundary. The point of intersection between the ray and the subbasin boundary was chosen as the starting point for the virtual transect. Because of the inconsistent geometries and orientation of a given subbasin, this method provided sufficiently random data for a representative look at a given subbasin. Although this method proved useful for the large majority of subbasins at the YTC, problems arose in areas where the subbasins were smaller or had less topographic relief. The virtual transects in these areas would often run parallel to the subbasin boundary for a distance before descending downslope into the basin and/or producing other spurious results. Various attempts at resolving these issues were employed, such as inseting the starting point of the virtual transect by 2 or 3 cell-resolution

distances, increasing the number of starting points, and employing more automated rule-sets for accepting a virtual transect. Although this was an improvement in the methodology, these efforts ultimately reduced the number of valid transects and often left these more difficult subbasins with only three or four transects to base the modeling on.

A new VTM was developed that derives a flow path from a random point along the stream network (concentrated flow line) and traces the flow back upslope to its origin along the subbasin boundary. Based on changes in slope, the derived virtual transect is then broken into segments and each segment is populated with various spatial data attributes (e.g., vegetation canopy cover and soil type). To achieve a virtual transect starting from the stream channel, a unique “channel-up” flow tracing approach was developed. This method required inverting the DEM so the channels were transformed from low points to ridges and thus, flow direction and flow accumulation values were recalculated. Once the virtual transects were derived, all other processing resumed on non-inverted elevation data. Because the “channel-up” approach was effective on the more difficult subbasins, the method was used consistently across the entire YTC. The automated rule-sets that were developed for assessing the validity of an extracted virtual transect were still employed. This typically resulted in approximately 10-20 valid transects for each subbasin. Figure 27 shows the results from the “channel-up” approach.

Approximately 52,000 virtual transects were constructed over the nearly 3,500 first-order subbasins at the YTC and required 4,800 CPU-hours (i.e., 200 days on a single processor computer) to complete. As described above, the coupled DHSVM-HEM models were parameterized for each of the approximately 10-20 virtual transects for each of the thousands of subbasins. Sufficient transects were used to characterize rangeland, unimproved roads, and firebreak roads within each subbasin. Sediment yield for each subbasin was calculated and then the DHSVM-HEM model results were related back into the spatial database. The specific sediment yield results for each of three land use and a combined total per subbasin are shown in Figure 29 - Figure 32.

The conditions determined by the VTM provide parameter inputs to the hydrology and erosion models and allow a consistent approach for determining sediment yield parameters at multiple scales (single subbasin to entire site). This modeling effort thus represents a heretofore unavailable methodology for using remote-sensing and geospatial technology to parameterize distributed hydrology and soil erosion models.

In a GIS environment, a site-wide sediment budget is calculated for thousands of virtual transects describing approximately 3,500 subbasins and represents a new and unique technology. The resulting sediment budget represents the extensive field data transects used for model calibration and evaluation, the thousands of virtual transects derived from remote sensing databases, the thousands of subbasin sediment yield calculations using state-of-the-art simulation models, and the GIS spatial analysis capabilities.

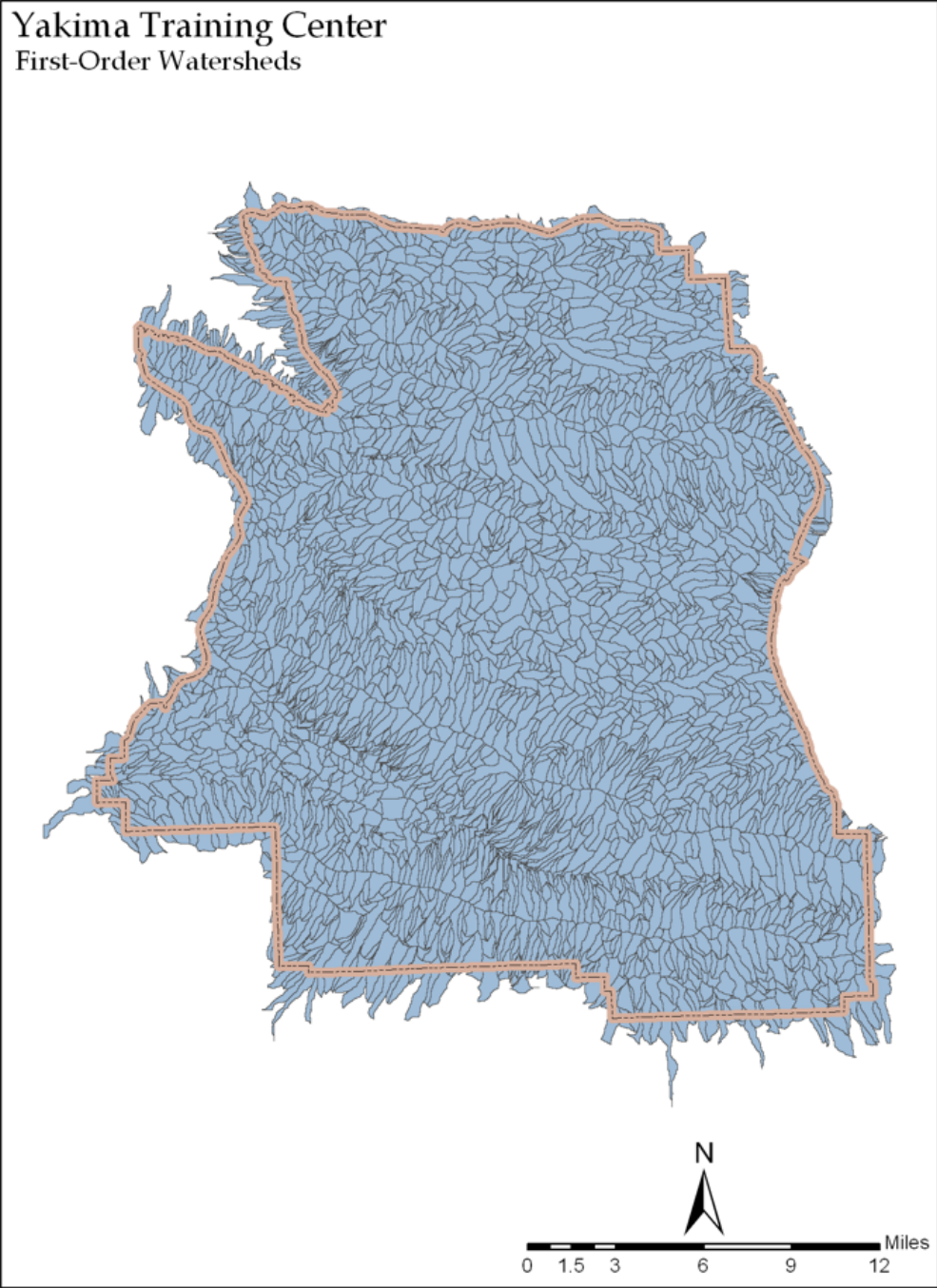


Figure 26. A total of 3,469 first-order subbasins were developed as a base for multi-scale sediment yield analysis.

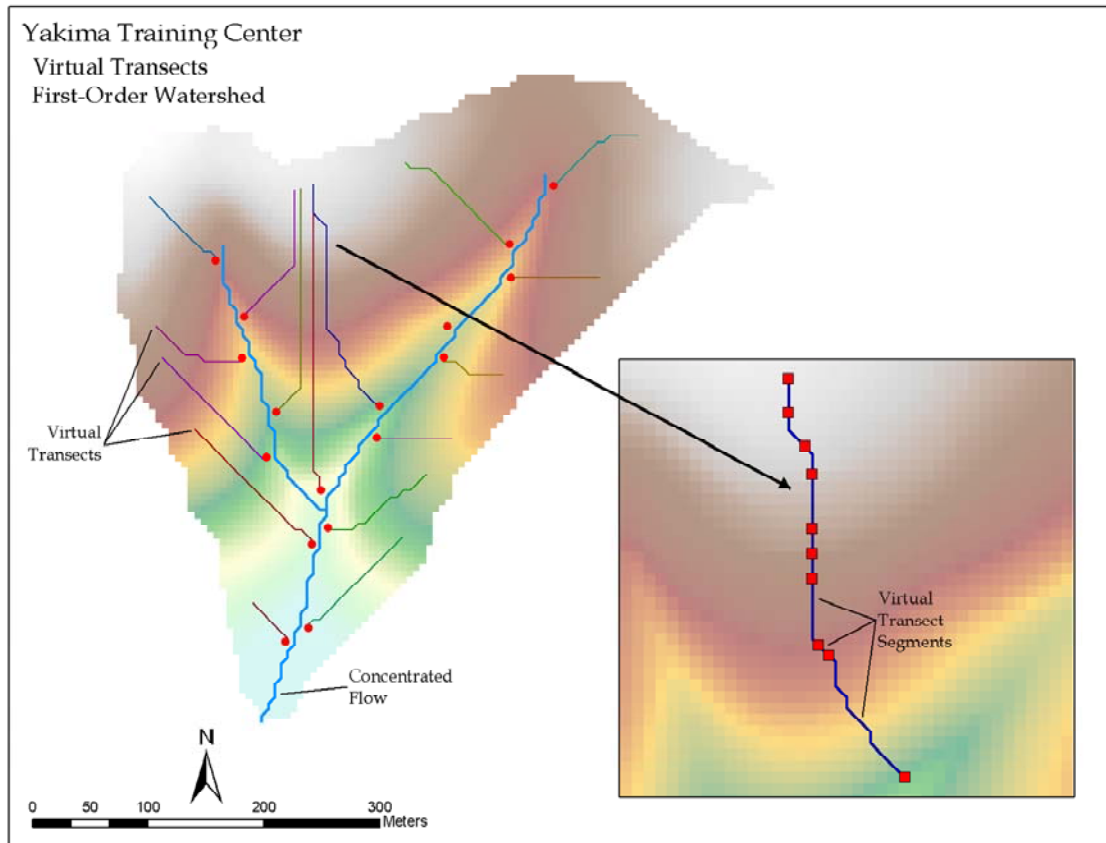


Figure 27. The Virtual Transect Model derives a flow path from a given starting point in a subbasin until it reaches a point of concentrated flow. A transect is broken into segments based on changes in slope.

Comparison Between Field-Measured and DEM-Derived Flow Paths - Pond 10

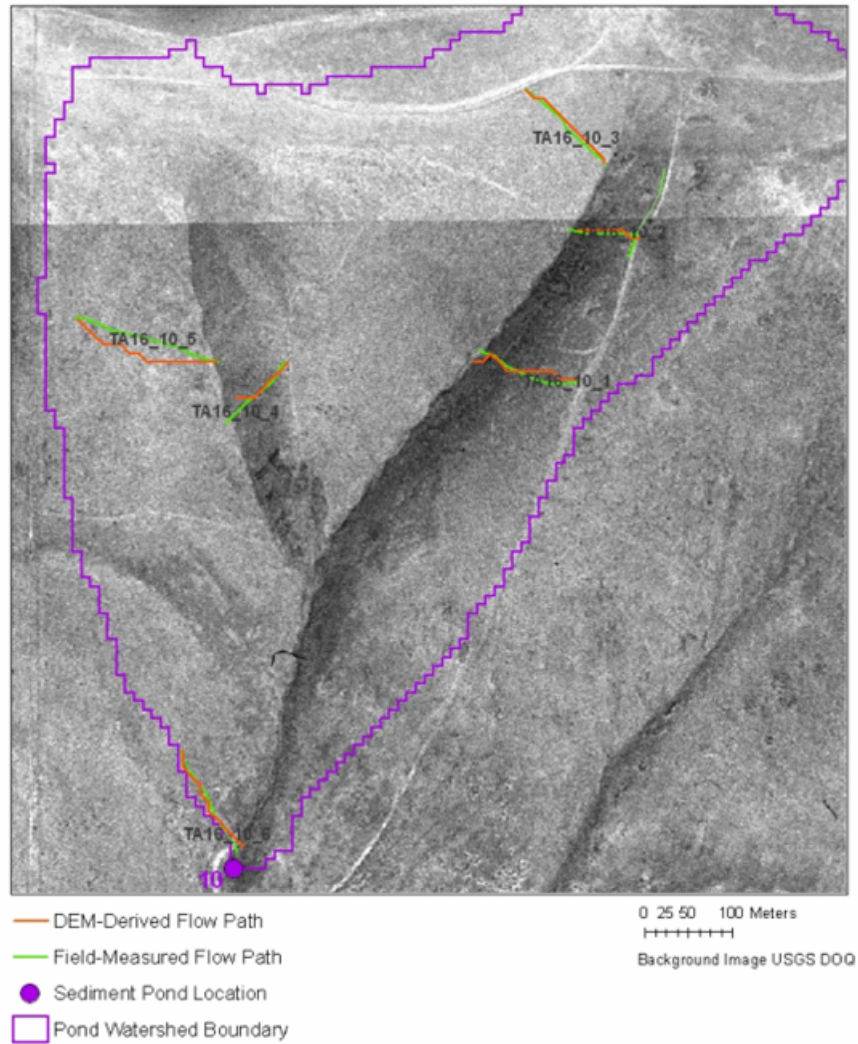


Figure 28. A spatial comparison of field measured flow paths and flow paths derived from the virtual transect model.

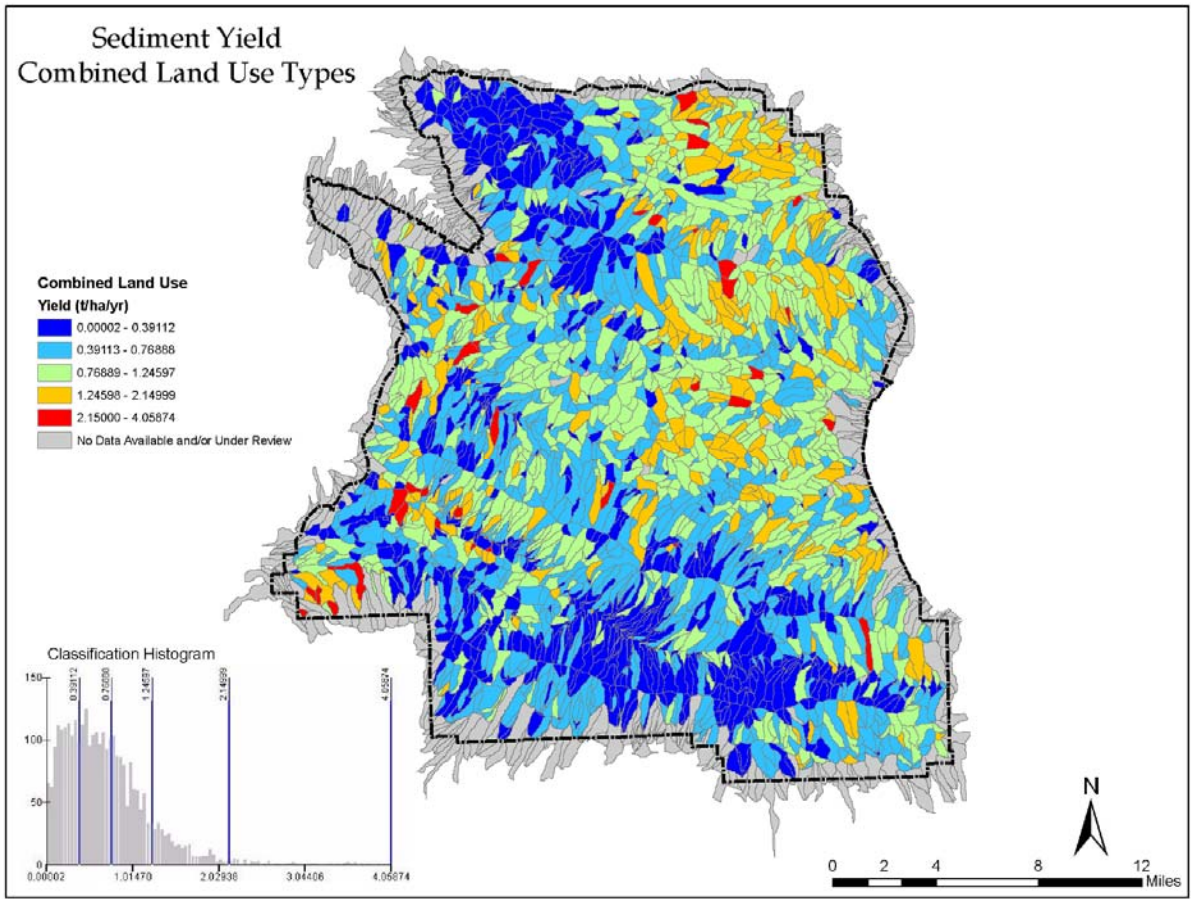


Figure 29. Total sediment yield (t/ha/yr) for subbasins fully contained within the YTC.

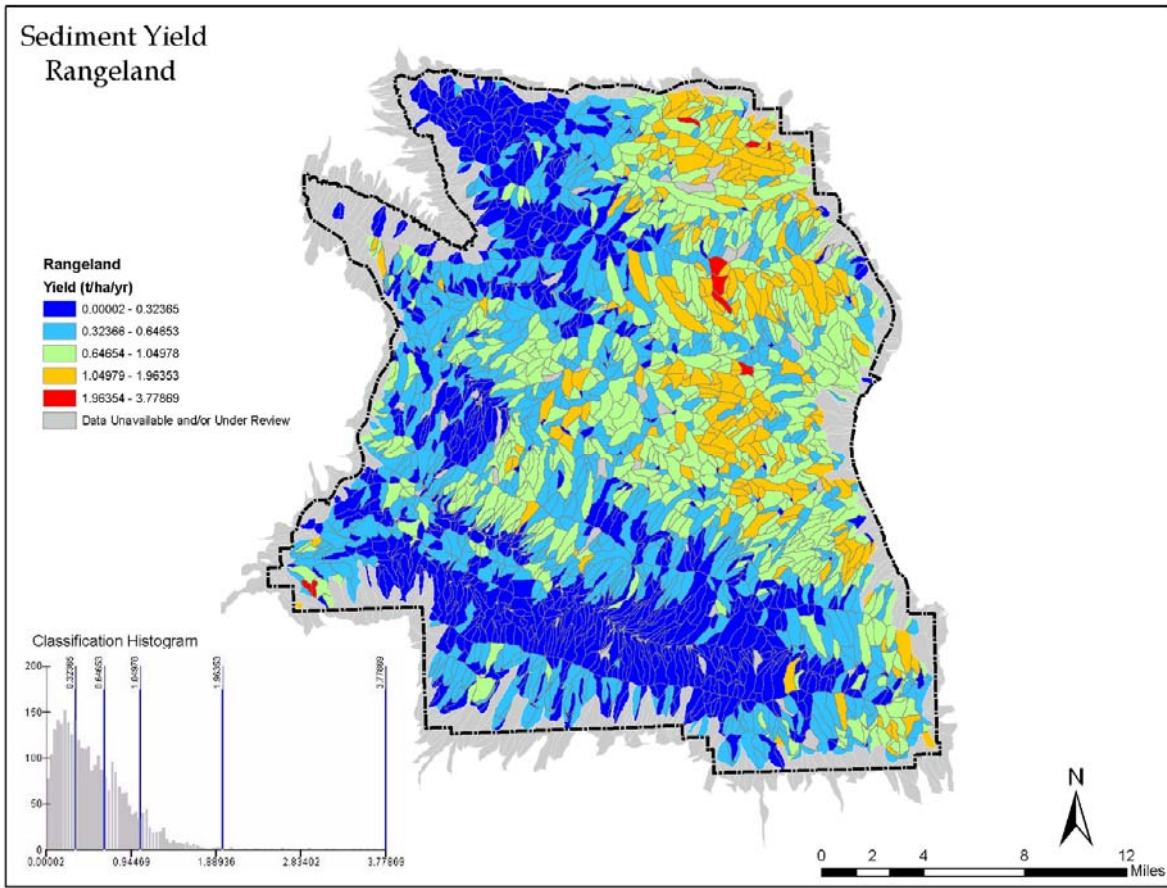


Figure 30. Sediment yield (t/ha/yr) generated from rangeland areas on subbasins fully contained within the YTC.

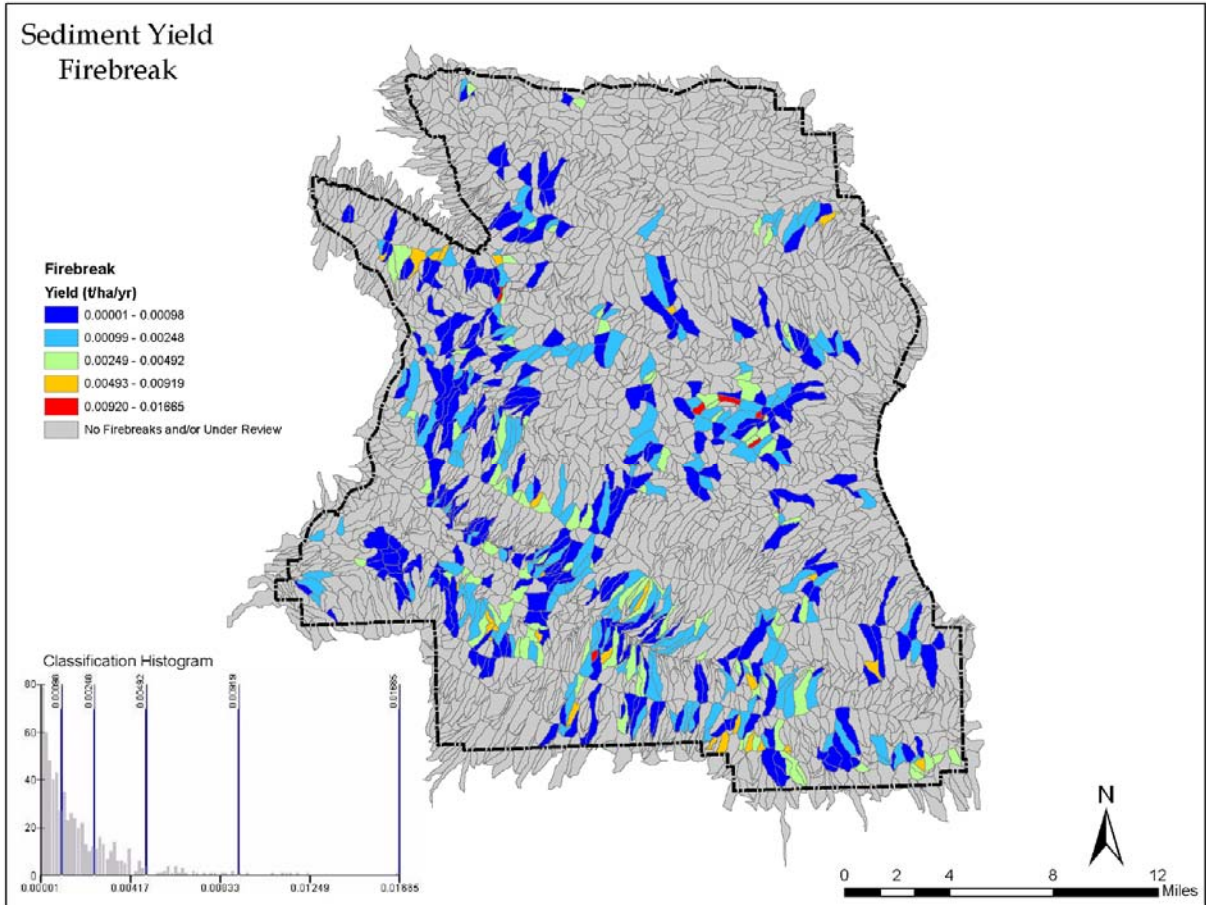


Figure 31. Sediment yield (t/ha/yr) generated from firebreaks. Only subbasins which contain firebreaks are shown.

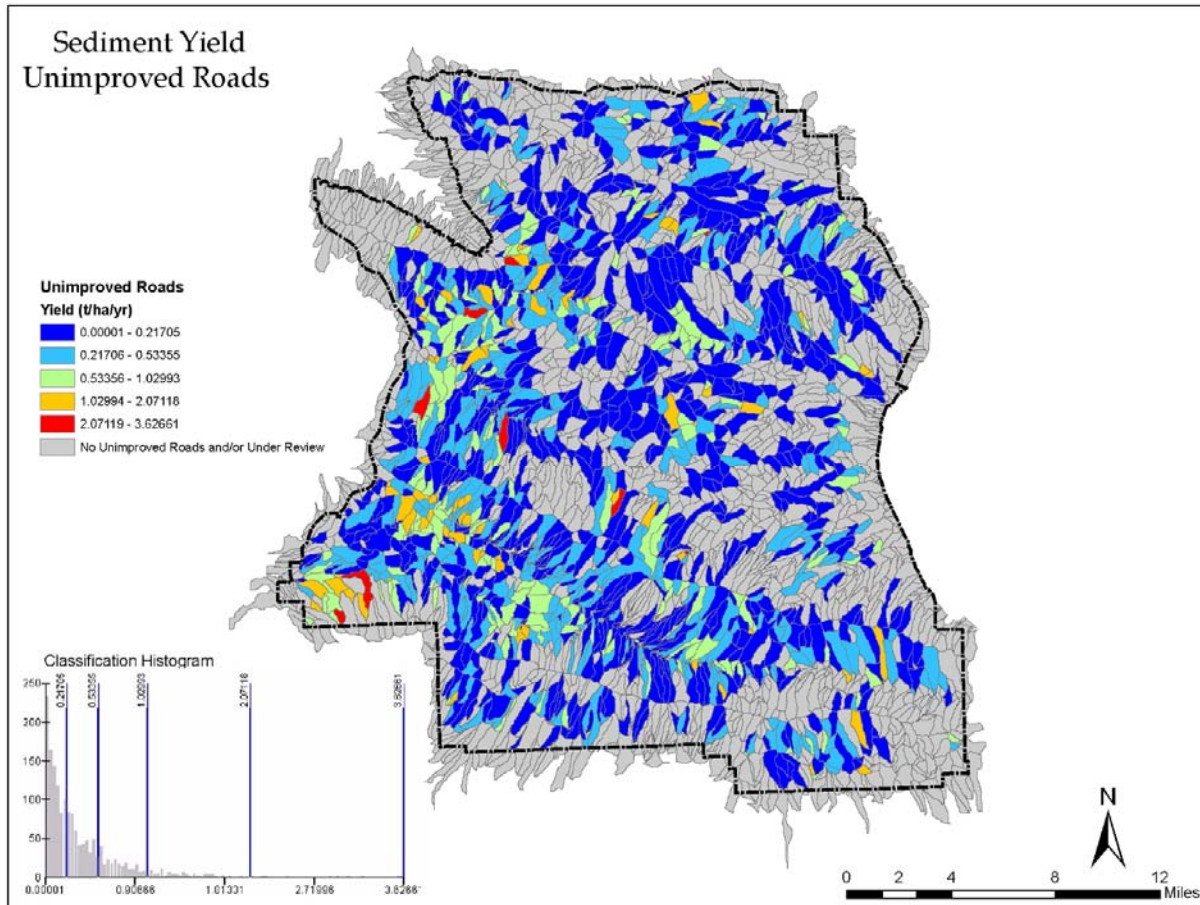


Figure 32. Sediment yield (t/ha/yr) generated from unimproved roads. Only subbasins which contain unimproved roads are shown.

4.7.3 Spatial Data Viewer

The Spatial Data Viewer is designed to allow the non-GIS specialist to easily navigate and query spatial data from the site sediment budget and associated vegetation and soils data. A large amount of valuable, detailed spatial data was developed in the preparation and post-processing of the YTC site-wide sediment modeling. The spatially based data were developed using GIS technologies and were tightly integrated to the modeling process. To provide input data and final modeling results into a format allowing decision processes by non-GIS personnel, an existing, off-the-shelf, freely available, and easy-to-use spatial data viewer was utilized (see Figure 33). The primary use of the spatial data viewer is to evaluate sediment yield conditions at the subbasin scale; however, other data including percent canopy cover, percent ground cover, soils, land use, hydrography, slope, aspect, erosion potential, elevation, flow direction, flow accumulation, and base imagery can all be accessed.

With the goal of providing a functional and easy-to-use decision environment, a simple user-interface based on Environmental Systems Research Institute's Java-based ArcExplorer software allows for easy identification of classified sediment yield areas and provides an interactive query

capability so the user can view the underlying database information (see Figure 34). This database provides information such as subbasin area, total subbasin sediment yield, sediment yield by land use type, mean elevation, mean slope, soil types, mean percent canopy, and mean percent ground cover. If the user requires additional information about the ground conditions within a subbasin, the aforementioned data themes can simply be loaded or turned on to help inform the decision maker. In addition to the basic maneuvering and query capabilities of the viewer, the user has the ability to reclassify data to define more detailed sediment yield patterns. The user also has the ability to develop customized data queries (e.g., define subbasins with silt loam soils and a combined sediment yield > 3.2 t/ha/yr), add a user's own data for overlays or access web-ready data via WMS (e.g., National Wetlands Inventory), develop customized map layouts, and perform linear measurements. Any altered ArcExplorer sessions can be saved and reopened for use later or for use by others.

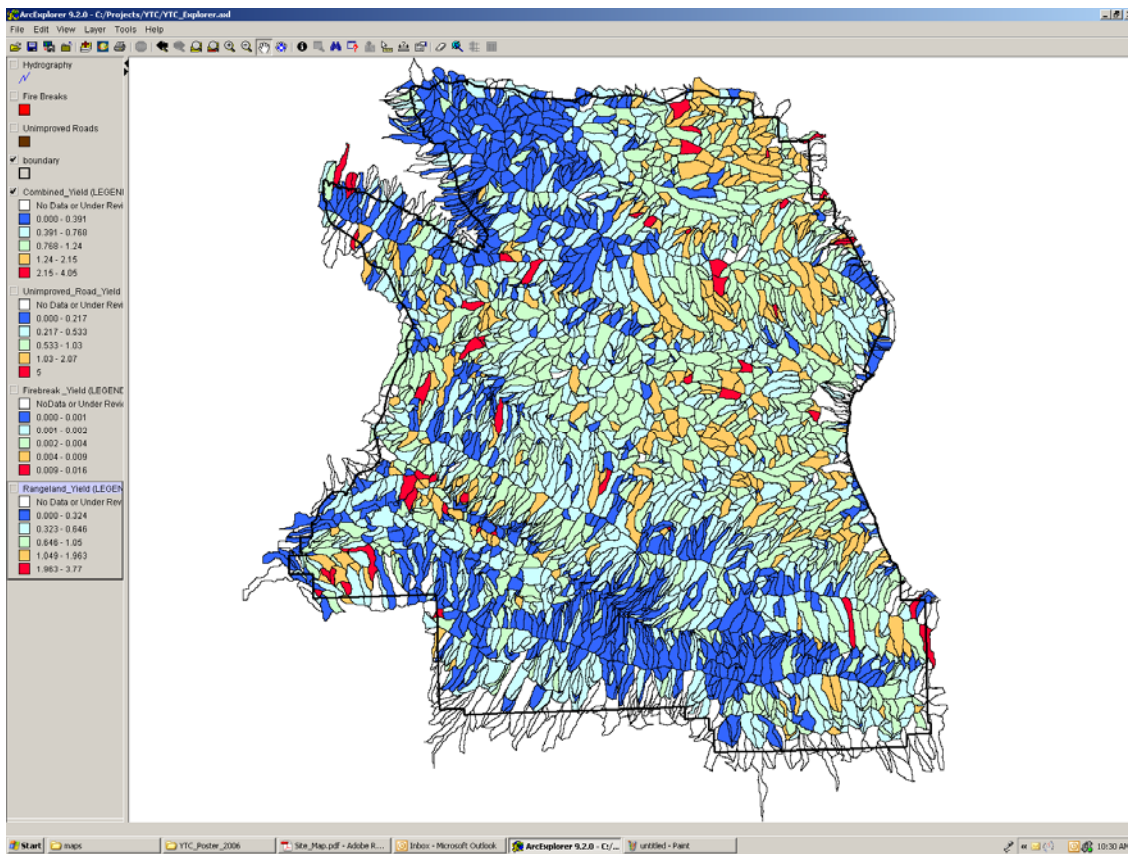


Figure 33. An easy-to-use spatial data viewer was developed for the YTC to allow easy access to spatially based model input and modeled sediment yield results.

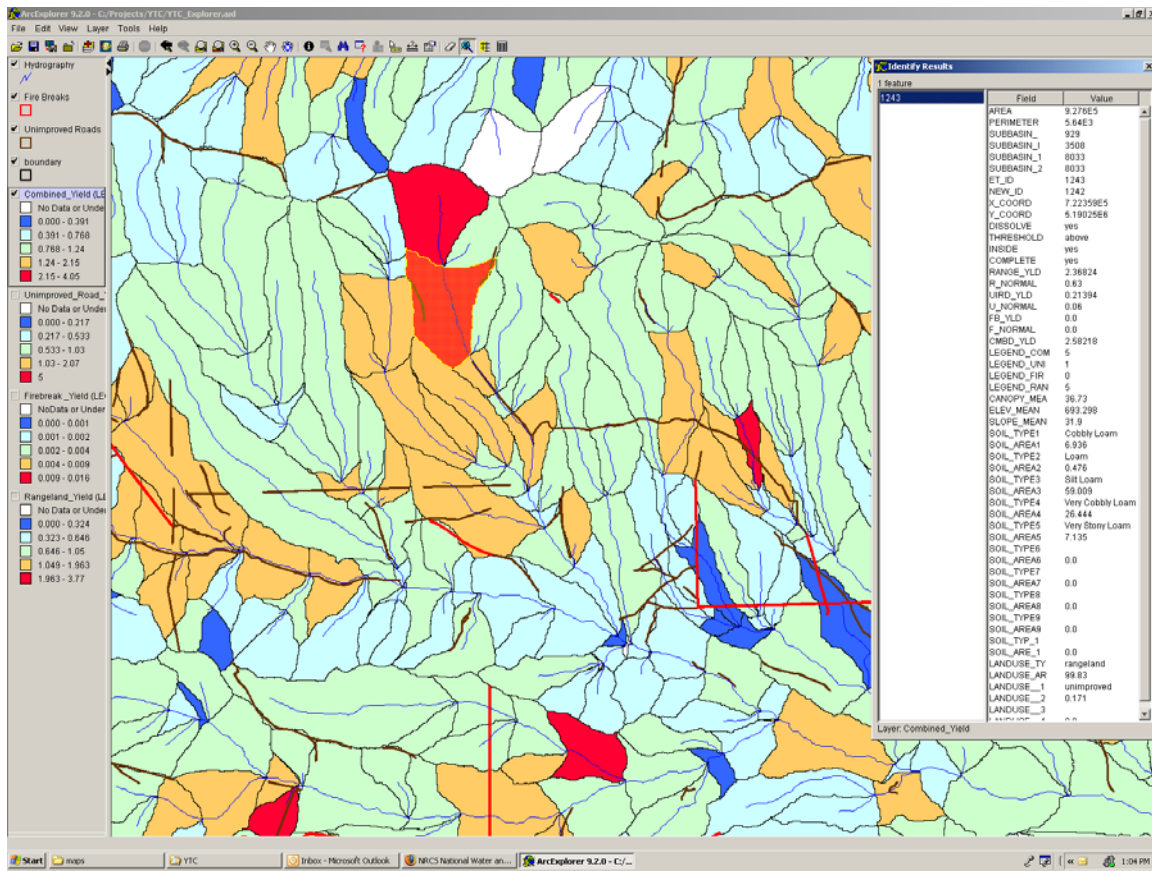


Figure 34. The spatial data viewer allows interactive queries to the underlying database of information, which includes information on sediment yield, soil types, land use, canopy, and ground cover. Also shown is the presence of unimproved roads (brown) and firebreaks (red) overlain on the classified subbasin boundaries.

4.8 Spatial and Temporal Analysis of Sediment Yield

The combined application of remote sensing, field data collection, geospatial analysis, distributed hydrologic modeling, and statistical analysis technologies allow new and unique methods of understanding and predicting watershed processes across a range of spatial scales from the hillslope to the subbasin to watersheds/basin and to the entire YTC. The associated temporal scales range from minutes for infiltration calculations to hours for runoff events on subbasins to daily water balance calculations, to annual yields and to several decades used to describe mean annual runoff and sediment yields across the spatial scales described above.

4.8.1 Basin-Scale Sediment Yield

To describe mean annual sediment yield on the 130,000 ha YTC, 3031 subbasins were used, as shown in Figure 29. Simulations of 42 years of runoff, soil erosion, and sediment yield were used to compute the mean annual sediment yield from each subbasin. The mean subbasin size

was 42.9 ha with an SD of 33.7 ha. To focus on topography, soils, vegetation, land use, and land-management practices and how their combined spatial variability influenced sediment yield across the entire YTC, we eliminated spatial variability of precipitation from this particular analysis. Long-term meteorological data (42 years of record) from the Yakima Airport site were used as climatic input for the simulations at the YTC.

With respect to the YTC mean annual sediment yield map, an obvious question is how these data are interpreted in the context of management and land-use decisions. These questions include the following:

1. Can the spatial distribution of sediment yield be used to target specific subbasins for treatment/rehabilitation efforts to reduce sediment yield from the YTC?
2. How does one maximize return on investment from rehabilitation of subbasins to minimize soil erosion and sediment delivery to streams?
3. Can the spatial distribution of sediment yield be used to schedule training/land use events to minimize resulting impacts on sediment yield while maximizing available training area?
4. When conducting water quality analyses, e.g., the TMDL procedure, if a water body is impaired, then the contaminant source area must be determined. If the contaminant is sediment, can the basin-wide sediment yield map be used to determine those source areas?

A map of YTC similar to Figure 29, but showing sediment yield from only those subbasins that contain firebreak roads, is shown in Figure 31. Notice the utility of being able to geospatially represent sediment yield from firebreak roads. A glance at Figure 29 gives information sufficient for targeting firebreak road management to reduce sediment yield on the YTC. Moreover, quantitative information is available for each subbasin with firebreak roads and sediment yield from the entire subbasin, from individual and from aggregated firebreak roads within the subbasin (see Section 4.7.3) for a description of the “Spatial Data Viewer”).

Similar maps (shown in Section 4.7) are available for only subbasins with unimproved roads and for only rangeland subbasins (without firebreak or unimproved roads). Thus, YTC land-management personnel now have the new and unique ability to display, and quantify simulated sediment yield by subbasin, and for the entire YTC, including various land uses such as firebreak roads, unimproved roads, and roadless rangeland areas.

Therefore, the geospatial analyses allowing mapping, quantification, and statistical analyses of subbasin sediment yields for a variety of land uses greatly enhances the opportunity to evaluate alternative management and land-use practices and thereby develop alternative management and land-use scenarios based on available site data and state-of-the-art simulation modeling results in useful visual and numerical forms. Moreover, because the soil erosion and sediment yield calculations are based on physical features of the landscape (i.e., presence or absence of roads, soils, topography, vegetation canopy cover, and ground surface cover), these distributed results

and the resulting maps are useful for several purposes. For example, in targeting areas for periodic monitoring and for remediation measures, especially those protecting or enhancing vegetative cover and minimizing soil surface disturbance.

The data shown in Figure 29 represent more than 3000 subbasins. To obtain a summary of the information presented, mean annual sediment yield by subbasins was binned into five class intervals, as shown in Table 7.

Table 7. Sediment yield class intervals by subbasins for the YTC. Computed values of sediment yield are from the DHSVM-HEM model in units of t/ha/y.

Class & Number in Class	Class Limits (t/ha/y)	% of YTC Area	% of YTC Sediment Yield	Comments
1 - 935	0.00–0.39	25.2	9.3	Lowest Yields
2 - 976	0.39–0.77	32.6	26.6	
3 - 760	0.77–1.24	28.7	34.9	
4 - 310	1.24–2.15	11.4	22.5	
5 - 50	2.15–4.05	2.0	6.6	Highest Yields

The percent of YTC area vs. the percent of YTC mean annual sediment yield data are shown in Table 7. Notice that the highest sediment yield class, #5: 2.15–4.05 t/ha/y, represents 2% of the total area but produces about 6.6% of the total sediment yield. The lowest sediment yield class, #1: 0.00–0.39 t/ha/y, represents 25.2% of the total area but only produces 9.3 % of the total sediment yield.

YTC Spatial Distribution of DHSVM-HEM Simulated Sediment Yield by Class Intervals

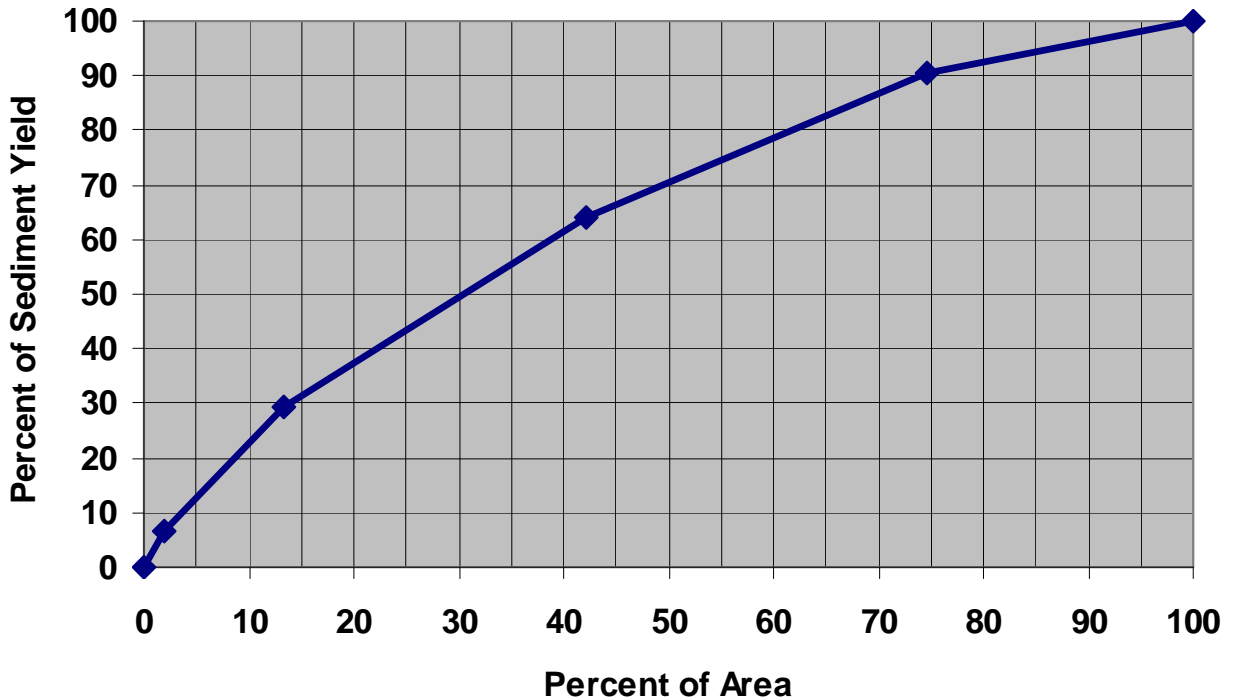


Figure 35. Illustration of the relationship between the percent of the YTC area and the percent of the total sediment delivery to streams. Simulations are for 42 years using the DHSVM-HEM model.

4.8.2 Interpretation and Utilization of Distributed Sediment Yield Data

Only 13% of the drainage area at YTC contributes nearly a third of the total sediment yield (classes 4 and 5 in Table 7 and Figure 35). By targeting rehabilitation measures for sediment yield reduction on the subbasins—making up this 13% of the area that reduced sediment yield by 75%—overall YTC sediment yield would be reduced by approximately 20%. Thus, targeting the higher sediment yield subbasins appears to be a logical approach. This approach would ensure maximum return on investment of rehabilitation funds.

Avoiding or minimizing training/land-use activities that increase sediment yield on only about 13% of the YTC area could have significant payoffs in preventing increases, or causing decreases, in mean annual sediment yield.

Impaired water bodies at YTC that trigger a contaminant source area analysis, could directly use information shown in Figure 29 to determine these source areas and to quantify their impacts.

The curve and its shape, shown in Figure 35 contain significant information about the spatial distribution of sediment yield. The curve is convex showing that the fraction of the subbasins with highest sediment yield dominates sediment delivery to streams. A management philosophy that targeted, or ranked in priority, those high sediment yield subbasins for remediation measures, in general, would maximize return on investment on erosion control measures. Of course, some streams may be more important for a variety of reasons, and this is easily included in the prioritization for remediation.

4.8.3 Temporal Variations in Sediment Yield – Role of Large Storms

Under a wide variety of land-use and climatic conditions and at locations around the world, we have found that large storms dominate sediment yield from experimental plots and small watersheds (e.g., Lane 2007).

For example, time series of sediment yield from two cropland areas and two semiarid rangeland areas in the United States and one subtropical area in New Zealand behave similarly with regard to the dominance of large storms in determining total sediment yield. The questions of relevance herein include the following. Are similar patterns observed in the Northwest, specifically at the YTC, and do the coupled DHSVM-HEM simulation models capture the dominance of large storm aspects as observed from monitoring data?

Because similar patterns of large storm influence have been found throughout the United States, we infer that similar patterns exist at the YTC. These areas include the previously mentioned experimental locations at Kingdom City, Missouri; Treynor, Iowa; Tombstone, Arizona; Santa Rita, Arizona; other sites in New Mexico, Idaho, and Colorado; and in New Zealand. We have demonstrated that the HEM captures these patterns observed in the measured data. Therefore, we have increased confidence that if the DHSVM-HEM models reproduce these patterns at the YTC, that both empirical data and theory (simulation modeling results) support the assumption of large storm dominance of sediment yield at the YTC.

The relation between storm size and sediment yield from a small hillslope watershed (Lucky Hills 5, 0.182 ha, semiarid rangeland) is shown in Figure 36. The top curve in this graph is for observed data for 40 events. Notice that the single largest event (% of events = $1/40 = 2.5\%$) accounts for approximately 35% of sediment yield from all 40 events. The calibrated HEM model applied to this watershed produced the results shown in the lower curve. Again, notice that the single largest simulated event accounted for approximately 25% of the sediment yield from all 40 events. In fact, the HEM model over predicted the mean sediment yield by about a third (observed mean = 103 Kg, simulated mean = 131 kg, Figure 36), but it under predicted the largest event as shown in the regression equation in Figure 36; $\text{Simulated} = 39 + 0.89 * \text{Observed}$. However, the shapes of the observed data and simulated curves are similar and both would lead to the conclusion that a few large events dominate total sediment yield from this watershed.

**Walnut Gulch, AZ HEM Calibration Data for Hillslope
Watershed Lucky Hills 5**

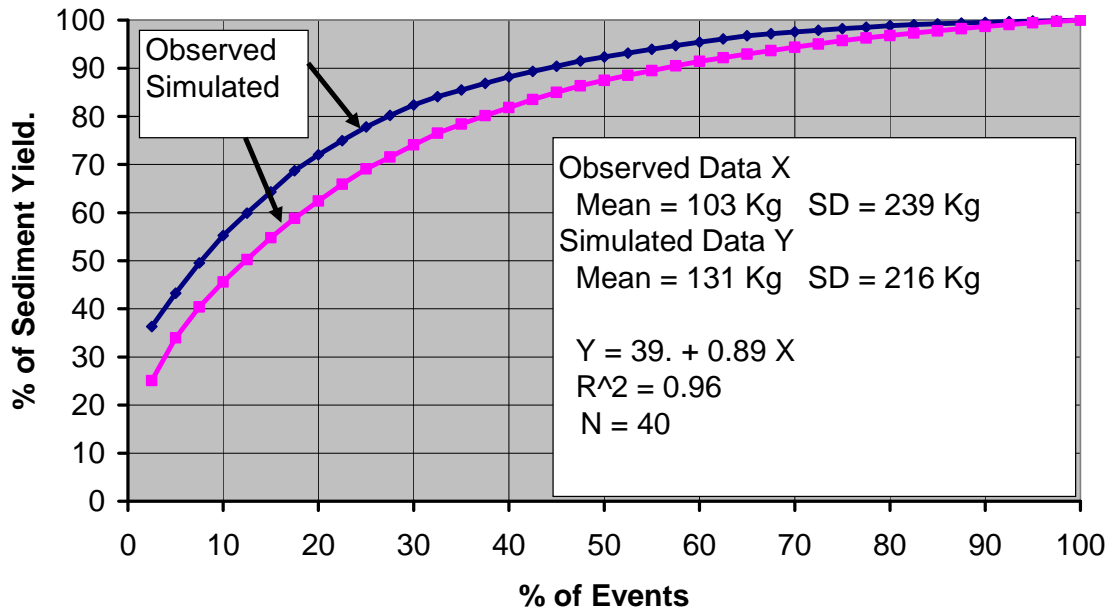


Figure 36. Illustration of the role of large storms in determining sediment yield from a small rangeland watershed in Arizona, United States.

The relation between storm size and sediment yield from experimental erosion plots in North Island, New Zealand (Pukekohe, bare plots 1 and 3, 0.0041 ha, cultivated cropland), is shown in Figure 37. The curves in this graph, labeled “observed” and “simulated,” are from data for 27 events. Notice that the single largest event (% of events = $1/27 = 3.7\%$) accounts for approximately 19% of sediment yield from all 27 events. The calibrated HEM model applied to this watershed produced the results shown in the simulated curve. Again, notice that the single largest simulated event accounted for approximately 28% of the sediment yield from all 27 events. In fact, the HEM model over predicted the mean sediment yield by about 10% (observed mean = 9.7 Kg, simulated mean = 10.9 kg, Figure 37), but slightly over predicted the largest event as shown in Figure 37 and the regression equation in Figure 37; Simulated = $0.93 + 1.03 \times$ Observed. However, the shapes of the observed data and simulated curves are similar and both would lead to the conclusion that a few large events dominate total sediment yield from these plots.

As stated earlier, similar analyses at various locations in the midwest and western United States have produced a similar conclusion: large storms dominate mean annual or total, sediment yield from plots and small watersheds. Therefore, empirical data and simulation modeling suggest that this is also the case for subbasins and watersheds at the YTC.

Pukekohe, NZ HEM Validation Data for Bare Plots 1 & 3

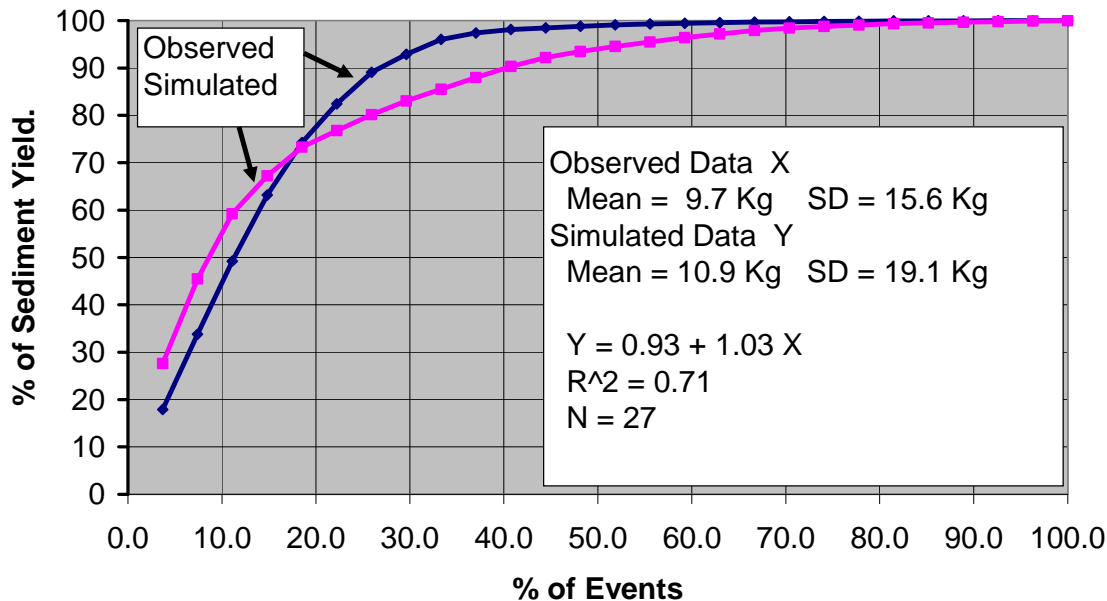


Figure 37. Illustration of the role of large storms in determining sediment yield for bare plots on cropland soils in New Zealand.

In cases such as the above two examples where the period of record is short, it is advantageous to use individual sediment yield events compared to the total sediment yield from all events. In other cases where longer observed or simulated periods of record are available or where mean annual, rather than mean event, sediment yield is of interest annual values of sediment yield are often used.

Lawrence (1996) presented annual sediment yield from four small watersheds on the Santa Rita Experimental Range near Tucson, Arizona. Four of these small watersheds (1.06 to 4.02 ha) with gullies are the subjects of this study. In 1974, two of the watersheds (6 and 7) were treated to control the invasion of mesquite (*Prosopis velutina* Woot.), and were subsequently retreated as needed. Watersheds 5 and 8 remained untreated. Grazing practices include yearlong cattle grazing on two watersheds (7 and 8) and a rotation system on the other two watersheds (5 and 6). Treatment and management have remained constant since the beginning of the study. The watersheds are instrumented to measure precipitation, surface runoff, and sediment yield (Lawrence 1996).

Annual sediment yields for each of the 16 years from 1976 to 1991 were computed and from them a mean annual sediment yield for all 16 years was computed for each of the small

watersheds. In a slight variation of the previous analyses, contributions of sediment yield from the individual years (not events) were used to analyze the relationship between sediment yield in “large sediment yield years” and the 16-year total sediment yield. The results of these analyses are shown in Figure 40.

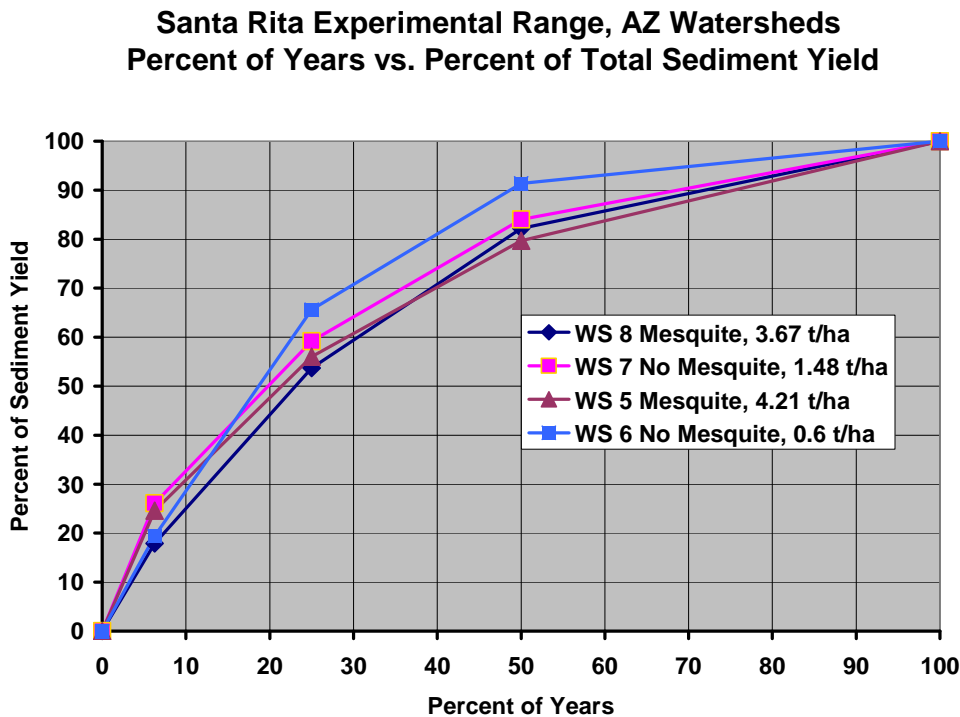


Figure 38. Illustration of the role of large storms in determining mean annual sediment yield from four small rangeland watersheds in Arizona, United States.

Notice that these curves are somewhat “flatter” than in the previous two graphs because annual rather than individual event data were used. Summing all the individual events in a year, to produce annual sediment yield, results in smoothing the data.

4.8.4 Role of Large Storms in Determining Sediment Yield at the YTC

The DHSVM-HEM model was calibrated using data from the Hanford Site and from 12 sedimentation ponds on the YTC. After calibration, the model was used with 42 years of meteorological data from Yakima, Washington (extended to the YTC),¹

for simulating mean annual sediment yield on more than 30,000 individual hillslope transects used to estimate subbasin sediment yield for 3031 subbasins on the YTC. In this section, we examine the importance of large storms in determining mean annual sediment yield for hillslope transects at the YTC. The results shown in Figure 39 are for all transects over the 42-year period.

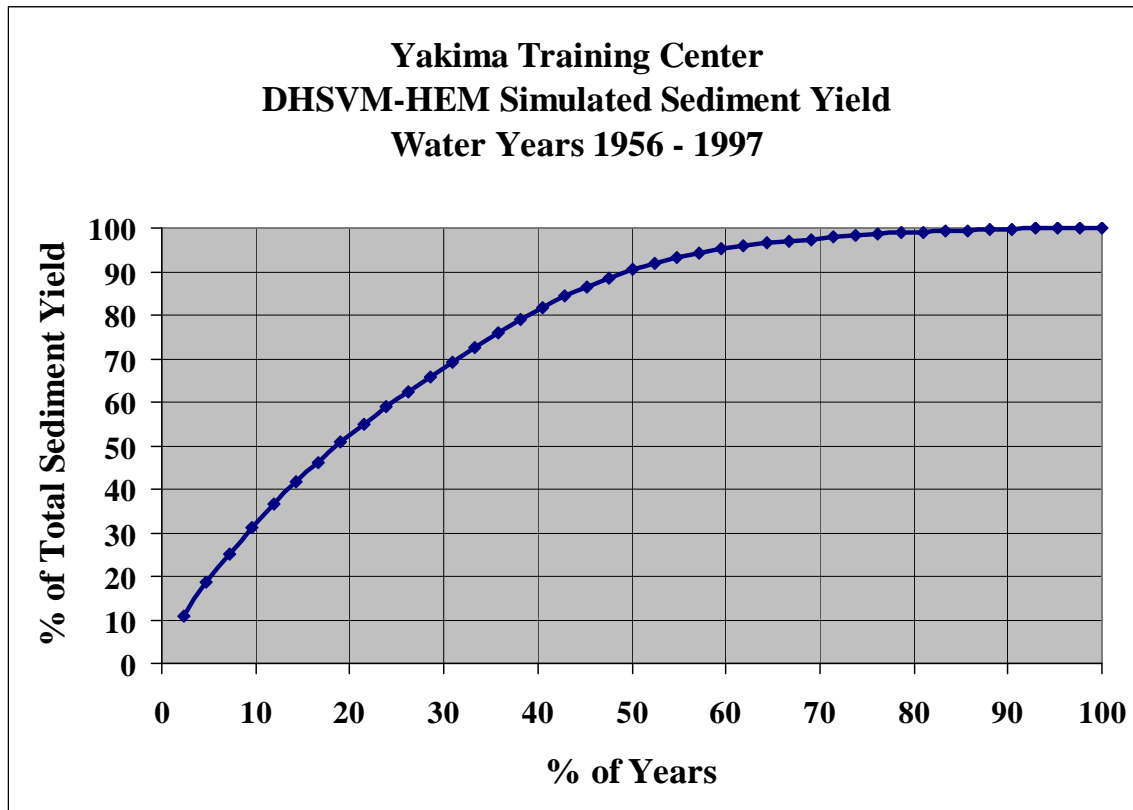


Figure 39. Illustration of the role of large storms in determining mean annual sediment yield from all transects on the YTC.

Notice that the single largest sediment yield year (percentage of years = $1/42 = 2.4\%$) produced more than 10% of total sediment yield in the entire 42-year period. In addition, the four largest years produced more than 30% of the total sediment yield. Finally, the combined sediment yield from the largest half of the 42 years produced more than 90% of the total sediment yield.

The curve in Figure 39, from simulation model results, is quite similar in shape to the curves in Figure 38 from measured data. This suggests that the DHSVM-HEM model is preserving the property of large storm dominance of long-term or mean annual sediment yield from small watersheds.

4.8.5 Discussion

The question of scale effects in hydrology has been a principal scientific problem in for decades. Synergistic effects of combining databases from long-term watershed monitoring programs, geospatial data acquisition and analysis technology, distributed hydrologic modeling, and targeted field data acquisition programs have resulted in a new and unique ability to simulate spatial and temporal sediment yield across a range of space-time scales. However, this has not

been purely a theoretical result of synergy; it has broad practical applications. Hydrologic problems positively impacted by these new developments include the development of targeting monitoring and remediation efforts to maximize return on investment of remediation resources to that fraction of the landscape producing soil erosion and sediment yield at a much higher rate than the spatial average. Implicit in these developments is the ability to display and analyze geospatial data based on combining sound scientific modeling procedures with improved databases.

Temporal analyses and results have profound implications for monitoring programs, hydrologic and hydraulic design criteria, and simulation model evaluation using extreme event simulation, within a long time series, to replicate the large storm dominance on sediment yield, as observed in nature. Simulation models, which lack the ability to account for the significance of large storms in a time series, are of limited value in determining required monitoring periods, estimating frequency distributions for event or annual sediment yields, and thus designing hydraulic structures based on exceedance probabilities, or evaluating management actions against typical environmental regulatory requirements,. In summary, simulation models, which do not reproduce the large storm dominance of sediment yield (e.g., USLE/RUSLE), significantly underestimate uncertainty of the processes producing soil erosion and sediment yield. The same is true for models that do not capture the spatial distribution of sediment yield.

Fortunately, the synergistic effects of combining databases, geospatial technology, distributed simulation modeling, and simulation models that capture the large storm dominance features on sediment yield were developed over expanded space-time scales to meet the needs of managing natural resources on large military training areas such as the YTC.

4.9 Decision Support Systems

A DSS, as used in SERDP Project SI-1340, is an integrative tool involving databases, simulation models, decision models, expert judgment, and alternative evaluation and comparison capabilities. As such, it is also an integral part of an AM system. The DSS research done for this project has resulted in the development and refinement of a spreadsheet version of the DSS.

4.9.1 The Spreadsheet Implemented Multi-objective Decision Support System (SIMDSS)

A SIMDSS uses a combination of decision variables (each quantifying an objective) to score each alternative management practice being valuated. The existing, or reference, management system by definition scores 0.5 on each decision variable. All other alternatives use a scoring function (defined by the existing management system and normalized to a range of [0,1] to score each decision variable). The individual scores are then “rolled up” using the following objective function for each of the i alternatives over each of the j decision variables.

$$G_i = \sum (S_j)(W_j) \quad (22)$$

where S_j is the score, and W_j is the weight for decision variable j .

Subject to:

$$W_1 \geq W_2 \dots W_n \quad (23)$$

and

$$\sum (W_j) = 1 \quad (24)$$

The procedure is to minimize equation (22) subject to constraints in equations (23 and 24) to get the minimum possible score for alternative *i* and then to maximize equation (22) subject to the same constraints to get the maximum possible score for alternative *i*, representing the worst and best possible performance of a given alternative under all combinations of weights subject to the selected preference order. A preference order for the importance of the decision variables (evaluation criteria) is specified in equation (23), and the sum of the weights over all decision variables must equal 1.0 is stated in equation (24). Notice that the user need not specify values for the weights, only their preference order and equation (22) computes a total score for all possible combination of weights.

Values of *G* from equation (22) are limited to the range 0 to 1, the average score for an alternative is the average of its minimum and maximum score, and the average score for the existing or reference management system is 0.5 by definition. The SIMDSS performs the above calculations and displays them graphically to assist the user in making a decision.

4.9.2 Example Application – Analysis of Firebreak Road Alternatives

The initial or data entry page of the spreadsheet is illustrated in Figure 5.8.2.1. The left-most column labeled “Decision Support System” has a “Solve/Solved” button to make the calculations shown in equations (22) and (23) and return the minimum, maximum, and average score for each alternative. The green “Solved” button, shown in Figure 40, is displayed after the spreadsheet has been updated and solved. The button changes to a red “Solve” label immediately after a change has been made to the spreadsheet, notifying the user that the system must be solved to reflect the changes. The next cell in column 1 is labeled “Management Alternative,” and it has – and + buttons to subtract alternatives removed from consideration, or to add rows for new alternatives. Each numbered cell below the “Management Alternative” cell briefly describes each alternative management system for firebreak roads at the YTC.

Decision Support System Solved		Totals		Evaluation Criteria & Objectives								
				1			2			3		
				Control Fire			Reduce Soil Erosion			Reduce Total Costs		
Management Alternative	Nmlzd Pts Min	Nmlzd Pts Max	Rank:	1		Rank:	2		Rank:	3		
	Wt Min	Wt Max	Score (10 best)	Wt Min	Wt Max	Score (10 best)	Wt Min	Wt Max	Score (10 best)	Wt Min	Wt Max	
	Pts Min	Pts Max	Pts Min	Pts Max	Pts Min	Pts Max	Pts Min	Pts Max	Pts Min	Pts Max		
1 REFERENCE ALTERNATIVE Current Management, Grade Firebreak Roads	0.50	0.50	Always Scores as 5			Currently acceptable			Assume cost index of 100.			
	100%	100%	5	34%	33%	5	34%	33%	5	32%	33%	
	5.0	5.0		1.7	1.7		1.7	1.7		1.6	1.7	
2 Construct Turnouts at Engineered Intervals	0.50	0.60	No Impacts			Breaks up downslope flow of water and diverts it			Cost index = 120			
	100%	100%	5	98%	50%	7	1%	50%	4	1%	1%	
	5.0	6.0		4.9	2.5		0.1	3.5		0.0	0.0	
3 Construct Turnouts at Engineered Intervals and Add Gravel at Specified Locations	0.47	0.64	No Impacts			Breaks up downslope flow, diverts it, and protects some road crossings, etc.			Cost Index of 200			
	100%	100%	5	33%	50%	8	33%	50%	1	33%	1%	
	4.7	6.4		1.7	2.5		2.7	4.0		0.3	0.0	
4 Construct Turnouts at Engineered Intervals, No Gravel, Use Herbicides, and thus Less Frequent Grading	0.67	0.84	Herbicides control regrowth and make grading effects longer lasting			Breaks up downslope flow of water and diverts it. Less disturbance to bare soil			Cost Index of 140			
	100%	100%	8	33%	50%	9	33%	50%	3	33%	1%	
	6.7	8.4		2.7	4.0		3.0	4.5		1.0	0.0	

Figure 40. Illustration of the data entry page for the SIMDSS. Alternatives are shown in the left-most column, and decision variables (evaluation criteria) are shown in the columns under the row labeled “Evaluation Criteria and Objectives.”

In this example, the decision variables (evaluation criteria) are efficiency of fire control, reduction of soil erosion rates, and total costs. This is a simple example with only three evaluation criteria, or decision variables, and four alternatives.

The first alternative (Alternative 1) is the existing or reference alternative and represents how firebreak roads are currently constructed and managed by periodic grading to remove vegetation. The second alternative (Alternative 2) is the same as the first except that water turnouts are constructed at engineered intervals (optimal spacing as calculated with the erosion simulation model). This reduces the effective slope length of the firebreak roads by diverting flowing water off the roadway at specified intervals along the road. As a result, rill and gully erosion are reduced.

The third alternative (Alternative 3) is the same as Alternative 2 except that water turnouts are constructed and gravel/cobble is added to critical points such as small stream crossings. This further reduces soil erosion by eliminating what are essentially point sources of erosion. As a result, total erosion from the firebreak roads is reduced further.

The fourth alternative (Alternative 4) has engineered turnouts, no gravel/cobble added at critical spots, and the use of herbicide on the firebreak roads and bar ditches for maintenance to control vegetative growth and reduce the number of annual road gradings required. Alternative 4 is unique in that it simultaneously increases the effectiveness of fire control, reduces soil erosion by decreasing the soil disturbances due to grading, and reduces total costs by eliminating the expensive practice of gravel/cobble additions at critical points. As a rule, the more objectives an alternative positively influences, the more likely it is to score high.

The next two columns labeled “Totals” contain the minimum and maximum total scores for each alternative. These are obtained by solving equations (22) and (23) for each decision variable (evaluation criteria), in this case effectiveness of fire control, reduction in soil erosion (shown), initial costs, maintenance costs, and user acceptance (not shown) and for each alternative. Notice that the minimum and maximum scores are 0.5 for the reference alternative and vary from a minimum of 0.67 to a maximum of 0.84 for Alternative 4. The remaining cells in column 2 provide additional technical details to verify that the DSS is operating correctly. For example, the small cells directly below the minimum and maximum total score for the alternatives all read 100% verifying that the sum of the weights for all of the objectives sum to 1 or 100%. Finally, the two cells below those with 100% list the minimum and maximum non-normalized points (10 times the minimum and maximum normalized points or normalized score and represent intermediate calculations used in verification of the DSS). Most users can ignore these smaller cells in column 2.

The second and third cells in columns 3-5 list the criteria number and a brief description of the criteria/objectives. The cells labeled “Rank:” give the preference order for each objective. In this example, Control Fire outranks Reduce Soil Erosion, which outranks Reduce Total Costs. The user can easily change the preference orders by clicking on these cells and entering the new ranks. Notice that after all changes are made in the spreadsheet entry, the new solution is obtained by clicking on the “Solve/Solved” button in the first cell of column 1.

The first cell for each alternative in columns 3-5 gives a brief narrative description of how each alternative influences that objective. For example, in column 4, these narrative entries explain how each alternative influences soil erosion. The left-most cell directly below each narrative gives the score (on an integer scale of 1-10) of how each alternative is evaluated relative to the reference alternative with respect to all the objectives. Alternative 1 is the reference or control alternative and is given a score of 5 for all objectives. However, for Alternative 2, the user enters a score for each objective. For example, the score is 5 for Control Fire because turnouts do not affect fire control. In contrast, the score is 7 for Reduce Soil Erosion, as shown in Figure 42. Similar scores are entered for all alternatives and objectives before the DSS is solved by clicking the “Solve/Solved” button.

Graphical output illustrating the minimum score (i.e., the composite, or overall, summed, and normalized score in each case), the maximum score, and the average of these scores for all the alternatives is shown in Figure 41. The solid line at 0.5 illustrates that the reference alternative is always scored as 0.5. All other alternatives have minimum, maximum, and average scores.

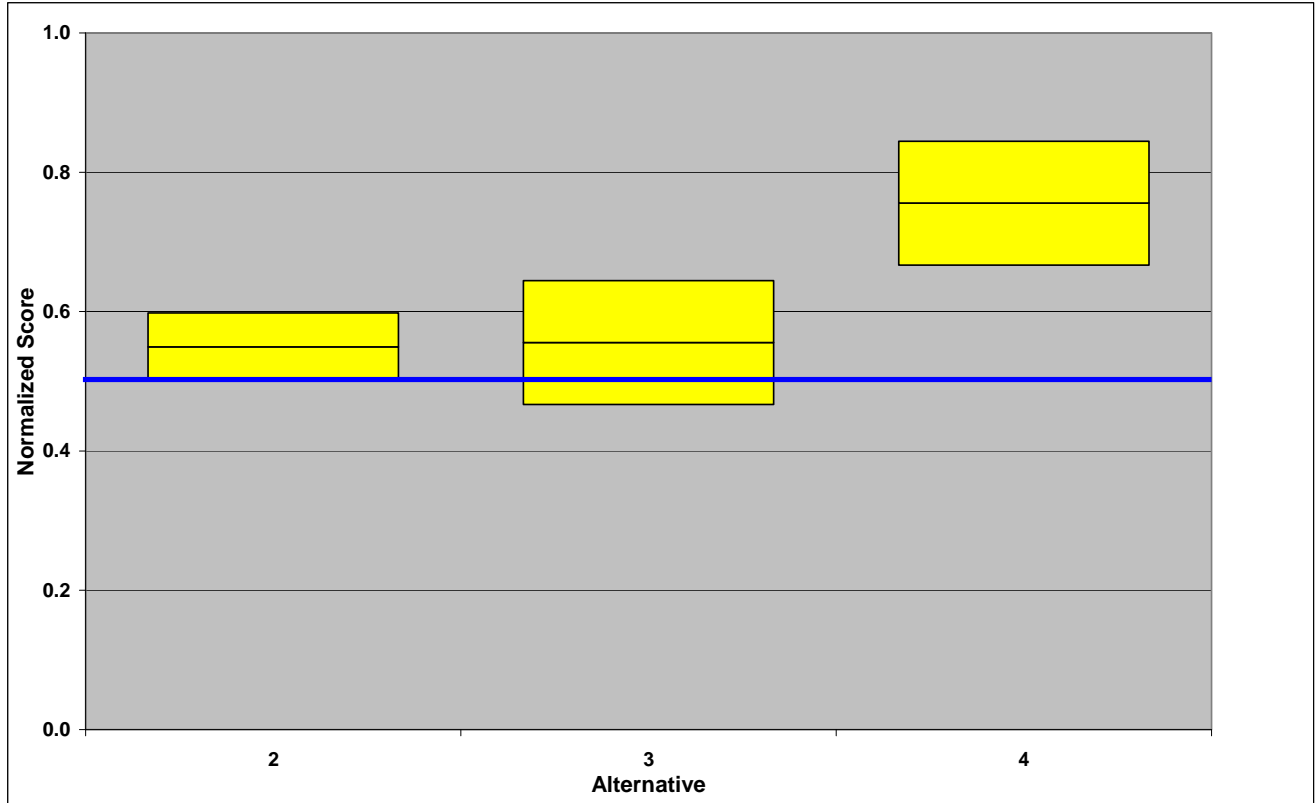


Figure 41. Illustration of minimum, maximum, and average scores for the reference management system for firebreak roads and three alternative management systems.

The scores for the reference firebreak management system (minimum=maximum = average = 0.5), Alternative 2 as the reference management system with engineered turnouts, Alternative 3 the same as 2 with gravel/cobble at critical points, and Alternative 4 is the same as 3 but with herbicide for vegetation control and without the gravel/cobble treatment.

The minimum, maximum, and average scores for the alternatives are Reference Alternative (0.5, 0.5, 0.5), Alternative 2 (0.5, 0.60, 0.55), Alternative 3 (0.47, 0.64, 0.56), and Alternative 4 (0.67, 0.84, 0.76). By this method, we conclude that the Alternative 2 is better than Alternative 1, Alternative 3 is somewhat worse than all other alternatives because its minimum score is 0.47, and Alternative 4 is the recommended firebreak road management system. Notice that this result is for the particular preference order selected, e.g. $W_1 \geq W_2 \geq W_3$, or fire control efficiency, then soil erosion, then total costs. If the weights had been ranked in a different order, the alternatives may have resulted in a different ranking. Thus, the DSS can be used to examine the importance of preference order for all possible combinations of weights.

In this example, the soil erosion rates would come from the DHSVM-HEM, the costs from user databases, and the fire control efficiency from expert judgment. This illustrates the ability of the DSS to use our best science (models and data) and our best judgment to rank alternatives for firebreak road management. Thus, the DSS brings our best science and judgment to bear on

improving the decision-making process. The improved decision-making process is then used to select the best alternative in the AM approach.

4.9.3 Example of User Input to the DSS – Firebreak roads at the YTC

Soil erosion/sediment yield information in most cases will come from a soil erosion–sediment yield model. In some cases it might come from monitored data. In the example described in the previous section, assume sediment yields from firebreak roads with and without turnouts and with and without vegetation re-growth on the road surface are estimated with the HEM and the impacts of graveled (hardened) stream crossings comes from field observations and databases. Furthermore, assume the cost information for these erosion control measures come from data documented in Site rehabilitation databases and the effectiveness of firebreak roads in reducing wildland fires comes from the expert judgment of Site personnel.

The values of the scores to input to the DSS as illustrated in Figure 40 are summarized in Table 8 as given below.

Table 8. User estimates and sources for scores in the firebreak road example. Under the conventional alternative 1.33 tons of sediment reach the adjacent stream and the cost index is 100.

Alternative #	Fire Control	Soil Erosion	Total Costs	Comments
1 – Reference or current management	Acceptable Score = 5	1.33 T Score = 5	Cost Index = 100 Score = 5	The Reference management always scores 5 for all objectives
2- Turnouts only	No impacts Score = 5	1.0 T Score = 7 ¹	Cost Index = 120 Score = 4 ²	See footnotes
3 Turnouts and gravel	No impacts Score = 5	0.7 T Score = 8	Cost Index = 200 Score = 1	Gravel emplacement is expensive
4 Turnouts and herbicide	Better fire control Score = 8 ³	0.4 T Score = 9	Cost Index = 140 Score = 3	

1. Score values come from scoring function as explained below.
2. Score values come from cost database maintained by Site personnel.
3. Score values come from expert judgment as to effectiveness of alternative in controlling fires.

When numerical data are available from monitoring or simulation modeling, it is possible to construct scoring functions to translate numerical values (such as sediment yield in tons) to a dimensionless score from 0 to 1.0 or (0 to 10.0). A scoring function is a mathematical formula which always scores 0.5 (5.0) for the reference alternative and then scores below or above 0.5 (5) depending upon whether or not the alternative scores worse or better with respect to the reference value of the specific objective.

Scoring functions can be derived in a number of ways. For example, a scoring function can be derived as a theoretical mathematical function as described by Wymore (1988), Lane, et al. (1991), and Lawrence et al. (1997), or as a “best fit” line to represent the data, or as a sketch of generalized relationship based on expert judgment. The scoring function used in Figure 42 was derived using Wymore’s (1988) procedure. The emphasis here is not on the source of the scoring function but on its general shape and properties for a decision variable such as soil erosion/sediment yield when less sediment yield is more desirable (and thus scores higher) than more sediment yield.

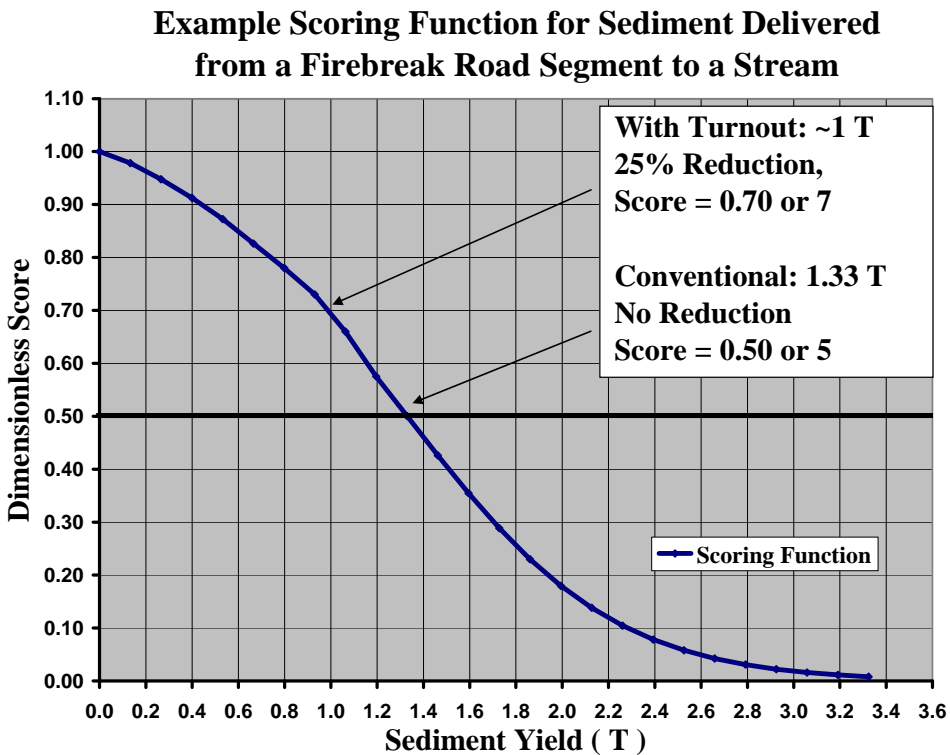


Figure 42. Illustration of a scoring function used to score sediment yield from alternative management practices for firebreak roads. In this example less sediment yield is desirable and thus alternatives which control erosion and result in less sediment delivery to streams scores higher than those with greater amounts of sediment yield.

4.9.4 Discussion

For our purposes herein, we can make some simple definitions to help describe the roll of decision support systems in technology transfer. If science is the organized search for truth to increase our knowledge, and technology is the practical application of science in problem solving, then technology transfer is the complex process of developing technology from science and then bringing it the user as a tool in problem solving. Notice that technology connotes everything from application of knowledge to development of apparatus for direct use by the consumer (broadest definition of user).

In this context, field data, remotely sensed data, smart change detection, hydrologic modeling, erosion/sediment transport modeling, and scientific judgment and expertise are brought together, or integrated, on a digital computer to implement what we call erosion prediction technology. Following the above steps to produce and implement erosion prediction technology results in a very complex data-modeling-interpretation process that requires advanced academic and practical training and experience for consistent and meaningful application in practical problem solving. The “data” step alone may require decades and millions of dollars to accomplish (e.g. see Lane et al., 2001, particularly pp. 214-222). Obviously, site users at military training facilities do not have the time or resources to develop databases and apply erosion prediction technology in assessing soil erosion impacts of training activities and remediation measures.

Therefore we have devised a spreadsheet implemented Multiple Objective Decision Support System to assist in applying erosion prediction technology as one part of a multi-objective analysis system for evaluation of alternative land management systems at military training facilities. The previously presented examples and the related text describe the DSS and how it includes application of erosion prediction technology as well as cost analysis, treatment effectiveness, etc. in a transparent (i.e. the DSS is documented and the user/reviewer/stakeholder can dig as deep as required to see how the system operates) and repeatable computer-based system. The DSS is integrated in a Windows environment and can be accessed through a simple spreadsheet. Results of erosion prediction technology analyses, cost data, etc. are imported into the spreadsheet, enabling the user to bring all of these components together to produce a graphical output summarizing the analyses (e.g. Figure 41).

Thus, the DSS is truly a technology transfer system as it enables a user to apply the complex technology to problem solving in a way that was heretofore impossible at worst and highly impractical at best. The following material elaborates on this assertion via examples for selected DSS components.

- Definition of the problem. Structuring the problem in a DSS framework can greatly simplify subsequent analyses by focusing efforts on specifics rather than taking a broader, unfocused approach. On the other hand, users are best able to state their needs and this information is crucial in building a DSS.
- Selection of decision variables. The decision variables must be measurable and precisely definable. For example, mean annual soil erosion in t/ha is a fine decision variable while “protecting the soil” is a higher level objective which may include reducing soil erosion, maintaining organic carbon content at a certain level, enhancing nutrient levels, and so on. The decision variable selection process forces scientific rigor while ensuring that each user (or even stakeholder) has a chance to have their management evaluation objectives (metrics) considered.
- Quantifying decision variables. If total initial cost is a decision variable then it can be quantified from historical project data files (i.e. contract costs, materials, etc.) or from expert judgment, or a combination of these for practices which have been implemented in the past and new practices under consideration. As described earlier, our best science can be used to quantify mean annual runoff volume, mean annual erosion, etc. through application of hydrologic modeling and erosion prediction technology. Databases of previous model runs, or databases of model input data for “on the fly” model running can

greatly simplify the modeling process and thus enhance the transfer of this modeling technology to the end user.

- Selection of scoring functions. Once the decision variables have been selected and quantified, we need to score them (decide the shape of the scoring function and then normalize the decision variables to a 0 to 1.0 range based on data/simulations from the conventional natural resources management system). This is a very transparent part of building a DSS. Everyone involved can see exactly which decision variables will be used to rank alternative management practices, how these decision variables reflect our shared objectives (e.g. do we want more runoff volume, less soil erosion, more vegetative cover for wildlife habitat, breaks in vegetation for fire control?), and which decision variables are excluded from the decision process. Selecting decision variables and their scoring functions in an interactive discussion setting can greatly enhance stakeholder participation, make the DSS more inclusive and transparent, and satisfy the practical needs of the users with respect to what they must do (regulations) and what they want to do (experience and expert judgment on management system needs) to solve a given natural resource problem.
- Selection of preference order for the decision variables. Ideally, a consensus can be achieved on which decision variables are most important and which are less important, and their relative rank from first to last. If this is not possible, then alternative preference orders can be selected and the DSS can then quantify the impacts of this uncertainty on ranking the feasible alternative natural resource management systems. Sometimes changing the preference order will change the ranking of the alternatives. Oftentimes, regardless of how many times the preference order is changed, one or two of the alternatives always rank as the best. In this happy circumstance, preference order does not dominate the problem and a consensus can easily be reached. Again, the weights are merely a numerical way of reflecting preference order. The weights can also be changed, given a preference order, to determine how important they are in determining the best alternative(s).

The above discussion illustrates the power of a DSS to facilitate stakeholder and user participation at all steps in the process from problem definition to ranking various natural resource management alternatives. The DSS can be as transparent as desired depending upon how much time and resources are available to facilitate stakeholder and user participation. The discussion also shows how our best science can be incorporated into a DSS and how the user can make the science as transparent as desired depending upon the time and resources available to “dig” into the science through the DSS documentation.

Thus, a DSS as proposed herein is invaluable in technology transfer through four main mechanisms or factors: 1) it assists in a focused, precise problem definition enhancing the possibility of reaching a solution, 2) it encourages stakeholder/user participation throughout the decision process from start to finish, 3) it enables us to bring our best science to bear on the decision process, and 4) it is transparent because of the opportunities for participation and the ability of the user/stakeholder/regulator to “dig” as deep as desired into the extensive documentation required.

5.0 Conclusions

To ensure sustainability and adaptability in managing training operations while minimizing impacts on watersheds, the DoD needs to identify activities that contribute to non-point source pollution and strategically locate and schedule operations. This project successfully developed decision tools that provide information to articulate tradeoffs between alternative management actions and resultant impacts and/or benefits to training range or adjacent downstream water bodies. The site-specific demonstration focused on management of training operations and ways to minimize impacts to training areas and downstream receiving waters at the YTC in south-central Washington State. The decision tools, and the data, science, technology, and knowledge upon which they are based, are necessary to bring the best science to bear on practical decision making.

The GIS-based decision support framework developed under this project provides the YTC stakeholders and DoD user community with the ability to plan for training activities and map the erosion potential response. This system is easy-to-use and provides meaningful results to help formulate the decision-making process. The presented methods, tools, and designs provide a new and unique ability to incorporate a multi-modal system incorporating field data, remote sensing, geospatial modeling, hydrologic and erosion modeling, and a DSS linked by a GIS-based user interface. The system works to articulate the multi-objective tradeoffs of management alternatives based on stakeholder decision criteria that allow for a scientifically defensible method of evaluating alternatives for the YTC site management needs.

The Distributed Hydrology Soil Vegetation Model (DHSVM), Green-Ampt infiltration model, and the HEM were enhanced and linked to simulate continuous runoff and sediment yield from rangeland, roads, firebreaks, and vehicle tracks associated with training activities at the site. The models were validated successfully against measured sediment yield from 12 sedimentation ponds within the YTC. The coupled DHSVM-HEM hydrologic and erosion models simulate the seasonal distribution of runoff and the resulting soil erosion at YTC as well as, or better than, RUSLE and WEPP. The coupled DHSVM-HEM modeling system represents a new generation of runoff and erosion prediction technology heretofore unavailable to land managers at the YTC, and to managers of lands hydrologically similar to the YTC.

The validated models were used with YTC hillslope profile data to develop “soil erosion condition classes” of poor, fair, good, and excellent in relation to the worst soil erosion conditions on the YTC. The soil erosion condition classes can now be used for analyses, on scales from individual subbasins to the entire YTC, evaluating existing conditions with respect to soil erosion. Because the erosion potential is analyzed on a pixel-by-pixel basis, in which each pixel is independent of one another, it cannot be used to estimate total sediment yield in a subbasin under varying conditions. However, for uses in which assessments of the influence of soil, vegetation, and land use on potential soil erosion are adequate, this methodology represents a new and unique decision tool for soil management on the YTC.

A complete and dynamic site-wide sediment budget was calculated in a GIS environment, for thousands of virtual transects describing approximately 3500 sub-basins, representing a new and unique technology. The resulting sediment budget represents the extensive field data transects

used for model calibration and evaluation, the thousands of virtual transects derived from remote sensing databases, the thousands of sub-basin sediment yield calculations using state-of-the-art simulation models, and the GIS spatial analysis and display capabilities. This modeling effort thus represents a heretofore-unavailable methodology for using remote sensing and geospatial technology to parameterize distributed hydrology and soil erosion models.

A Spatial Data Viewer was developed to allow the non-GIS specialist to easily navigate and query spatial data from the site wide sediment budget and associated vegetation and soils data. With the goal of providing a functional and easy-to-use decision environment, a simple user-interface based on Environmental Systems Research Institute's Java-based ArcExplorer software allows for easy identification of classified sediment yield areas and provides an interactive query capability so the user can view the underlying database information. This database provides information such as subbasin area, total subbasin sediment yield, sediment yield by land use type, mean elevation, mean slope, soil types, mean percent canopy, mean percent ground cover, etc. In addition to the viewer's basic maneuvering and query capabilities, the user can reclassify data to define more detailed sediment yield patterns and develop customized data queries (e.g., define subbasins with silt loam soils and a combined sediment yield > 3.2 t/ha/yr). The user also can add their own data for overlays or access web-ready data via WMS (e.g., National Wetlands Inventory), develop customized map layouts, and perform linear measurements.

A SIMDSS, adapted from an early standalone United States Department of Agriculture - Agricultural Research Service (USDA-ARS) prototype called WQDSS, was developed. The SIMDSS uses a spreadsheet environment to evaluate multiple-criteria alternative weighting into an easy-to-understand format for the end-user by providing summary statistics, graphs, and a familiar spreadsheet environment to facilitate various management scenarios. Data supporting SIMDSS can come from various sources including simulation models, measured data, and/or expert opinion to quantify decision criteria. SIMDSS provides this flexibility by using a scoring function, which converts numerical values into a dimensionless quantity. This built-in capability enables system users to mesh data from differing sources to arrive at the best possible decisions.

The potential for extreme spatial and temporal variability in hydrologic conditions during land-based training exercises can directly influence the level of associated environmental impacts from non-point source pollutants such as eroded sediment, petroleum products, and heavy metals. Under a wide variety of land-use and climatic conditions and at locations around the world, studies have shown that large storms dominate sediment yield from experimental plots and small watersheds. This project found similar results with only 13% of the drainage area at the YTC contributing nearly a third of the total sediment yield. A management philosophy that targeted, or ranked in priority, those high sediment yield subbasins for remediation measures, in general, would maximize return on investment on erosion control measures. Of course, some streams may be more important for a variety of reasons and this is easily included in the prioritization for remediation.

The single largest sediment yield year (one out of 42 years, or 2.4% of years) produced more than 10% of total simulated sediment yield in the entire 42-year period. In addition, the four largest years produced more than 30% of the total sediment yield. Finally, the combined sediment yield from the largest half of the 42 years produced more than 90% of the total

sediment yield. These simulated results are quite similar to measured data from a variety of locations throughout the globe, suggesting that the DHSVH-HEM model is preserving the property of large storm dominance of long-term or mean annual sediment yield from small watersheds.

The question of scale effects in hydrology has been a principal scientific problem for decades. Synergistic effects of combining databases from long-term watershed monitoring programs, geospatial data acquisition and analysis technology, distributed hydrologic modeling, and targeted field data acquisition programs have resulted in a new and unique ability to simulate spatial and temporal sediment yield across a range of space-time scales. However, this has not been purely a theoretical result of synergy; it has broad practical applications. Hydrologic problems positively impacted by these new developments include the development of targeting monitoring and remediation efforts to maximize return on investment of remediation resources to that fraction of the landscape producing soil erosion and sediment yield at a much higher rate than the spatial average. Implicit in these developments is the ability to display and analyze geospatial data based on combining sound scientific modeling procedures with improved databases.

Temporal analyses and results such as those derived under this project have profound implications for monitoring programs, hydrologic and hydraulic design criteria, and simulation model evaluation using extreme event simulation, within a long time series, to replicate the large storm dominance on sediment yield as observed in nature. Simulation models, which lack the ability to account for the significance of large storms in a time series, are of limited value in determining required monitoring periods, estimation of frequency distributions for event or annual sediment yields, and thus design of hydraulic structures based on exceedance probabilities or for evaluating management actions against typical environmental regulatory requirements. In summary, simulation models, which do not reproduce the large storm dominance of sediment yield (e.g., USLE/RUSLE), significantly underestimate uncertainty of the processes producing soil erosion and sediment yield. The same is true for models that do not capture the spatial distribution of sediment yield.

Fortunately, the synergistic effects of combining databases, geospatial technology, distributed simulation modeling, and simulation models that capture the large storm dominance features on sediment yield were developed over expanded space-time scales to meet the needs of managing natural resources on large military training areas such as the YTC.

6.0 References

- Blackburn, W. H., Pierson F. B., and Seyfried, M. S. 1990. Spatial and Temporal Influence of Soil Frost on Infiltration and Erosion of Sagebrush Rangelands. *Water Res. Bull.* 26(6):991-997.
- Clark, D. L., Janecky, D. R., and Lane, L. J. 2006. Science-based cleanup of Rocky Flats. *Physics Today*, Sept. 2006, pp 34-40 (Feature Article).
- Cogle, A. L., Lane, L. J., Basher, L. 2003. Testing the hillslope erosion model for application in India, New Zealand and Australia. *Environ. Modelling & Software* 18:825-830.
- Doe, W. E., Jones, D. S., and Warren, S. D. 1999. *The Soil Erosion Model Guide for Military Land Managers: Analysis of Erosion Models for Natural and Cultural Resources Applications*. U.S. Army Engineer Waterways Experiment Station Tech. Rept. ITL 99-XX: 122p.
- Foster, G. R., and Meyer, L. D. 1972. Transport of soil particles by shallow flow. *Trans. Am. Soc. Agric. Eng.*, 15:99-102.
- Goodrich, D.C., Lane, L.J., Shillito, R. A., Miller, S. N., Syed, K. A., and Woolhiser, D. A. 1997. Linearity of basin response as a function of scale in a semi-arid ephemeral watershed. *Water Res. Res.* 33(12): 2951-2965.
- Haupt, H.F. 1967. Infiltration, overland flow, and soil movement on frozen and snow-covered plots. *Water Res.. Res.* 3:145-161.
- Laflen, J. M., Elliot, W. J., Simanton, J. R., Holzhey, C. S., and Kohl, K. D. 1991a. WEPP soil erodibility experiments for rangeland and cropland soils. *J. Soil Water Conserv* 46:39-44.
- Laflen, J. M., Lane, L. J., and Foster, G. R., 1991b. WEPP: A new generation of erosion prediction technology. *J. Soil Water Conserv* 46:30-34.
- Lane, L. J., Simanton, J. R., Hakonson, T. E., and Romney, E. M. 1987. Large-Plot Infiltration Studies in Desert and Semiarid Rangeland Areas in the Southwestern U.S.A. Y. S. Fok, (ed.) In: Proc. Int'l. Conf. on Infiltration on Development and Applications, Honolulu, HI, Jan. 6-9, 1987, pp. 365-376.
- Lane, L. J., Shirley, E. D., and Singh, V. P. 1988. Modeling Erosion on Hillslopes. Chapter 10 In: *Modeling Geomorphological Systems* (ed.) M. G. Anderson, John Wiley and Sons Ltd., Chichester, England, pp. 287-308.
- Lane, L. J., Nichols, M. H., Levick, L. R., and Kidwell, M. R. 2001. A simulation model for erosion and sediment yield at the hillslope scale. Chapter 8 *In: Landscape Erosion and Evolution Modeling* (Harmon, R. S. and Doe, W. W., III), Kluwer Academic/Plenum Publishers, New York, 2001 pp. 201-237.
- Lane, L. J., Renard, K. G., Foster, G. R., and Laflen, J. M. 1992. Development and application of modern erosion prediction technology - the USDA experience. *Aust. J. Soil Res* 30:893-912.
- Lane, L. J., Nichols, M. H., and Simanton, J. R. 1995a. Spatial variability of cover affecting erosion and sediment yield in overland flow. In: *Effects of Scale on Interpretation and*

- Management of Sediment and Water Quality, Proc. Boulder Symposium, (W. R. Osterkamp, ed.), *Int. Assoc. Hydrol. Pub. No. 226*: 147-152.
- Lane, L. J., Nichols, M. H., and Paige, G. B. 1995b. Modeling erosion on hillslopes: concepts, theory and data. Proc. Int. Congr. on Modelling and Simulation, (P. Binning, H. Bridgman, and B. Williams, eds.), 1: 1-7.
- Lane, L. J., Hernandez, M., and Nichols, M. 1997. Processes controlling sediment yield from watersheds as functions of spatial scale. *J. Env. Model. Software* 12: 355-369.
- Lane, L. J., Nichols, M. H., Levick, L. R., and Kidwell, M. R. 2001. A Simulation Model for Erosion and Sediment Yield at the Hillslope Scale. Chap. 8 In: Landscape Erosion and Landscape Evolution Modeling, Ed. R. Harmon and W. Doe, Kluwer Academic/Plenum Pub. Co., pp. 201-237.
- Lane, L. J., and Wigmosta, M. S. 2006. The role of processes-based models and scaling in geomorphic designs. Paper was presented at the 2006 Billings Land Reclamation Symposium, June 5-8, 2006, Billings, MT and jointly published by BLRS and ASMR, 3134 Montavesta Rd., Lexington, KY 40502.
- Lane, L.J., M. Wigmosta, M Hernandez., 2007. Extreme Events and Stochastic Processes of Sediment Yield. Accepted for presentation/publication at the World Environmental & Water Congress, Honolulu, HI, May 13-16, 2008
- Lawrence, P. A. 1996. The role of data sources and simulation model complexity in using a prototype decision support system. Unpublished PhD Dissertation, School of Renewable Natural Resources, University of Arizona, Tucson, AZ, 332 pp.
- Lawrence, P. A., Stone, J. J., Heilman, P., and Lane, L. J. 1997. Using measured data and expert opinion in a multiple objective decision support system for semi-arid rangeland. *Trans. of the ASCE* 40(6):1589-1597.
- Nicks, A. D., and Lane, L. J. 1989. Chapter 2. Weather Generator. In USDA-Water Erosion Prediction Project: Hillslope Profile Model Documentation. L. J. Lane and M. A. Nearing (editors). NSERL Report No. 2. USDA-ARS National Soil Erosion Research Laboratory. West Lafayette, IN.
- National Research Council (NRC), 1999. New Strategies for America's Watersheds. National Academy Press, Washington, D.C.
- National Research Council (NRC). 2001. Assessing the TMDL Approach to Water Quality Management. Washington, D.C.: National Academy Press, Washington, D.C.
- O'Callaghan, J. F., and Mark, D. M. 1984. The extraction of drainage networks from digital elevation data. *Computer Vision, Graphics and Image Processing* 28:323-344.
- Rawls, W. J., Brakensiek, D. L., and Saxton, K. E., 1982. Estimation of soil water properties. *Trans. Am. Soc. Agric. Eng.* 25:1316-1320.
- Renard, K. G., Foster, G. R., Weesies, G. A., McCool, D. K., and Yoder, D. C. (coords.), 1997. Predicting soil erosion by water: a guide to conservation planning with the Revised Universal Soil Loss Equation (RUSLE). *USDA Agricultural Handbook No. 703*.
- Rodriguez-Iturbe, I., and Rinaldo, A., 1997. *Fractal River Basins: Chance and Self Organization*. Cambridge, University Press, Cambridge, U.K, 547 p.

- Seyfried, M. S., and Flerchinger, G. N. 1994. Influence of frozen soil on rangeland erosion. In: Variability of Rangeland Water Erosion Processes, SSA Special Publ. 38, pp. 67-82. *Soil Science Society of America, Inc.*, Madison, WI.
- Shirley, E. D., and Lane, L. J. 1978. A sediment yield equation from an erosion simulation model. *Hydrol. Water Res. Arizona Southwest* 8: 90-96.
- Stone, J. J., Lane, L. J., and Shirley, E. D. 1992. Infiltration and runoff simulation on a plane. *Trans. Am. Soc. Agric. Eng* 35: 161-170
- Storck, P., Bowling, L., Wetherbee, P., and Lettenmaier, D. P. 1998. An application of a GIS-based distributed hydrology model for the prediction of forest harvest effects on peak streamflow in the Pacific Northwest. *Hydrologic Processes* (12):889-904.
- Walters, C. J., and Holling, C. S. 1990. Large-scale management experiments and learning by doing. *Ecology* 71(6), 2060-2068.
- Wigmosta, M. S., Vail, L. W., and Lettenmaier, D. P. 1994. A distributed hydrology-vegetation model for complex terrain. *Water Res. Res.*, 30(6):1665-1679.
- Wigmosta, M. S., Nijssen, B., and Storck, P. 2002. The Distributed Hydrology Soil Vegetation Model. In *Mathematical Models of Small Watershed Hydrology and Applications*, V. P. Singh, D. K. Frevert, eds., *Water Res. Pub.*, Littleton, CO, p. 7-42.
- Wigmosta, M. S., Lane, L. J., Tagestad, J. D., and Coleman, A.M., 2006. Hydrologic and erosion models to assess land use and management practices affecting soil erosion. In Press.
- Wilson, C. J., Carey, J. W., Beeson, P. C., Gard, M. O., and Lane, L. J. 2001. A GIS-based hillslope erosion and sediment delivery model and its application in the Cerro Grande burn area. *Hydrol. Proc.* 15:2995-3010.
- Wischmeier, W. H., and Smith, D. D., 1978. Predicting rainfall erosion losses, a guide to conservation planning, *USDA Handbook No. 537*, U.S. Government Printing Office, Washington, D.C.
- Wymore, A. W. 1988. Structuring system design decisions. *Systems science and engineering. Proc. International Conf. on Systems Science*, pp. 704-709.
- Yakima Training Center (YTC). 2002. *Cultural and Natural Resource Management Plan* YTC, Yakima, WA.
- Yakowitz, D.S., Lane L.J. Lane and Szidarovszky, F. 1993a. Multi-attribute decision making: dominance with respect to an importance order of the attributes. *Appl. Mathem. and Comput.* 54:p167-181.
- Young, R. A., Romkens, M. J. M., and McCool, D. K. 1990. Temporal Variations in Soil Erodibility. Pp 41-53 in: *Soil Erosion: Experiments and Models* (Rorke B. Bryan, ed), Cantena Supplement 17, Cremlingen-Destedt, West Germany.
- Zuzel, J. F., and Pikul, J. L., Jr., 1987. Infiltration into Seasonally Frozen Agricultural Soil. *J. Soil Water Conserv.* 42:447-450.

Appendix

Technical Publications

Journal Articles

Coleman, A.M., M. Wigmosta, L.J. Lane, J. Tagestad, and D. Roberts, 2007. A GIS-based adaptive management decision support system to support a multi-objective framework. Published in *J. Map and Geog. Libraries*, 2007.

Wigmosta, M., L.J. Lane, and J. Tagestad, 2008. Coupled hydrologic and erosion modeling for assessment of military training activities affecting soil erosion. In review, *ASCE J. Hydrological Engineering*.

Tagestad, J, Coleman, A.M., L.J. Lane, and M. Wigmosta, 2008. Analyses of hydrologic-erosion model performance using field and remotely sensed data: A case study. In preparation.

Technical Reports

Wigmosta, M., L.J. Lane, J. Tagestad, A.M. Coleman, and D. Roberts, 2003. Development of an Adaptive Framework for Management of Military Operations in Arid/Semi-Arid Regions to Minimize Watershed and Instream Impacts from Non-Point Pollution, SERDP Project SI-1340 2003 Annual Report.

Wigmosta, M., L.J. Lane, J. Tagestad, A.M. Coleman, and D. Roberts, 2003. Development of an Adaptive Framework for Management of Military Operations in Arid/Semi-Arid Regions to Minimize Watershed and Instream Impacts from Non-Point Pollution, SERDP Project SI-1340 2004 Annual Report.

Wigmosta, M., L.J. Lane, J. Tagestad, A.M. Coleman, and D. Roberts, 2003. Development of an Adaptive Framework for Management of Military Operations in Arid/Semi-Arid Regions to Minimize Watershed and Instream Impacts from Non-Point Pollution, SERDP Project SI-1340 2005 Annual Report.

Wigmosta, M., L.J. Lane, J. Tagestad, A.M. Coleman, and D. Roberts, 2003. Development of an Adaptive Framework for Management of Military Operations in Arid/Semi-Arid Regions to Minimize Watershed and Instream Impacts from Non-Point Pollution, SERDP Project SI-1340 2006 Annual Report.

Conference Proceedings and Papers

Lane, L.J, M. Wigmosta, 2006. The Role of Process-Based Models and Scaling in Geomorphic Designs. Paper was presented at the 2006 Billings Land Reclamation Symposium, June 5-8, 2006, Billings, MT and jointly published by BLRS and ASMR, 3134 Montavesta Rd., Lexington, KY 40502.

Lane, L.J, M. Wigmosta, and M. Hernandez, 2008. Extreme Events and Stochastic Processes of Sediment Yield. Accepted for presentation/publication at the World Environmental & Water Congress, Honolulu, HI, May 13-16, 2008.

Published Abstracts

Wigmosta, M., L.J. Lane, J.Tagestad, A.M. Coleman, and D. Roberts, 2003. Development of an Adaptive Framework for Management of Military Operations in Arid/Semi-Arid Regions to Minimize Watershed and Instream Impacts from Non-Point Pollution, SERDP 2003 Annual Symposium.

Wigmosta, M., L.J. Lane, J.Tagestad, A.M. Coleman, and D. Roberts, 2003. Development of an Adaptive Framework for Management of Military Operations in Arid/Semi-Arid Regions to Minimize Watershed and Instream Impacts from Non-Point Pollution, SERDP 2004 Annual Symposium.

Wigmosta, M., L.J. Lane, J.Tagestad, A.M. Coleman, and D. Roberts, 2003. Development of an Adaptive Framework for Management of Military Operations in Arid/Semi-Arid Regions to Minimize Watershed and Instream Impacts from Non-Point Pollution, SERDP 2005 Annual Symposium.

Wigmosta, M., L.J. Lane, J.Tagestad, A.M. Coleman, and D. Roberts, 2003. Development of an Adaptive Framework for Management of Military Operations in Arid/Semi-Arid Regions to Minimize Watershed and Instream Impacts from Non-Point Pollution, SERDP 2006 Annual Symposium.

Published Book Chapters

Wigmosta, M, R Prasad, L.J. Lane, and K. Gill, 2008. Upscaling and Downscaling – Dynamic Models. (Update of Chapter 11) Encyclopedia of Hydrologic Sciences. Submitted